

Georgia State University

ScholarWorks @ Georgia State University

Chemistry Dissertations

Department of Chemistry

8-2024

Carbon Monoxide Donors: From Synthetic Applications to Reassessment of Commercially Available Compounds

Nicola Bauer

Follow this and additional works at: https://scholarworks.gsu.edu/chemistry_diss

Recommended Citation

Bauer, Nicola, "Carbon Monoxide Donors: From Synthetic Applications to Reassessment of Commercially Available Compounds." Dissertation, Georgia State University, 2024.
doi: <https://doi.org/10.57709/37236073>

This Dissertation is brought to you for free and open access by the Department of Chemistry at ScholarWorks @ Georgia State University. It has been accepted for inclusion in Chemistry Dissertations by an authorized administrator of ScholarWorks @ Georgia State University. For more information, please contact scholarworks@gsu.edu.

Carbon Monoxide Donors: From Synthetic Applications to Reassessment of Commercially
Available Compounds

by

Nicola Bauer

Under the Direction of Binghe Wang, PhD

A Dissertation Submitted in Partial Fulfillment of the Requirements for the Degree of

Doctor of Philosophy

in the College of Arts and Sciences

Georgia State University

2024

ABSTRACT

Carbon monoxide (CO) is known for various reasons. The general public sees CO as the “silent killer”, while organic chemists see CO as a reagent for carbonylation, and medicinal chemists and biologists see CO as an endogenous signaling molecule with therapeutic potential. Along these lines, we have developed and assessed CO donors for wide ranging applications.

In terms of synthetic organic chemistry, our lab has developed a light-activated CO donor for Pd-catalyzed and light-mediated carbonylation. This low-molecular-weight, solid CO surrogate that only requires a low-power LED for activation to release 2 equivalents of CO can be universally implemented in various palladium-catalyzed carbonylative transformations. It is also compatible with protocols that employ blue-light to activate conventionally inaccessible substrates such as nonactivated alkyl halides.

In the focus of its medicinal and biological applications, CO is produced in mammals primarily through heme degradation mediated by heme oxygenases, HO-1 and HO-2, with the inducible form HO-1 being cytoprotective and immunomodulatory. Much of HO-1's effects have been recapitulated by exogenous administration of CO and have been pharmacologically validated for its therapeutic benefits in animal models. For the further development of CO-based therapeutics, new delivery forms are needed to address the inherent limitations of using inhaled CO for therapeutic applications. Along this line, there have been metal-based CO-releasing molecules (CORMs), photo-sensitive organic donors, and organic CO prodrugs that release CO under physiological conditions. Among these, four commercially available carbonyl complexes with either a transition metal or borane (CORM-2, CORM-3, CORM-A1, and CORM-401) have played prominent roles appearing in over 650 publications. Detailed CO-releasing characteristics in buffer and cell culture media have been reported by various labs for the two ruthenium

compounds: CORM-2 and CORM-3. In this work, we characterize the other two, CORM-A1 and CORM-401, for its CO release properties under various conditions important for its application in studying CO biology. Specifically, we report the idiosyncratic CO production and redox activity of CORM-A1, as well as the variable CO production and impure commercial samples of CORM-401.

This work highlights the foundational issues and unreliability of the commercially available CORMs including a lack of idiosyncratic CO production, CO-independent chemical and biological activity, and lack of good negative controls of the carrier. The significance of this work includes highlighting the convolution the CORMs have had caused in the CO field, as well as confronting the issues of influence from prominent researchers and commercial vendors.

INDEX WORDS: Carbon monoxide, CO donor, Gasotransmitter, Carbonylation

Copyright by
Nicola Bauer
2024

Carbon Monoxide Donors: From Synthetic Applications to Reassessment of Commercially
Available Compounds

by

Nicola Bauer

Committee Chair: Binghe Wang

Committee: Jun Yin

Maged Henary

Electronic Version Approved:

Office of Graduate Services

College of Arts and Sciences

Georgia State University

August 2024

DEDICATION

This dissertation is dedicated to my parents, Andrea and Brian, and my brother, Andrew.
None of this would have been possible without you, your love, and unconditional support.

ACKNOWLEDGEMENTS

I want to start off by acknowledging and expressing my deepest gratitude to my Ph.D. advisor, Dr. Binghe Wang. His mentorship, in research and in life, has been incredibly inspiring. I struggle to find the words to express how thankful I am for him putting his faith in me and supporting all my curiosity-driven endeavors. The time I have spent under his advisement has not only made me a strong researcher, but his dedicated mentorship, patience, empathy, and ocean of knowledge has inspired me for years to come. I am truly honored to have trained under his advisement and hope to carry the impact he has had on me throughout my career and personal life.

I would like to extend gratitude to my dissertation committee, Dr. Jun Yin and Dr. Maged Henary, for their time and insights on my projects, as well as helping form my future career.

I would also like to thank the lab members who have made my time in this lab enjoyable and made time just fly by. I could probably write a full dissertation of just how thankful I am for each of these wonderful people, so just know this is the abridged version.

First, I'd like to thank my first mentor Dr. Ladie Kimberly De La Cruz for her kindness, trust and belief in my abilities early on, and strong guidance to set me up for success. I'd also like to thank Dr. Zhengnan Yuan for his guidance in research and in my career.

It is imperative that I express my gratitude to Dr. Xiaoxiao Yang. Not only as a fantastic mentor in research, but Dr. Yang has also been a mentor in my life. Thank you for listening to all my crazy research ideas and questions, patiently working with me on things I didn't understand, teaching me things in and outside of research, mentoring me on my career decisions, and talking to me about all things food, history, space, and travel. I aspire to one day reach his level of knowledge, skill, and patience.

I would also like to acknowledge my peers, with special appreciation for Lester Liu, Dr. Ravi Tripathi, and Dr. Qiyue Mao. Lester was not only my bench mate, but I am proud to call him a dear friend, and I am so thankful for the time we have spent discussing research, talking about our personal goals, and of course, eating hot pot. Thank you to Ravi for advising me on research questions and projects, but a special thank you to the time he spent talking about the depths of life and advising me through my own personal life during my time in the lab. Lastly, I'd like to extend a special thank you to Dr. Qiyue Mao, who joined the lab only a year before my defense, but in that short time has become an inspiring mentor and a great friend. Finally, thank you to everyone else in the lab that has helped me get here: Shameer, Ce, David, Zach, Phat, Rujuta, Liang, Shubham, Dr. Wen Lu, Dr. Rohit, Dr. Priti, Dr. Zhu, Aditi, and Muskan. I'd also like to thank my three undergraduate mentees during my time at GSU: Christel, Fabiola, and Mark. Thank you for allowing me to grow my mentoring skills and teaching me how to teach!

Importantly, I'd like to acknowledge my parents, Andrea and Brian, and my brother, Andrew, for supporting me through this journey. Thank you for everything you've done to lead me here.

Last but not least, I'd like to acknowledge the friends that have provided me with unconditional support: my best friend, Dottie Ruth, and the amazing people of Awkward: Andrew, Amanda, and Harry. Thank you for your unconditional love and support.

I also gratefully acknowledge the support and funding from the Department of Chemistry and GSU Neuroscience Institute Brains and Behavior Program.

TABLE OF CONTENTS

ACKNOWLEDGEMENTS	V
LIST OF TABLES	X
1 INTRODUCTION	1
2 ANALYSIS OF COMMERCIALLY AVAILABLE CARBON MONOXIDE DONOR, CORM-A1.....	5
2.1 Introduction	5
2.1.1 CORM-A1	7
2.2 Results and Discussion.....	9
2.2.1 Criterion I. The chemical reactivity of CORM-A1 towards biorelevant molecules	9
2.2.2 Criterion II. Assessment of commonly used negative controls: iCORM-A1	14
2.2.3 Criterion III: The ability for CORM-A1 to generate CO in a reproducible and reliable fashion: CO production under various conditions	18
2.2.4 Consideration on the viability of CORM-A1 as a CO surrogate	31
2.3 Conclusion.....	35
2.4 Experimental	36
2.4.1 General Information	36
2.4.2 UV-Vis Analysis.....	37
2.4.3 LC-MS/MS Analysis.....	39
2.4.4 B NMR Analysis	40

2.4.5	<i>Quantitative CO Analysis</i>	40
2.4.6	<i>Reaction of 1-methylnicotinamide (1 mM) and CORM-A1 (5 mM) or NaBH₄ (10 mM) in PBS</i>	43
3	ANALYSIS OF COMMERCIALLY AVAILABLE CARBON MONOXIDE DONOR, CORM-401	44
3.1	Introduction	44
3.2	Results and Discussion	45
3.2.1	<i>CO Production using GC</i>	45
3.2.2	<i>CO-releasing ability of CORM-401 translates into hemoglobin binding</i>	54
3.2.3	<i>EPR Characterization of CORM-401</i>	58
3.3	Conclusion	60
3.4	Experimental	62
3.4.1	<i>General Information</i>	62
3.4.2	<i>UV-vis Analysis</i>	63
3.4.3	<i>Quantitative CO Analysis</i>	63
3.4.4	<i>CO-oximetry</i>	65
3.4.5	<i>EPR</i>	65
4	DESIGN OF CARBON MONOXIDE DONOR FOR CARBONYLATION REACTIONS	67
4.1	Introduction	67

4.1.1	<i>Preliminary Work Conducted by Dr. Ladie Kimberly De La Cruz</i>	69
4.2	Results and Discussion	72
4.3	Conclusion	75
4.4	Experimental	76
4.4.1	<i>General</i>	76
4.4.2	<i>Synthesis of CO-501</i>	77
4.4.3	<i>General Protocol</i>	80
4.4.4	<i>Reaction Vessel</i>	80
4.4.5	<i>Proof-of-concept- CO-501 as a CO source for various carbonylative reactions</i> .	81
4.4.6	<i>Light-assisted Carbonylation using CO-501 as a CO Source</i>	85
5	CONCLUSION	90
	REFERENCES	92
	APPENDICES	105
	Appendix A: LC-MS Chromatographs for Chapter 1	105
	<i>Appendix A.1 B NMR Spectra for Chapter 1</i>	120
	<i>Appendix A.2</i>	120
	Appendix B: NMR Spectra for Chapter 3	121

LIST OF TABLES

Table 1-1. CO production of CORM-A1 in unbuffered water (n = 3)	21
Table 1-2. Effect of Buffer on CO Production from CORM-A1 (n = 3).....	22
Table 1-3. Effect of different reagents on the CO production from 10 mM CORM-A1 in 100 mM PBS (n=3)	23
Table 1-4. Effect of NAD ⁺ on the stability of 1 mM CORM-A1 in unbuffered water (n=3).....	24
Table 1-5. Effect of different ions on CO production from 10 mM CORM-A1 (n=3)	26
Table 1-6. Effect of nicotinamide variations on the CO production from 10 mM CORM-A1 in 100 mM PBS. (n=3).....	27
Table 1-7. CO production from CORM-A1 in the presence of different DMSO solutions and oxidants (n=3)	29
Table 1-8. Effect of H ₂ O ₂ on CO production from CORM-A1 in 100 mM PBS (n=3).....	30
Table 1-9. CO production from CORM-A1 in different biological media (n=3).....	31
Table 1-10. Summary of factors that alter CORM-A1 CO production	33
Table 2-1. CO production from 1 mM and 100 μ M CORM-401 in PBS or unbuffered water detected via GC-FID (n=3). *P \leq 0.05 vs CORM-401 in PBS (1 mM and 100 μ M) via one-tailed, equal variance t-test	45
Table 2-2. CO production from CORM-401 in PBS detected via GC-FID (n=3).....	48
Table 2-3. CO production from 1 mM and 100 μ M CORM-401 in 100 μ M H ₂ O ₂ detected via GC-FID (n=3). *P \leq 0.05, **P \leq 0.01 vs CORM-401 in PBS (1 mM and 100 μ M) via one-tailed, equal variance t-test	51

Table 2-4. CO production from 1 mM and 100 μ M CORM-401 in 100 μ M GSH or cysteine detected via GC-FID (n=3). *P \leq 0.05, **P \leq 0.01 vs CORM-401 in PBS (1 mM and 100 μ M) via one-tailed, equal variance t-test	52
Table 2-5. CO production from 1 mM and 100 μ M CORM-401 in 100 μ M myoglobin (Mb) or albumin detected via GC-FID (n=3). *P \leq 0.05 vs CORM-401 in PBS (1 mM and 100 μ M) via one-tailed, equal variance t-test	53
Table 2-6. Maximum %COHb in mouse blood in vitro achieved within 2 h when incubated with CORM-3, CORM-401, CORM-A1, or CO gas. The ratio to CO gas is calculated by %COHb CORM/%COHb CO gas.	55
Table 2-7. CO production of 1 mM CORM-3 in different solvent detected via GC-FID (n=3) ..	56
Table 3-1. Proof-of-concept studies on the applicability of CO-501 as a CO surrogate for various carbonylation reactions (\approx 0.1 mmol scale) under different reaction conditions. [#] \approx 1 mmol scale.	73

LIST OF FIGURES

Figure 1-1. (Blue) Structures of CORM-2, CORM-3, and CORM-401 and brief overview of their reported CO-independent biological and chemical reactivities and (Purple) structure of CORM-A1 and an overview of the work presented here.	8
Figure 1-2. Investigation of NAD ⁺ reduction by CORM-A1	10
Figure 1-3. Reaction kinetics of 2 mM NAD ⁺ with CORM-A1 (1:1, 2 mM) incubated at 37 °C for 30 minutes monitored using UV-Vis.	11
Figure 1-4. Kinetic studies of reaction of NAD ⁺ with different concentrations of CORM-A1 (1:1, 2 mM or 200 μM; 7:1 1.4 mM; 11:1 2.2 mM). The 1:1 reaction (2 mM CORM-A1: 2 mM NAD ⁺) was incubated at in PBS at 37 °C. At each time point, the reaction was either conducted at or diluted by 10-fold to 200 μM for UV measurements. Other reactions were conducted at 200 μM (NAD ⁺) for UV-Vis detection. Reactions were monitored using UV-Vis at 340 nm.	11
Figure 1-5. A: Reaction of 2 mM NAD ⁺ with CORM-A1 (1:1, 2 mM) incubated at 37 °C for 30 minutes. Reactions monitored and AUC determined using LC-MS/MS (right) and UV-Vis (left). B: Reaction of 1 mM NAD ⁺ with CORM-A1 (10:1, 10 mM) incubated at 37 °C for 15 minutes. Formation of NADH (μM) over 30 minutes by reaction of 200 μM NAD ⁺ and CORM-A1 (11:1, 2.2 mM) monitored by LC-MS/MS (right) and UV-Vis (left), quantification done using AUC. Ratios are calculated using the average AUC from duplication experiments.	13
Figure 1-6. Kinetic studies of reaction of NADP ⁺ with CORM-A1 at different concentrations and ratios (1:1, 100 μM; 3.5:1 350 μM; 10:1 1 mM). Reactions were conducted at 100 μM NADP ⁺ . NADPH generation was monitored by UV-Vis absorbance at 340 nm.	13

Figure 1-7. Reactions of NAD⁺ with CO gas, CORM-A1 and other relevant boron species. A.

Reactions of 1 mM NAD⁺ with CO gas (2 mL), CORM-A1 (10:1, 10 mM), boric acid (10:1, 10 mM), or BH₃-THF (10:1, 10 mM) at 37 °C for 15 minutes. Reactions monitored and AUC determined using LC-MS/MS. Ratios are calculated using the average AUC from duplication experiments. B. Reaction of 1 mM NAD⁺ with iCORM-A1 (10:1, 10 mM), boric acid (10:1, 10 mM) and NaBH₄ (10:1, 10 mM). Unreacted CORM-A1 (2mM) provided as a control. Reactions were diluted to 200 μM after 15 minutes for UV-vis measurements..... 17

Figure 1-8. Structures of NAD⁺/NADP⁺, NADH/NADPH, 1-methylnicotinamide, N-methylpyridine, and N-methyl DABCO 27

Figure 2-1. Previously proposed CO release and “re-backbonding” mechanism⁹⁵ 47

Figure 2-2. A. UV-vis spectra of OxyHb and COHb (78.9 μM) and UV-vis spectra of 1:1 reaction between CORM-401 and Hb, with and without Na₂S₂O₄. B. UV-vis spectra of 2:1 reaction between CORM-401 and Hb, with and without Na₂S₂O₄. C. %COHb Yield calculated using Hb assay from 25 mM and 150 mM CORM-401, respectively 58

Figure 2-3. X-Band EPR spectra of CORM-401 solutions (400 μM). A. CORM-401 dissolved in PBS at RT (blue); B. CORM-401 dissolved in PBS, incubated at 37 °C for 120 min (green), and in PBS with excess Na₂S₂O₄ for 5 min incubation at 37 °C (red) and C. CORM-401 dissolved in PBS incubated at 37 °C for 120 min, then bubbled with excess CO gas (black). The EPR conditions were shown in SI. 60

Figure 3-1. (A) For light-assisted carbonylation reactions using CO surrogates, a two-chamber reaction vessel is needed. (B) Photoactivated CO donor simplifies set-up and protocol. 68

Figure 3-2. Strategy to prepare **CO-501** that undergoes photochemical transformation to release two equivalents of CO and by-product **3**. 70

Figure 3-3. A) UV-Vis spectrum **CO-501** (1 mM in DMSO) upon exposure to blue LED light.

(B) **CO-501** is stable under ambient light but releases CO when exposed to blue LED.

(C) NMR studies confirming conversion of **CO-501** to photoproduct **3**..... 72

Figure 3-4. Light-activated CO surrogate for light-assisted carbonylation reactions of challenging substrates. (A) non-activated alkyl iodides (B) bulky nucleophile. (^aisolated yield,

^bliterature yield, ^cNMR yield) 75

1 INTRODUCTION

Since the 1940's, it has been known that carbon monoxide (CO) is produced endogenously in humans¹ through heme degradation as part of red blood cell turn overs.² Incidentally, human red blood cells have an average lifetime of about 120 days, leading to a sustained level of CO production at an "average" rate of ~10 ml/day.³⁻⁵ Heme degradation is mediated by heme oxygenases-1 and -2 (HO-1, 2). Despite the public perception of its poisonous nature at high concentrations, CO has been shown to play important pathophysiological roles in immunoregulation, anti-inflammation, cyto-/organ-protection, and circadian clock regulation. A recent book comprehensively examines the various pathophysiological roles of CO and its validated pharmacological functions.⁶ For example, CO has been shown to vary in concentrations under pathological conditions and has been pharmacologically validated to offer beneficial effects in animal models of acute kidney injury,^{7, 8} chemically induced liver injury,⁹⁻¹¹ organ transplantation,^{12, 13} systemic inflammation,¹⁴ and cancer metastasis.^{15, 16} Interestingly, CO also has reported roles in neuromodulation and cognition, and recently a CO-HO-Dopamine axis was proposed for the first time.¹⁷ Earlier studies largely employed gaseous CO through inhalation.¹⁸ For safety reasons and for ease of administration and dose control, alternative delivery approaches are desired. Along this line, Motterlini and Mann introduced metal-CO complexes as CO-releasing molecules (CORMs) in 2002.¹⁹ Later, many other varieties of metal-CO complexes,²⁰⁻²⁴ CO in solution,²⁵ and photo-sensitive organic CO donors²⁶⁻²⁹ were reported. In 2014, we reported the first organic CO prodrugs by employing a cheletropic reaction of a norbornadienone scaffold for CO release.³⁰ Subsequently, organic CO prodrugs of different types capable of CO release under physiological conditions have been reported.³¹⁻³⁵

When it comes to studying CO biology, four compounds termed “carbon monoxide-releasing molecules” or “CORMs” have played a prominent role for the past two decades; CORM-2, CORM-3, CORM-A1, and CORM-401 have collectively appeared in about 650 publications. CORM-2 and CORM-3 are ruthenium-based carbonyl complexes; CORM-401 is a manganese carbonyl complex; and CORM-A1 is a borane complex. A PubMed search in February 2023 yielded 407 publications for CORM-2, 200 for CORM-3, 29 for CORM-401, and 79 for CORM-A1, clearly indicating the importance and broad impacts of these four CORMs. These four have been reported to have a large number of pharmacological and therapeutic functions including effects on autophagy, coagulation/platelet activation, non-alcoholic steatohepatitis, myocardial infarction, neuronal differentiation, blood brain barrier dysfunction, cancer metastasis, autoimmune uveoretinitis, inflammation and fibrosis, arthritis, injuries of various types and organs, and neonatal vascular injury, among many other indications. These activities were all originally attributed to the “CO released” from these CORMs. However, recent studies have revealed very pronounced CO-independent effects and chemical reactivities of these four CORMs. These effects and reactivities should be taken into consideration when using any of these CORMs for studying CO biology and/or pharmacology.

The issues summarized in a recent review³⁶ are expected to have profound impacts on how results from these four CORMs should be interpreted. However, it is important to emphasize that despite all the issues identified with these CORMs, this in itself raises no question about the pharmacological effects that have been discovered for these CORMs. The only issue is whether these pharmacological effects can be attributed to CO, partially, fully, or not at all. It is important to note that these four CORMs have not only been used to examine CO delivery properties, but also to define CO pharmacology, physiology, and mechanism(s) of actions of a wide range of

biological activities. As such, there is a heavy burden on these CORMs to meet certain threshold conditions for these applications. At the outset, we set four essential criteria for a CORM to be so-named and to be used for CO biology as a surrogate: (1) the ability to reliably and reproducibly donate CO with known kinetics under near physiological conditions in order to meet the minimal requirement needed to be called a “CO-releasing molecule” or CORM; (2) being devoid of chemical reactivities that may interfere with critical biomolecules and/or intercept with CO signaling pathways or cause significant biological consequences; (3) being free from significant CO-independent biological activities; and (4) the availability of at least one proper negative control. It is unfortunate that all four CORMs failed to meet any one of these criteria. Especially alarming is the lack of or unreliable production of CO by these “CORMs” under normal physiological conditions, which directly undermines the foundation for these CORMs to be used as CO surrogates to study CO biology. It is unfortunate that these complications have been amplified over a 20-year period. We would like to further emphasize that the failure of these four CORMs to meet the requirements for an adequate CO donor does not invalidate discoveries using them thus far, but only subtracts the role of CO from the possible pharmacological mechanisms. Once again, we would like to emphasize that the commercial availability and ease of use of these CORMs has promoted a 20-year snowball effect that is to no fault of any individual researcher. Although we only highlight these four CORMs, all other CORMs or CO donors with reactive metal cores (or reactive functional groups) need to be thoroughly assessed for chemical reactivity and CO-independent biological activity before their use in studying CO biology. It is also sad to see that in some cases, CO fluorescent probe development also solely relied on a CORM to study feasibility, leading to some “CO probes” that only detect the “CORM” because of its unique chemistry, but not CO.³⁷ We hope that future CO donors will meet the four threshold criteria set

out and future biological studies and fluorescent probe work will emphasize the need to cross validate with a proven CO source. We also hope that our work not only addresses the tangible issues on hand with these four CORMs, but also stimulates conversations within the field, encourages discussions of the lessons learned, and helps to enhance the level of rigor in developing CO donors and studying CO biology.

Regarding contributions to the CO field, this work is broad. Chapters 2 and 3 describe the reassessment of two commercially available compounds, CORM-A1 and CORM-401. These chapters bring to light the idiosyncratic CO production, CO-independent reactivity, and lack of proper controls of these two commercially available CORMs for the first time. The third chapter involves the demonstration of the light-activated CO surrogate developed in our lab to be used for one-pot, Pd-catalyzed and light-mediated carbonylation reactions. Other work conducted in the CO field that is not included in this dissertation includes the proposal of a CO-HO-Dopamine axis, as well as work in CO prodrug development and CO probes. In summary, the work completed during this PhD broadly impacts the CO field in many different areas of research.

2 ANALYSIS OF COMMERCIALY AVAILABLE CARBON MONOXIDE DONOR, CORM-A1

This chapter is mainly based on my publications: Bauer, N. et al. *Chem. Sci.*, **2023**,14, 3215-3228. Bauer, N. et al. *Biochem Pharmacol.* **2023**, 214, 115642.

2.1 Introduction

Carbon monoxide (CO) is an endogenous signaling molecule with functional importance on par with that of two other gaseous signaling molecules: nitric oxide and hydrogen sulfide.^{2, 38, 39} CO is produced in mammals primarily through heme degradation mediated by heme-oxygenase (HO). Exogenous CO has been pharmacologically validated to provide therapeutic benefits in animal models of ischemia-reperfusion injury of various organs, organ transplantations, anti-inflammation, and even cancer. A recent book comprehensively summarizes CO biology and its therapeutic potential including clinical trials.⁴⁰ Early studies of CO biology mostly used gaseous CO, which has the advantage of little ambiguity in terms of the active principal and the disadvantage of difficulty in controlling dosage and concentration, lack of portability, health hazards to lab personnel, and dosage variations depending on individual characteristics such as lung capacity, breathing rate, and physiological state.³² The last point is especially problematic if CO-based therapeutics ever go into human studies. To address these issues, new forms of CO have been developed including metal-based CO-releasing molecules (CORMs),⁴¹⁻⁴⁴ and organic CO donors capable of releasing CO upon photolysis, mechanical force, or chemoexcitation.⁴⁵⁻⁵⁰ There have also been efforts to use various triggers for CO release from metal-based CORMs.⁵¹⁻⁵⁵ In 2014, we reported the first organic CO prodrugs by taking advantage of a cheletropic reaction for CO release from a norbornadienone scaffold; this was followed by a series of reports of CO prodrugs of various properties^{30, 56-58} including one that uses saccharine and acesulfame as carrier

molecules for CO delivery.⁵⁹ Among the large number of CO donors published, CORM-2, CORM-3, CORM-401, and CORM-A1 are probably the most well-known (Figure 1).^{20, 41, 60} Due to their commercial availability and ease of use, these four CORMs have been widely used as CO surrogates in a large number of studies examining the biological effects of CO.^{20, 61, 62} Combined, they had appeared in about 650 publications, based on a Pubmed search in January 2023. Recently, extensive CO-independent chemical reactivities for these molecules have been reported that could impact the interpretation of results from using these CORMs. Specifically, ruthenium-based molecules CORM-2 and CORM-3 have been shown to react with nucleophiles such as the thiol group on cysteine and the imidazole group in histidine and to have catalase-like, redox, and radical scavenging activity.⁶³⁻⁶⁷ Under near-physiological conditions, aqueous solutions of CORM-2 and CORM-3 have been shown to mostly produce CO₂ instead of CO, through an redox reaction.^{63, 64,}⁶⁸ Along a similar line, CORM-401 has been shown to react with reactive oxygen species (ROS) such as hydrogen peroxide and free radicals, which are commonly recognized as key mediators in CO's signaling actions.⁶³ Similarly, CO-independent biological activities have been reported by various studies.^{65-67, 69-71} Incidentally, some of these CORMs (CORM-2, CORM-3) have been used as the sole CO source in developing CO-sensing methods, leading to "CO probes" that fail to detect CO and only detect the CORM used.

In our own work of developing CO prodrugs for various applications, we were frequently asked to compare against a widely used CORM as a "positive control."⁵⁷ Therefore, we took an interest in examining CORM-2, CORM-3, CORM-401, and CORM-A1, which were considered as the "standard" positive controls. We have already conducted extensive studies of the first two (Figure 1). In the next two chapters, we examine CORM-A1 and CORM-401.

2.1.1 CORM-A1

Based on an earlier literature report of a borane-based compound capable of CO release in aqueous solutions, Motterlini and coworkers proposed its use as a CO surrogate for studying CO biology and pharmacology and named the compound CORM-A1.⁶⁰ The mechanism of CO release was described as decomposition upon protonation to liberate CO spontaneously via an unstable borane carbonyl intermediate (Scheme 1).⁶⁰ This mechanism is distinctly different from other metal-based CORMs such as CORM-2 and CORM-3, which dissociate CO through light irradiation or ligand substitution.^{41, 63, 64} Further, if BH_3 is an intermediate, it is expected to either release molecular hydrogen upon reaction with active protons or undergo reductions reactions with an “oxidizing partner,” though this was not part of the originally proposed mechanistic aspect. Due to its commercially availability, solubility in water, lack of a transition metal, and stated fast CO release rate ($t_{1/2}$, 2-21 min), CORM-A1 has been widely used in biological studies as a CO donor with the assumption that it is benign otherwise and donates near stoichiometric amounts of CO with the release half-life as indicated in the original report.^{60, 61, 72, 73}

A search of the term “CORM-A1” in Pubmed in January 2023 yielded 79 publications covering studies examining CO’s effects on autophagy, coagulation/platelet activation, non-alcoholic steatohepatitis, myocardial infarction, neuronal differentiation, blood-brain barrier dysfunction, cancer metastasis, autoimmune uveoretinitis, inflammation and fibrosis, and neonatal vascular injury, among many other indications. Such a broad range of activities and the large number of publications using CORM-A1 clearly indicate its broad impact in the CO field. However, among these four widely used CORMs, CORM-A1 is the least characterized in terms of CO release properties and chemical reactivity, despite the presence of a BH_3 moiety, which is known to be chemically reactive. Further, reports of CO-independent biological activity are emerging.

Therefore, we took an interest in examining the chemical reactivity of CORM-A1 and its CO production characteristics under various conditions. To us, a viable CO surrogate for studying CO biology and pharmacology should meet three basic criteria. First, the “surrogate” should not have pronounced chemical reactivity toward biomolecules commonly seen in cellular functions or *in vivo*. Second, there is a good negative control of the “carrier” portion of the delivery system; in the case of a CORM, the CO-depleted product (referred to as iCORM) is commonly considered as the most acceptable negative control. Lastly, and probably most importantly: it should be able to reproducibly generate near stoichiometric amount of CO under near physiological conditions with well-defined kinetics and well-established release profiles. Further, factors that could affect the CO release yield and kinetics should be well understood within the confines of commonly-encountered variations in lab experiments and *in vivo*. Herein, we describe our work in examining CORM-A1 along these three lines, starting with the examination of chemical reactivities because these properties directly impact both CO yields and the analysis of the issue of a negative control (Figure 1).

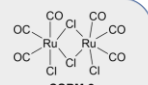
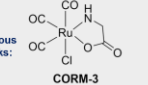
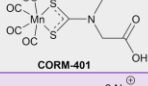
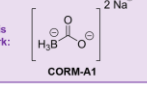
	Variable or lack of CO production	CO-Independent Chemical Reactivity	CO-Independent Biological Activity
<div> <div>  <p>CORM-2</p> </div> <div> <p>Previous Works:</p>  <p>CORM-3</p> </div> <div>  <p>CORM-401</p> </div> </div>	<div>✓</div> <div>✓</div> <div>✓</div>	<div>✓</div> <div>✓</div> <div>✓</div>	<div>✓</div> <div>✓</div> <div>?</div>
<div> <p>This Work:</p>  <p>CORM-A1</p> </div>	<div>✓</div>	<div>✓</div>	<div>?</div>

Figure 2-1. (Blue) Structures of CORM-2, CORM-3, and CORM-401 and brief overview of their reported CO-independent biological and chemical reactivities and (Purple) structure of CORM-A1 and an overview of the work presented here.

2.2 Results and Discussion

2.2.1 Criterion I. The chemical reactivity of CORM-A1 towards biorelevant molecules

CORM-A1 is a complex of borane, which is a textbook case of a common reducing agent for a wide range of functional groups and molecules. Though, the presence of a borane moiety in CORM-A1 is strongly indicative of its reducing power and suggests the need to carefully examine this issue, it is not readily predictable, at least not conclusively, as to whether this specific complex would be reactive enough to pose a reactivity issue in solution and in biological milieu. Earlier, we have reported the ability for CORM-A1 to react and consume H_2O_2 and free radicals, which are very important in redox signalling of CO.⁶³ Therefore, initial indications are that the direct reactivity of CORM-A1 could pose a challenge to the examination of CO's roles in various redox signalling processes when it is used as a CO surrogate. In this study, we are interested in examining the direct reaction of CORM-A1 with biomolecules important to cellular functions. Among the different possibilities, we chose to study the effect of CORM-A1 on NAD^+ and NADP^+ , because of their widely recognized roles in essential cellular processes (Fig 2). Further, changes in the concentration of NAD^+ and the ratio of NAD^+/NADH have been specifically implicated in CO's roles in regulating platelet activation and energy metabolism.^{61, 62} Again, CORM-A1 has structural similarity with other BH_3 complexes and borohydride reagents such as sodium borohydride and sodium cyanoborohydride, which are known to reduce *N*-methylated nicotinamides.^{74, 75} Therefore, it is important to study the reactivity issue of CORM-A1 in redox processes either to eliminate such reactivity as a confounding factor in result interpretation or to raise caution in using CORM-A1 as a pure "CO surrogate." In doing so, we focused on three key aspects as shown in Fig 2. First, is there significant chemical reactivity between CORM-A1 and NAD^+ or NADP^+ respectively? If so, is it the borane moiety that is responsible for the observed reduction? Secondly,

does the CO-depleted product (commonly referred to as iCORM) serve as an adequate control based on chemical reactivity? Boric acid is sometimes used as a negative control for CORM-A1. Is it an adequate control based on chemical reactivity? Thirdly, does the reaction between CORM-A1 and NAD^+ or NADP^+ have any impact on the CO-releasing property of CORM-A1? Below we describe our findings and analyses.

CORM-A1 reduces NAD^+ to NADH and NADP^+ to NADPH: First, the reaction of CORM-A1 and NAD^+ was analyzed using UV-Vis by taking advantage of the lack of absorbance for NAD^+ at 340 nm, where there is an intense peak for NADH.⁷⁶ We conducted the experiments at μM to low mM concentrations, since cellular NAD^+ concentrations range between approximately 0.2-0.5 mM.⁷⁷ Specifically, when NAD^+ and CORM-A1 (2 mM each) were incubated in 10 mM PBS at 37 °C for 15 minutes, time-dependent increase of the peak corresponding to NADH (340 nm) was observed. Fig 3 shows a representative set of UV spectra. Further, the observed spectral changes are also dependent on the concentration and relative ratio between CORM-A1 and NAD^+ . In order to quantitatively assess the yield of NADH, a standard curve of absorptions of NADH ($\lambda_{\text{max}} = 340$ nm) was established (Fig. S1A). For the reaction between 2 mM NAD^+ with 2 mM CORM-A1, 1.4 mM NADH was formed at the 15-min point (70%, marked by a red dash line) and 1.75 mM (88%) was formed at the 30-minute point (Fig 3).

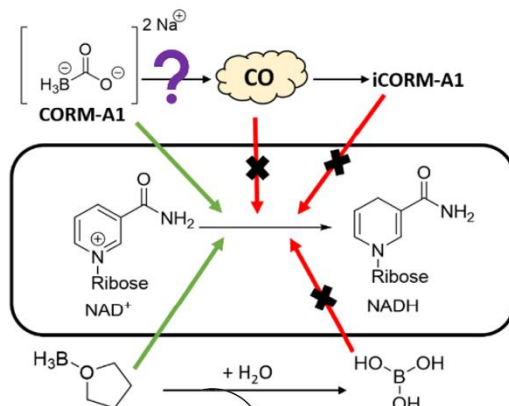
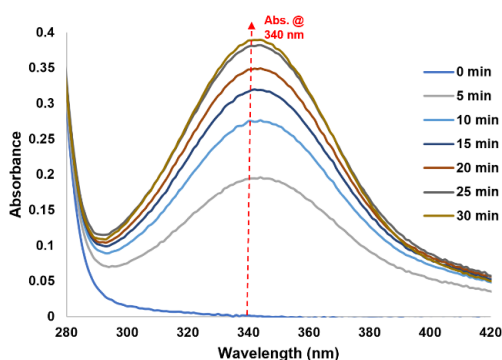


Figure 2-2. Investigation of NAD^+ reduction by CORM-A1

When CORM-A1 was used in excess (11:1, 2.2 mM CORM-A1: 200 μ M NAD^+), about 200 μ M NADH was formed after 15 min (Fig. 4), indicating 100% completion (Fig 4). These results confirmed the ability for CORM-A1 to chemically reduce NAD^+ in an aqueous solution. When an equal molar ratio was used at 200 μ M CORM-A1, a significant decrease in the rate was observed in comparison to the reaction at 2 mM CORM-A1. These expected concentration-dependent changes in reaction rate are consistent with the biomolecular nature of the reaction. Consequently, only when CORM-A1 was in a ≥ 10 -fold molar ratio, complete reaction was observed within 15



minutes.

Figure 2-3. Reaction kinetics of 2 mM NAD^+ with CORM-A1 (1:1, 2 mM) incubated at 37 °C for 30 minutes monitored using UV-Vis.

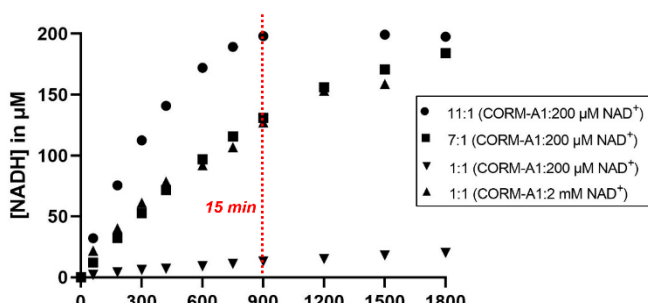


Figure 2-4. Kinetic studies of reaction of NAD^+ with different concentrations of CORM-A1 (1:1, 2 mM or 200 μ M; 7:1 1.4 mM; 11:1 2.2 mM). The 1:1 reaction (2 mM CORM-A1: 2 mM NAD^+) was incubated at in PBS at 37 °C. At each time point, the reaction was either conducted at or diluted by 10-fold to 200 μ M for UV measurements. Other reactions were conducted at 200 μ M (NAD^+) for UV-Vis detection. Reactions were monitored using UV-Vis at 340 nm.

The conversion of NAD^+ to NADH was further confirmed with LC-MS/MS (Fig. S4-S18). Specifically, LC-MS/MS results indicated complete reduction of NAD^+ to NADH within 15 minutes at 10:1 CORM-A1: NAD^+ ratio and 30 minutes at 1:1 CORM-A1: NAD^+ ratio, corroborating findings of the UV-Vis experiments. When reactions were conducted at 37 °C in unbuffered water (pH 5.5), LC-MS/MS studies (Figures S4-S18) confirmed NADH formation and showed an increase in NADH/ NAD^+ ratio. Using an equivalent molar ratio (1:1) of CORM-A1 and NAD^+ at 2 mM each, a 65-fold change in NADH/ NAD^+ ratio was observed within 30 minutes (Fig. 5A). When the molar ratio of CORM-A1: NAD^+ was increased to 10:1, NAD^+ was completely consumed within 15 minute and NADH/ NAD^+ ratio increased by 260-fold (Fig. 5B). These results are consistent with observations in the UV-Vis experiments and confirm the ability for CORM-A1 to quantitatively reduce NAD^+ to NADH in a pure chemical reaction.

Similar studies were conducted to evaluate the reaction between NADP^+ and CORM-A1. It was found that CORM-A1 was able to reduce NADP^+ to NADPH, in a similar fashion as the reduction of NAD^+ . In one example, reaction between 1 mM CORM-A1 and 100 μM NADP^+ in PBS at 37 °C (Fig 6) led to the formation of 78 μM of NADPH within 60 minutes. At the same time point, lower concentrations of CORM-A1 at 350 μM and 100 μM led to the formation of 40 μM and 10 μM of NADPH, respectively. Combined, the results presented suggest that CORM-A1 has the chemical reactivity to play a significant role in affecting the concentrations of two biological cofactors (NAD^+ and NADP^+), which are important for biochemical processes such as glycolysis and the pentose phosphate pathway.

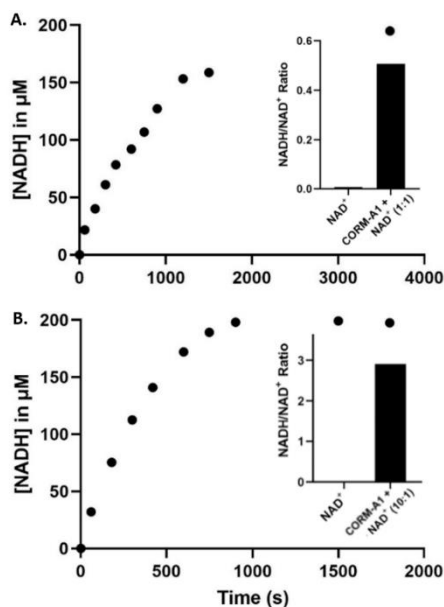


Figure 2-5. **A:** Reaction of 2 mM NAD^+ with CORM-A1 (1:1, 2 mM) incubated at 37 °C for 30 minutes. Reactions monitored and AUC determined using LC-MS/MS (right) and UV-Vis (left). **B:** Reaction of 1 mM NAD^+ with CORM-A1 (10:1, 10 mM) incubated at 37 °C for 15 minutes. Formation of NADH (μM) over 30 minutes by reaction of 200 μM NAD^+ and CORM-A1 (11:1, 2.2 mM) monitored by LC-MS/MS (right) and UV-Vis (left), quantification done using AUC. Ratios are calculated using the average AUC from duplication experiments.

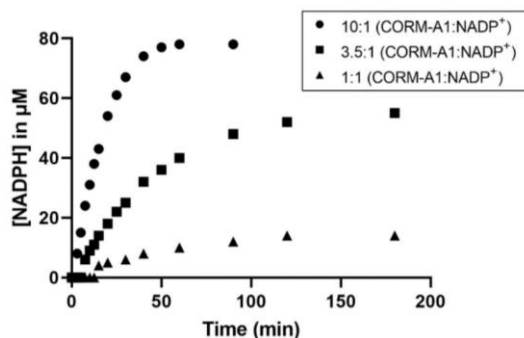


Figure 2-6. Kinetic studies of reaction of NADP^+ with CORM-A1 at different concentrations and ratios (1:1, 100 μM ; 3.5:1 350 μM ; 10:1 1 mM). Reactions were conducted at 100 μM NADP^+ . NADPH generation was monitored by UV-Vis absorbance at 340 nm.

We also conducted ^{11}B -NMR experiments to monitor the consumption of the BH_3 moiety in CORM-A1 by NAD^+ in D_2O . In the presence of 33.3 mM NAD^+ , a significant decrease in intensity of the borane peaks was seen within 10 minutes. When the same reaction was tested at 30 minutes, no further change in peak intensity was observed, indicating fast reaction. When an additional 66.6

mM of NAD^+ was added to the reaction, giving a final reaction of 1:1 CORM-A1: NAD^+ , the borane peaks disappeared within 10 minutes. These results further support a direct reaction between NAD^+ and the borane moiety on CORM-A1 (Fig. S19).

The chemical reactivities of CORM-A1 observed are in general agreement with basic organic chemistry and the known reactivity of borohydride and borane reagents such as cyanoborohydride. This newly observed chemical reactivity of CORM-A1 needs to be taken into consideration when CORM-A1 is used for studying the effect of CO. It should be noted that there have been some specific examples, in which $\text{NAD(P)}^+/\text{NAD(P)H}$ were reported to be involved in the biological functions of CO. In one set of studies, the platelet inhibition effects of CORM-A1 were proposed to be through conversion of NAD^+ to NADH .^{61, 62} In another study, the role of CORM-A1 was proposed to regulate the concentrations of biological co-factors, such as NADP^+ . For CORM-A1's ability to improve neuronal differentiation through increasing GSH levels, an earlier report suggested the pathway involving enhanced generation of NADPH .⁷³ The newly established chemical reactivity of CORM-A1 toward NADP^+ and NAD^+ suggests the likely need to re-evaluate the functions of CO and its mechanism(s) of action by taking into consideration of the redox properties of CORM-A1. However, it is understood that the cellular environment is much more complex than solution-phase chemistry. Therefore, factors beyond the reactivity of CORM-A1 in solution-phase may need to be considered in any re-evaluation efforts. In any case, there is a high degree of certainty that the chemical reactivity of CORM-A1 is a strong confounding factor to consider in result interpretations.

2.2.2 Criterion II. Assessment of commonly used negative controls: iCORM-A1

iCORM-A1 does not serve as an adequate negative control for the reducing ability of CORM-A1. In addressing the implications of the newly established chemical reactivity of CORM-

A1 in its use in studying CO biology, one key question is whether there are adequate negative controls to allow for examination of only CO-dependent effects. One commonly used “negative control” is “CO-depleted” CORM-A1 (inactivated CORM or iCORM). In this context, we would like to note that it is nearly impossible to have a “perfect” negative control of a prodrug of almost any active agent. Thus, when we look at the “negative control” issue, we bear this in mind and only examine truly significant issues that have a high likelihood of significantly complicating result interpretation, not mere minor or remote possibilities. As such, there are many ways of looking at this issue. In this study, we only examine the negative control issue in the context of chemical reactivity, specifically, the chemical reactivity of the iCORM preparations towards NAD(P)^+ . It should be noted that several recent publications have already revealed complications in using various iCORMs to properly control for the reactivity of the donor itself.^{41, 60, 64, 66, 78} Typically, iCORM-A1 is prepared by adding 0.1 M HCl to a stock solution of CORM-A1 and then bubbling the solution with N_2 gas to remove any residual CO. In doing so, it is assumed that CORM-A1 is converted to sodium borate and/or boric acid in equilibrium, depending on the pH.⁶⁰ This assumption is certainly in agreement with what one would expect based on borane chemistry.⁷⁹ The borane moiety present in the structure of CORM-A1, as well as the previously published mechanism of CO release, permits the assumption that the by-product is boric acid, given that borane, the only remaining component after CO release, produces boric acid and hydrogen gas when in aqueous solution.⁸⁰ The production of boric acid from borane in aqueous solution is an intrinsic redox reaction. Based on the CO release mechanism in Scheme 1, it is reasonable that the transformation from CORM-A1 to iCORM-A1 is analogous to this redox reaction. Therefore, we studied the reactivity of the same iCORM-A1 preparation, with NAD^+ using UV-Vis and found no indication that iCORM-A1 was able to reduce NAD^+ in the same

fashion as CORM-A1 (Fig. 7B).⁶⁰ Agreeing with UV-Vis data of iCORM-A1, LC-MS and UV-Vis studies also showed that boric acid had no effect on NAD^+ depletion (Fig. 7A, 7B). Overall, it is clear that CORM-A1 participates in a CO-independent redox reaction with NAD^+ , which cannot be achieved with iCORM-A1 or boric acid. Therefore, these results suggest that iCORM-A1 and boric acid are not proper negative controls for the redox properties of CORM-A1 in its use as a CO donor, at least in the context of their chemical reactivity.

Other controls for CORM-A1.

CO gas. Chemically, one would unambiguously expect CO to be inert toward NAD^+ . For the sake of thoroughness, we further confirmed this aspect using data. Thus, 1 mM NAD^+ was incubated with an excess amount of pure CO gas (2 mL, approximately 90 μmol of CO) in a 1 mL HPLC vial at 37 °C for 15 minutes. LC-MS studies of this reaction mixture indicated no change to this solution that could suggest a reduction of NAD^+ (Fig 7A), as one would expect.

Borane-based compounds. The direct chemical reduction of NAD^+ and NADP^+ by CORM-A1, along with the lack of redox reactivity seen with iCORM-A1 and boric acid, suggests the complexed borane being the reducing agent. As discussed earlier, borane is a textbook case of a strong reducing agent, especially when complexed with a Lewis base.^{81, 82} Examples include BH_3 -ether, BH_3 -THF, and sodium cyanoborohydride, which is known to reduce NAD^+ .^{74, 75, 83} For comparison, we conducted additional studies of NAD^+ reduction by NaBH_4 and BH_3 -THF using UV-Vis and LC-MS, respectively. The reaction between BH_3 -THF and NAD^+ (10:1) in 5% water in THF solution similarly led to a significantly reduced level of NAD^+ with the concomitant formation of NADH. At the 15-min point, the ratio of NADH/NAD^+ increased to 1.33 from the initial 0.026 (Fig 7A). Using UV-Vis, the reaction between NaBH_4 and CORM-A1 was probed. When incubated for 15 minutes at a 10:1 molar ratio, 10 mM NaBH_4 led to the formation of 440

μM NADH from 1 mM NAD^+ , suggesting a weaker reducing ability as compared to CORM-A1 (Fig. 7B). The decreased level of reduction may be due to a slower reaction rate or increased hydrolysis of NaBH_4 . Collectively, these results are consistent with the borane moiety on CORM-A1 being a strong reducing agent, analogous to other BH_3 complexes. In summary, CORM-A1 has redox activity that is independent of gaseous CO and is not properly controlled with iCORM-A1 or boric acid (Fig 2).

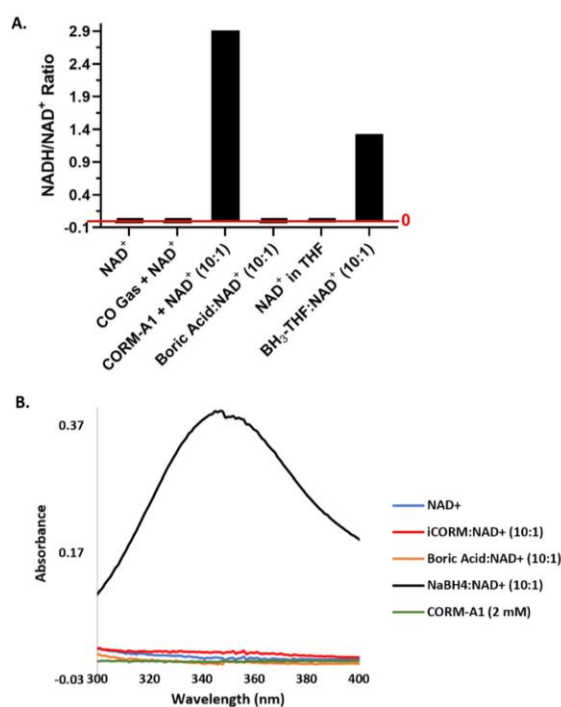


Figure 2-7. Reactions of NAD^+ with CO gas, CORM-A1 and other relevant boron species. A. Reactions of 1 mM NAD^+ with CO gas (2 mL), CORM-A1 (10:1, 10 mM), boric acid (10:1, 10 mM), or BH_3 -THF (10:1, 10 mM) at 37 °C for 15 minutes. Reactions monitored and AUC determined using LC-MS/MS. Ratios are calculated using the average AUC from duplication experiments. B. Reaction of 1 mM NAD^+ with iCORM-A1 (10:1, 10 mM), boric acid

(10:1, 10 mM) and NaBH_4 (10:1, 10 mM). Unreacted CORM-A1 (2mM) provided as a control.

Reactions were diluted to 200 μM after 15 minutes for UV-vis measurements.

2.2.3 Criterion III: The ability for CORM-A1 to generate CO in a reproducible and reliable fashion: CO production under various conditions

The entire premise of using CORM-A1 as a CO donor or surrogate for studying CO biology is predicated on its presumed ability to donate an adequate amount of CO in a reproducible and controllable fashion. Along this line, there have been studies of CO release yield and kinetics from CORM-A1 using the myoglobin assay. In doing so, sodium dithionite is used to keep myoglobin in the reduced form, which scavenges CO in solution, leading to spectroscopic changes. Using such a method, CORM-A1 was reported to show pH- and temperature-dependent CO release, with a half-life of 2.5 minutes and 21 minutes at 37 °C when incubated at pH 5.5 and pH 7.4, respectively.⁶⁰ Given the redox activity of CORM-A1 (described above), we were interested in using an GC quantification method to examine CO release to avoid introducing additional factors in CO detection. Specifically, without the need to add sodium dithionite (used in the myoglobin assay), the possible chemical interactions between two redox-active species in dithionite and CORM-A1 is eliminated. It should be noted that Klein and co-workers reported pH-dependent CO release of up to 0.91 ± 0.09 mole of CO liberated per mole of CORM-A1 using gas-phase vibrational spectroscopy.⁸⁴ When incubated at 27.5 °C and pH 7.4, Klein and co-workers determined the half-life of CORM-A1 being 106 minutes for the formation of the borane carbonyl intermediate, suggesting an overall half-life of about 2 hours. The authors suggested this half-life as being comparable to previous reports due to the slight difference in pH and temperature.

Aimed at probing the effect of temperature and pH, we incubated CORM-A1 in 100 mM PBS at both 37 °C and room temperature and did not observe significant changes in the rate of CO production. At 37 °C, the CO yield was 15% in the first 15 minutes and 60% within 24 hours (Table 2, Entry 3). In contrast, 13% CO was generated in the first 15 minutes and 54% within 24 hours at room temperature (Table S1, Entry S1). These results, along with the results reported by Klein and co-workers, suggest that CO production from CORM-A1 does not have the kind of temperature-dependence to account for the reaction half-life difference between the original report and that of Klein and co-workers. Although FTIR of the gas headspace removes the complications of additional reagents (i.e., dithionite), this is an indirect method of quantification of CO involving a fit line calculated from a sum of CO concentration and intermediate H_3BCO concentration.⁸⁴ Given the various numbers in the literature under different conditions, we feel the need to use the gold-standard method, GC, to conclusively assess CO release from CORM-A1. Therefore, we conducted quantitative analysis of CO release of CORM-A1 under near physiological condition in both unbuffered water (pH = 5.5) and PBS (pH = 7.4) by using a methanizer coupled GC-FID, which is much more sensitive than the GC-TCD method and ensures the detection of CO at sub-ppm level.

In examining the ability for CORM-A1 to release CO, there are aspects that need to be characterized. First, we are interested in studying CO release from CORM-A1 in water, as it has been reported to be stable in water, as well as the effect of buffer.²⁰ We are also interested in the pH effect on CO release in pure water, as the somewhat basic nature of the CORM-A1 was stated to be the reason for its stability in water. Second, we are interested in how CORM-A1's reducing capability of NAD^+ and NADP^+ may affect CO production. Third, we are interested in probing other factors that could play a role in affecting CO release from CORM-A1, including its redox

activity, the presence of organic and inorganic ions, oxidants, and commonly used reagents and media commonly used in experiments to study CO's biology.

2.2.3.1 Criterion III, Assessment 1. CO production in unbuffered water and buffered solutions

CO production in water and pH effect. CORM-A1 was reported to be stable in water due to its basic nature, ultimately changing the pH of the solution to around pH 11.²⁰ To our knowledge, there are no concentration information reported or in-depth stability studies of CORM-A1 in aqueous solution. As the conjugate base of a weak acid, we expect the pH of the solution to be dependent on the concentration of CORM-A1. Therefore, we prepared CORM-A1 solutions at 20 μ M, 100 μ M, 500 μ M, 1 mM, 10 mM, and 100 mM. Indeed, the pH values of these solutions were determined to be 5.5, 6.0, 6.5, 7.5, 9.0 and 9.5, respectively. As expected, the pH depends on the concentration of CORM-A1; such results are different from the common belief that CORM-A1 solution is basic. Apparently, CORM-A1 is a weak base and can bring the pH to 9.5 only at a high concentration. At low concentrations (e.g., 20 μ M), the pH remains about the same as the water used (pH 5.5). Further, these solutions of CORM-A1 in unbuffered water showed initial CO release of $\leq 2\%$ at the 15-min point regardless of the final pH (Table 1). Especially surprising was the low CO yield of the solution at pH 5.5, which was reported to allow for CO release with a $t_{1/2}$ of 2.5 min in buffer with a similarly adjusted pH.⁶⁰ Such results suggest that low pH (e.g., 5.5) does not automatically lead to rapid CO release and CORM-A1 stability in aqueous solution is not exclusively pH-dependent.

Table 2-1. CO production of CORM-A1 in unbuffered water ($n = 3$)

Entry	[CORM-A1]	Initial CO Yield % (15 min)	Total CO Yield % (20+ h)	Final pH
1	20 μ M	1 ± 0.4	24 ± 6.5	5.5
2	100 μ M	2 ± 1.4	24 ± 7.3	6.0
3	500 μ M	0.7 ± 0.2	24 ± 3.6	6.5
4	1 mM	0.5 ± 0.2	25 ± 4.0	7.5
5	10 mM	0.6 ± 0.2	33 ± 2.4	9.0
6	100 mM	0.4 ± 0.2	23 ± 3.5	9.5

Effect of Buffer. As previously discussed, CORM-A1 was reported to have a rapid CO release at low pH, something we did not observe in unbuffered water solutions. The sole difference between the data in Table 1 and the high CO release yield at low pH (5.5) reported by the literature was the use of buffer. Specifically, CORM-A1 was reported to release CO in buffered aqueous conditions such as PBS with a $t_{1/2}$ of 2.5 min at pH 5.5. Considering the low CO production yield in water regardless of pH (Table 1), we became interested in examining the effect of buffer by using PBS at different buffer strengths and CORM-A1 concentrations, respectively. First, different concentrations of CORM-A1 were tested in 100 mM PBS solution at 37 °C. In 100 mM PBS (pH 7.4), CORM-A1 at 10 mM was found to release CO with a 15% yield at the 15-min point (hereafter denoted as initial period) and a total of 60% after 20+ hours (Entry 3, Table 2). At 1 mM of CORM-A1, an average of 13% CO was released within the first 15 minutes and 71% overall CO yield after 20 h. At 100 μ M of CORM-A1, CO release of 3% and 45% was seen for the initial period and after 20 h, respectively (Entries 1-2, Table 2). These numbers are much higher than what was observed in the absence of a buffer. To further probe the instability of CORM-A1 in buffered aqueous solutions, CO release from CORM-A1 in different concentrations of PBS was tested. Commercially available PBS solutions of 1 \times (10 mM), 10 \times (100 mM), and 20 \times (200 mM) were used. As can be seen in Table 2, at 10 mM of PBS (1 \times), the initial CO yield from 10 mM CORM-

A1 was only 1%, followed by a total CO yield of 48% (Entry 4, Table 2). Higher concentrations of PBS (100 mM and 200 mM) showed initial CO yields of 15% and 18%, respectively (Entry 3 and 5, Table 2). However, the total CO yields after 20 h are in the range of 45-71% with lower yields observed at either a low CORM-A1 concentration (e.g., 100 μ M) or a low buffer concentration (e.g., 10 mM). The observed dependence of CO yield for the initial period on the concentration of the buffer and CORM-A1 suggests a bimolecular event involving the buffer components. The low yields and release rate from the experiments in water further support this notion. Overall, the initial CO release yield is low. Further, the overall results are substantially different from the literature report of $t_{1/2}$ of 21 min in PBS at neutral pH. Again, it is important to note that a reducing agent (sodium dithionite) was used in the experiments using the literature-described myoglobin assay. Sodium dithionite has been previously reported to interact with other CORMs to promote CO production. Thus, the conditions we used by assessing gas production directly are different from that of the original report via an indirect method for measuring gas production using myoglobin in the presence of dithionite.

Table 2-2. Effect of Buffer on CO Production from CORM-A1 (n = 3)

Entry	[CORM-A1]	Solvent	Initial CO Yield % (15 min)	Total CO Yield % (20+ h)
1	0.1 mM	100 mM PBS	3.0 ± 0.7	45 ± 10.5
2	1 mM	100 mM PBS	13 ± 5.0	71 ± 1.9
3	10 mM	100 mM PBS	15 ± 5.5	60 ± 3.6
4	10 mM	10 mM PBS	1.0 ± 0.15	48 ± 5
5	10 mM	200 mM PBS	18 ± 2	57 ± 10.3

2.2.3.2 Criterion III, Assessment 2. The effect of CORM-A1's redox activity with NAD^+ and NADP^+ on CO production

NAD^+ and NADP^+ accelerate CO release from CORM-A1 in PBS. Solutions containing an equal molar ratio of NAD^+ showed a higher initial CO yield in 100 mM PBS by about two-fold, 35% at 10 mM and 21% at 1 mM within 15 minutes (Entry 2, Table 3 and Entry 4, Table 4) than in the absence of NAD^+ . To further examine this issue, we also studied the effects of excess NAD^+ . Specifically, when 10 mM CORM-A1 was incubated with 30 mM NAD^+ in 100 mM PBS solution, initial CO yield of 55% was obtained (Entry 3, Table 3). Obviously, the presence of 3-fold excess of NAD^+ led to an approximately 3.5-fold increase in the initial CO yield over the reaction in solely PBS. However, the overall CO yield (20+ h) was comparable to solutions that did not contain NAD^+ . In a similar fashion to NAD^+ , equal molar equivalents of NADP^+ increased the CO release yield from 10 mM CORM-A1 with an initial CO yield of 49% and an overall CO yield of 58% (Entry 4, Table 3).

Table 2-3. Effect of different reagents on the CO production from 10 mM CORM-A1 in 100 mM PBS (n=3)

Entry	Added Reagent:	Initial CO Yield% (15 min)	Total CO Yield% (20+ h)
1	-	15 ± 5.5	60 ± 3.6
2	10 mM NAD^+	35 ± 9.8	64 ± 4
3	30 mM NAD^+	55 ± 5.7	60 ± 8.3
4	10 mM NADP^+	49 ± 2.9	58 ± 2.7

NAD^+ reverses CORM-A1's stability in water. As previously discussed, CORM-A1 is kinetically more stable in unbuffered water solutions than in PBS. With the demonstrated acceleration effect of NAD^+ on CO release in PBS, we became also interested in studying the effect of NAD^+ on the stability of CORM-A1 in unbuffered water and thus CO release from CORM-A1. The addition of NAD^+ had the same general effect in water as in PBS. For example, NAD^+ at 1

mM increased the initial CO release from CORM-A1 (1 mM) by 16-fold from 0.5% to 8% (Entry 1 and 3, Table 4). Such results highlight the interesting ability of NAD^+ to trigger CO release from CORM-A1 at a rate comparable to that in buffered solution. Such results further suggest that CO release from CORM-A1 is not solely pH-dependent. More mechanistic studies need to be done to probe the stability of CORM-A1 in aqueous solution.

Table 2-4. Effect of NAD^+ on the stability of 1 mM CORM-A1 in unbuffered water (n=3)

Entry	Solvent	Added Reagent:	Initial CO Yield % (15 min)	Total CO Yield % (20+ h)
1	Unbuffered Water	-	0.5 ± 0.2	25 ± 4.0
2	100 mM PBS	-	13 ± 5.0	71 ± 1.9
3	Unbuffered Water	1 mM NAD^+	8 ± 2.0	47 ± 8.3
4	100 mM PBS	1 mM NAD^+	21 ± 7.8	54 ± 4

2.2.3.3 Criterion III, Assessment 3. Probing other factors that impact CO production from

CORM-A1: the idiosyncratic nature of CO production

In an attempt to define a clear mechanism for CO production from CORM-A1 to account for the above observations, many different factors were probed. These factors were selected based on previously reported studies using CORM-A1 or relevance to the literature studies that give us reasons to examine their effects. Some of these factors include the effect of ions, the redox activity of CORM-A1, the presence of different oxidants including H_2O_2 , DMSO, DDQ, and sGC inhibitor, ODQ. We also examined CO production from CORM-A1, or lack thereof, in biological media. The studies discussed hereon reveal that the mechanism of CO release from CORM-A1 is difficult to define, following a seemingly idiosyncratic pattern. Along the same lines, these studies bring to light complications in studies using CORM-A1 as a CO surrogate to study CO's biology.

Effect of Ions. To examine the effects of various ions, other solutions containing similar anions and cations were tested. First, the CO production from 10 mM CORM-A1 in the presence

of 100 mM NaCl was tested to see whether it was the sodium cation in PBS that led to the rate enhancement. In the presence of NaCl in unbuffered water at pH 5.5, CORM-A1 produced negligible amounts of CO, 0.4% in the first 15 minutes, and 33% over the course of 20 hours (Entry 4, Table 5). These results are comparable to the CO production of CORM-A1 in unbuffered water solutions, suggesting no significant role for sodium cations (or chloride anions) in CO release from CORM-A1. Such results further suggest the important roles of phosphate, but not chloride. Second, the role of inorganic cations was further probed by testing CO production from 10 mM CORM-A1 in two concentrations of lithium phosphate buffer (25 mM and 100 mM) at pH 7.4. Both concentrations produced comparable initial CO yields of 16% and 18%, respectively, within 15 minutes (Entry 1 and 3, Table 5). These results are similar to the CO production from CORM-A1 in PBS, further suggesting the lack of a direct role for inorganic cations. On the other hand, the presence of phosphate anions seems beneficial to the production of CO from CORM-A1. Along the same line, in the presence of NAD^+ , the CO yield from 10 mM CORM-A1 in 25 mM lithium phosphate buffer was 51% in the first 15 minutes, a significant increase in comparison to PBS solutions containing the same concentrations of CORM-A1 and NAD^+ (Entry 2, Table 5). Because NAD^+ also has a pyrophosphate group (Figure 8), we cannot readily conclude whether the CO release rate was due to the cation, the anion, the redox reaction, or a combination of three. Due to CORM-A1's ability to reduce the nicotinamide moiety (an organic cation), additional organic cations were tested (Figure 8). Neither the presence of 10 mM methylated pyridine nor 10 mM methylated DABCO in 100 mM PBS enhanced the CO production from 10 mM CORM-A1, giving initial CO yields of 12% and 15% in 15 minutes, respectively (Entries 5-6, Table 5). These results suggest that NAD^+ being an organic cation is unlikely to be what triggers the accelerated CO release. Then, we reasoned that the role of NAD^+ is likely through its reduction by CORM-A1, as

further discussed in the next section. In summary, organic anions, but not organic or inorganic cations seem to play a role in the CO production from CORM-A1.

Table 2-5. Effect of different ions on CO production from 10 mM CORM-A1 (n=3)

Entry	Solvent	Added Reagent:	Initial CO Yield% (15 min)	Total CO Yield% (20+ h)
1	25 mM Lithium Phosphate Buffer	-	16 ± 1.1	51 ± 12.4
2	25 mM Lithium Phosphate Buffer	10 mM NAD ⁺	51 ± 5.5	68 ± 7.5
3	100 mM Lithium Phosphate Buffer	-	18 ± 0.7	55 ± 1.1
4	100 mM NaCl	-	0.4 ± 0.0	33 ± 7.1
5	100 mM PBS	10 mM <i>N</i> -methylpyridine	12 ± 4.9	47 ± 4
6	100 mM PBS	10 mM <i>N</i> -methyl DABCO	15 ± 1.2	47 ± 5.7

Redox Activity Promotes CO Production. To broaden the chemical reactivity studies, we also examined the reaction with the *N*-methylnicotinamide moiety (Figure 8), which is present in both NAD⁺ and NADP⁺ and is the redox center of these two co-factors. Specifically, reaction between 10 mM *l*-methylnicotinamide and 10 mM CORM-A1 led to an initial CO release yield of 32% (Entry 2, Table 6). Similar to NAD⁺ and NADP⁺, CORM-A1 reduced *l*-methylnicotinamide in the same manner as NaBH₄, further supporting the reduction of the nicotinamide moiety on NAD⁺ and NADP⁺ by CORM-A1 being responsible for its acceleration in CO release (Fig. S3). The role of CORM-A1's reducing capability in accelerating CO release was investigated using NADH, which is already reduced. The addition of NADH (10 mM) to CORM-A1 (10 mM) led to a 13% yield of CO release in the first 15 min, which is comparable to buffer alone (Entry 1, Table 6). These results suggest that the reduction of the methylated nicotinamide moiety on NAD⁺ and NADP⁺ by CORM-A1 facilitates its CO release. Since methylated pyridine did not enhance CO production, it is possible that the electron-withdrawing nature of the amide group on nicotinamide could play a role in the ease of its reduction, which facilitates CO release.

Further, borane has long been shown to coordinate to carbonyl oxygens to promote reduction reactions. Therefore, these results also suggest the possibility of coordination of a boron species to the carbonyl oxygen on the nicotinamide of NAD^+ , leading to accelerated NAD^+ reduction to NADH and CO release.⁸³ Further the phosphate group of NAD(P)^+ might also play a role in the same way as phosphate buffer.

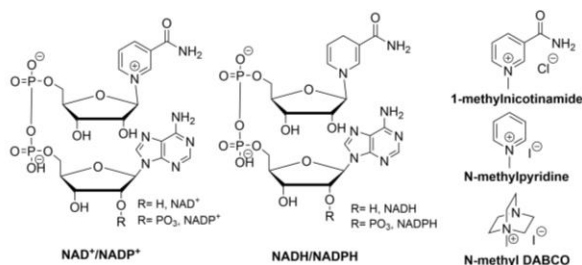


Figure 2-8. Structures of $\text{NAD}^+/\text{NADP}^+$, NADH/NADPH , 1-methylnicotinamide, N-methylpyridine, and N-methyl DABCO

Table 2-6. Effect of nicotinamide variations on the CO production from 10 mM CORM-A1 in 100 mM PBS. ($n=3$)

Entry	Added Reagent:	Initial CO Yield% (15 min)	Total CO Yield% (20+ h)
1	10 mM NADH	13 ± 5.3	49 ± 3.9
2	10 mM 1-methylnicotinamide	32 ± 8.8	51 ± 9

Oxidants alter CO Production. The ability to accelerate CO release from CORM-A1 through reduction of NAD^+ begs the question as to whether oxidation of the BH_3 moiety would lead to CO release. Therefore, the effect of a few different types of relevant oxidants were examined. This section discusses this and a few other factors.

DMSO inhibits CO production from CORM-A1. First, CO production from CORM-A1 in DMSO, an oxidant and commonly used solvent, was absent. At first, it seemed that CORM-A1 was stable in DMSO, but further experiments showed that stock solutions of CORM-A1 in DMSO failed to produce CO when diluted in 100 mM PBS (Entry 1, Table 7). We recognize that biological

studies often use a very small amounts of DMSO in PBS, with an acceptable level often being about 0.1-0.5% DMSO. Therefore, CO release from CORM-A1 in 0.5%DMSO/PBS solutions was also probed (Entry 2, Table 7). CO production from 1 mM CORM-A1 in 0.5% DMSO/PBS solutions was diminished in comparison to 1 mM CORM-A1 in just PBS solutions (10 mM) with an initial CO yield of 2% and total CO yield of 42%. These results suggest that CORM-A1 has some chemical reactivity with DMSO that diminishes or completely inhibits its CO production. Surprisingly, when a different organic oxidant, DDQ, was included in DMSO-only solutions, this inhibition was slightly ameliorated, increasing the CO release from 0% to 18% in the first 15 minutes and 2% to 26% within 24 hours (Entry 3, Table 7).

sGC inhibitor, ODQ, alters CO production from CORM-A1. The therapeutic role of CO gas is often studied in the context of its ability to activate soluble guanylate cyclase (sGC).⁸⁵ To such an effect, many of the biological studies using CORMs also include studies with a sGC inhibitor, ODQ.^{62, 86, 87} ODQ is not soluble in aqueous solutions and must be administered using a mixed solvent of DMSO/PBS. CORM-A1 is readily soluble in aqueous solution, so its CO production in DMSO has not yet been discussed in literature to our knowledge. When 100 μ M CORM-A1 was incubated with 10 μ M ODQ in DMSO, significantly increased CO production was observed in the first 15 minutes (14%) as compared to unbuffered water and in DMSO. Such results are similar to the addition of DDQ as described earlier. However, the overall production at 24 hour-point was still only 20% (Entry 4, Table 7). Although DMSO was not used as a solvent for CORM-A1, the change in CO production in the presence of ODQ suggests chemical reactivity between ODQ and CORM-A1. The mechanistic aspects of the reaction need to be further investigated, but ultimately the results suggest that the presence of CORM-A1 may impact biological results involving ODQ.

Furthermore, these results convolute the role of oxidants in the CO release mechanism of CORM-A1.

Table 2-7. CO production from CORM-A1 in the presence of different DMSO solutions and oxidants (n=3)

Entry	[CORM-A1]	Solvent	Added Reagent (Oxidant):	Initial CO Yield % (15 min)	Total CO Yield % (20+ h)
1	10 mM	DMSO	-	0 ± 0.1	2 ± 1.0
2	1 mM	0.5% DMSO/PBS	-	2 ± 0.4	42 ± 2.6
3	10 mM	DMSO	10 mM DDQ	18 ± 4.5	26 ± 3.3
4	100 μ M	DMSO	10 μ M ODQ	14 ± 5.5	20 ± 4.3

H₂O₂ diminishes CO release from CORM-A1. The unclear role of oxidants brings concerns in the interaction between commonly used redox reagents in CORM-A1 experiments studying CO's biology. Therefore, we probed CO production from CORM-A1 in the presence of H₂O₂, a commonly used reagent to induce oxidative stress. Incidentally, H₂O₂ is also well-established in textbook hydroboration reactions to oxidizes the -BH₂ moiety, after its reduction of an alkene. Our lab has previously reported that 100 μ M CORM-A1 degrades 300 μ M H₂O₂ in a non-catalytic manner.⁶³ Due to CORM-A1's ability to degrade H₂O₂ in a non-catalytic manner, one can assume a stoichiometric redox process involving relevant structural moiety of CORM-A1, similar to its reaction with NAD⁺. The previously reported reaction was further investigated in the context of CO release in H₂O₂/PBS solutions. In the presence of 300 μ M H₂O₂, 100 μ M of CORM-A1 had an initial CO yield of <1% and a total CO yield of 2% after 20 h (Entry 3, Table 8). In the presence of lower concentrations of H₂O₂ (100 μ M), the CO release from 100 μ M CORM-A1 was still diminished with an initial yield of 2% and a total yield of 4% (Entry 2, Table 8). At higher concentrations of CORM-A1 (1 mM) in the presence of H₂O₂ (100 μ M), the initial CO release yield was 7%, which is slightly higher than that of the reaction in water (Entry 1, Table 8). Since

H₂O₂ is commonly used to induce oxidative stress in biological studies and is produced intracellularly under stress, these results also suggest difficulties in interpreting the results when CORM-A1 is used as a CO surrogate in biological studies. The ability for CORM-A1 to act as a reducing agent may introduce new mechanisms that could change the CO release rate and overall CO yield. Although, it is well-established in textbook hydroboration reactions that H₂O₂ oxidizes the -BH₂ moiety formed following reduction of an alkene by borane, further mechanistic studies are necessary to determine the different chemical interactions involving CORM-A1.

Table 2-8. Effect of H₂O₂ on CO production from CORM-A1 in 100 mM PBS (n=3)

Entry	[CORM-A1]	Added Reagent:	Initial CO Yield % (15 min)	Total CO Yield % (20+ h)
1	1 mM	100 μ M H ₂ O ₂	7 \pm 2.4	44 \pm 9.9
2	100 μ M	100 μ M H ₂ O ₂	2 \pm 0.4	4 \pm 1.2
3	100 μ M	300 μ M H ₂ O ₂	0.8 \pm 0.3	2 \pm 1.2

Biological Media. The preceding results suggest that the CO release from CORM-A1 is dependent on substrates and reagents present in solutions. Normal variations in intracellular concentrations of components such as NAD⁺, NADP⁺, metal ions, and peroxides may lead to substantial fluctuations of CO release rate and yield. As previously discussed, there are many emerging reports on the CO-independent effects of other CORMs in chemical and biological studies.^{63, 64, 66, 70, 71, 78} Finally, there was one last, incredibly important aspect to probe: CO production from CORM-A1 in biological media.

CO production from CORM-A1 is dependent on the biological media used. Naturally when examining the biology of CO, studies using CO surrogates are often conducted in biological media. The idiosyncratic nature of CO production from CORM-A1 in the studies in simple solvents, as discussed thus far, compelled a brief investigation into its CO production in biological media. In solutions of DMEM containing 10% FBS, 1 mM CORM-A1 released low yields of CO similar to

that in PBS solutions (~18% in the first 15 minutes and 44% within 24 hours) (Entry 1, Table 9). To our surprise, when incubated in RPMI1640 culture medium (without FBS) solutions, 1 mM CORM-A1 had significantly diminished CO production, 2% in the first 15 minutes and 41% within 24 hours (Entry 2, Table 9). The mechanistic underpinnings of why the starved media led decreased initial CO production compared to media containing FBS is difficult to probe without knowing the exact composition of FBS. Determination of all the mechanistic differences proves to be inconsequential, as these results further show that CORM-A1 has unreliable CO production that seems to follow intractable patterns. Such results present a convoluted picture for result interpretation. The new data described should further encourage researchers to consider various variables and uncertain chemical reactivities when using CORM-A1 as a CO donor for studying CO biology.

Table 2-9. CO production from CORM-A1 in different biological media (n=3)

Entry	[CORM-A1]	Media	Initial CO Yield % (15 min)	Total CO Yield % (20+ h)
1	1 mM	DMEM, 10% FBS	18 ± 2.9	44 ± 3.7
2	1 mM	RPMI1640 culture medium (without FBS)	2 ± 0.4	41 ± 1.1

2.2.4 Consideration on the viability of CORM-A1 as a CO surrogate

In this section, we summarily address these issues described in various section with the aim of synthesizing a cohesive set of characteristics of CORM-A1 for easy correlation with implications in its use as a “CO surrogate.” Table 10 summaries key findings for discussion. First, the newly found redox reactions of CORM-A1 with biologically important molecules such as NAD⁺ and NADP⁺ raise concerns of its biological effects way beyond CO alone, i.e., significant CO-independent effects. This is especially true considering the reported involvement of NAD(P)⁺ in CO-related signaling events. In addition, CORM-A1 had already been reported to scavenge ROS,

which are known mediators of CO-related signaling events. The complexity of the redox issues seems hard to untangle in interpreting the CO-dependent effects from CORM-A1. Further, there are many other redox-active species involved in cellular functions including reactive sulfur species (RSS), reactive nitrogen species (RNS), and reactive electrophiles such as aldehydes (e.g., glucose, pyridoxal/vitamin B₆, retinal, pyruvate, among many others), which could be subjected to borane-mediated redox reactions. All these factors combined seem to make the redox reaction issue almost intractably complex in separating the putative CO-mediated biological response of CORM-A1 from that of chemical reactions. Second, there does not seem to be a viable negative control to cancel the effects of chemical reactivity from CORM-A1 in biological studies. The traditionally used iCORM-A1 is essentially boric acid/borate, an oxidized form of BH₃, which is devoid of the redox activity of BH₃ under normal physiological conditions.

A third point touches upon the most critical issue, i.e., whether CORM-A1 releases a sufficient amount of CO within a reasonable period of time reproducibly and reliably to qualify CORM-A1 as a CO donor for studying CO biology. At this point, we start with the issue of reproducibility and reliability and then come back to the points of “sufficient amount” and “within a reasonable period of time.” This is because a lack of reproducibility and reliability renders the issue of “sufficient amount” and “within a reasonable period of time” moot points in analyzing CO-dependent effects from CORM-A1.

Table 2-10. Summary of factors that alter CORM-A1 CO production

<u>Aspect Probed</u>	<u>Reagents Used</u>	<u>Effect on CO Production</u>
<i>Buffer/phosphate anions</i>	Phosphate buffered saline, lithium phosphate buffer	Concentration-dependent acceleration
<i>CO-independent redox activity</i>	NAD ⁺ , NADP ⁺ , NADH, 1-methylnicotinamide	Acceleration
<i>Oxidants</i>	H ₂ O ₂ , DMSO	Inhibition
<i>Oxidants in DMSO</i>	DDQ, ODQ	Reversal of inhibition; indicating chemical reactivity
<i>Cations (organic and inorganic)</i>	N-methyl pyridine, N-methyl DABCO, Na ⁺ (in PBS and NaCl) and Li ⁺ (in lithium phosphate buffer)	No effect
<i>Biological Media</i>	DMEM (10% FBS)	Acceleration (when compared to PBS)
<i>Biological Media</i>	RMPI (starved)	Decrease of initial CO production

On the issue of “reproducibility and reliability,” it is important to highlight the salient CO-release features already presented. It should be noted that for a volatile molecule such as CO, its release rate from a given donor is a critical factor to consider because of its rapid exchange with the environment and the known effects of release rate on its sustained concentration in solution.⁸⁸ The wide variability reported here implicates each future biological experiment to carefully determine CO release yields and kinetic profiles under the specific experimental conditions used before analyzing CO-dependent effects and dose-response relationship. The convoluted interplay of effects of various anions, cations, redox reactions, and biological media on CO release defies a unified mechanism for explanation and seems to be idiosyncratic. This level of perturbation of CO release yields by various factors make it extremely difficult to decipher CO-dependent effects when CORM-A1 is used as a CO donor. Further, the level of complexity of the intracellular environment and *in vivo* is guaranteed to be greater than the experimental conditions that we used in solution, which makes an intractable situation impossible to deconvolute. With the intractable nature of CO release, it is clear that using CORM-A1 as a CO donor in studying CO biology will

be faced with many CO-independent problems. At this time, it almost seems inconsequential whether we know the mechanism(s) of actions of all the perturbation factors because these factors all lead to intractable problems.

In addition to the issue of overall suitability for CORM-A1 to be used as a CO donor for studying its biology, there is another important experimental question to address. Earlier reports state CORM-A1 being stable in water. There needs to be an important conversation on the definition of stability and what “stable” means in the case of CORM-A1. This is especially important if a stock solution of CORM-A1 in water is used in experiments. In our opinion, the adjective “stable” carries little meaning if not defined with numbers within the context of specific conditions and/or factors. The following discussions summarize the data presented in this work and show the idiosyncratic nature of CO production from CORM-A1 and the lack of stability for CORM-A1 stock solution to be used after hours of storage. The stability data presented in the Criterion III, Assessment 1 section clearly indicate that such a broad-stroke statement of “stable” is incorrect. First, in the case of unbuffered water solutions, where CORM-A1 has been reported to be stable previously, it still releases up to 33% within a 24-hour period. This inconsistency could alter the true concentration of CO that is delivered from a degrading stock solution. Second, the addition of certain reagents such as NAD(P)^+ reverses CORM-A1’s stated stability in unbuffered water. Third, the data suggest that CORM-A1 releases CO in a concentration-dependent manner with regard to phosphate anion, a concept yet to be discussed with the stability of CORM-A1. Finally, CO production from CORM-A1 is easily altered, whether accelerated or diminished, in the presence of simple reagents commonly encountered in bioassays such as peroxide, inorganic cations, and anions. Furthermore, one can only assume that the complex differences that exist in

biological studies, in comparison to the simplicity of *in vitro* chemical reactivity studies, could only introduce more uncertainty in the use of CORM-A1 as an efficient CO donor.

Overall, the chemical reactivity and idiosyncratic nature of CO production from CORM-A1 in the presence of different substrates makes CORM-A1's role as a CO "surrogate" uncertain to say the least, as it fails to meet three basic criteria for a viable CO surrogate. There are already multiple reports on the CO-independent effects of other CORMs; therefore these results only further accentuate the complexities of chemical reactivity when using these chemically reactive CORMs with inadequate CO release under normal physiological conditions.^{63, 64, 66, 70, 71, 78} With the understanding of the complexities and differences between biological and chemical studies, we urge the need to consider these chemical aspects when evaluating controls in studies using CORM-A1. Finally, to truly understand the mechanism on how various factors affect CO release from CORM-A1, much more extensive work is needed. However, if CORM-A1 is not a suitable CO donor for biological applications, the emphasis is to avoid its usage, not on additional resources being expended on studying the in-depth mechanism.

An additional point related to the idiosyncratic nature of CO release from CORM-A1 is its unfortunate use as the recommended standard in calibrating a certain commercially available CO electrode. In our hand, the electrode was unable to produce consistent and reproducible data after calibrating using CO gas instead of CORM-A1. We urge caution in quantitative studies when using any electrodes that recommend CORM-A1 as the standard for calibration.

2.3 Conclusion

The results presented clearly demonstrate three key points. First, CORM-A1 does not reproducibly and reliably release an adequate amount of CO. Therefore, CORM-A1 fails the most basic test for it to be qualified as a CO surrogate in studying CO biology. Second, CORM-A1 has

extensive chemical reactivity, leading to intractable chemical reaction problems, which is bound to result in CO-independent effects and potentially serious side effects. Third, there is no adequate control available in using CORM-A1 as a CO surrogate. All these new findings do not affect the reliability of the biological results from CORM-A1 in the literature, but they do affect interpretation of the results in the context of CO-related activity.

In view of the different issues discovered with regard to the four most widely used CORMs: CORM-2, CORM-3, CORM-401, and CORM-A1, we would like to urge consideration of the following issues in future work in developing new CO donors for studying CO biology. First, the CO donors need to be devoid of significant chemical reactivity, especially if such reactivity is non-selective and hard to control (e.g., BH_3 and Ru complexes) . This is not a high bar, but very important. Second, CO release kinetics needs to be carefully defined under normal physiological conditions. Without a good understanding of the kinetics, CO concentration is hard to define at a given time even if the concentration of the donor molecule is known. Third, there needs to have at least one adequate control for the donor molecule. Another point of consideration is the release half-life of a donor molecule. Given the biological half-life of CO is 20 min in mice⁸⁹ and a few hours in humans,^{56, 90} a donor molecule with a release half-life much longer than CO's biological half-life is unlikely to lead to the delivery of a meaningful amount of CO.

2.4 Experimental

2.4.1 General Information

All reagents and solvents were of reagent grade from commercial suppliers (Sigma-Aldrich, etc.). Absorption spectra were measured and observed at 340 nm (NADH) and 260 nm (NAD^+) on Varian Cary 100 Bio UV–visible spectrophotometer (UV-Vis). Liquid chromatography–mass spectrometry (LC–MS/MS) data were collected on an API 3200

LC/MS/MS system, a triple quadrupole mass spectrometer coupled with an Agilent 1200 series HPLC and UV-DAD. Gas chromatography studies were performed on an Agilent 7820A system equipped with flame ionization detector (FID) coupled with a methanizer (CH4izer, Restek, USA). Column: Packed; 80/100 5A molecular sieve solid support, L \times I.D. 2m \times 0.53 mm (Restek). Carrier gas: Helium (Airgas). Gas tanks (Helium, H₂, CO, and Air) were purchased from Airgas.. CORM-A1, nicotinamide adenine dinucleotide (NAD⁺), reduced nicotinamide adenine dinucleotide (NADH), nicotinamide adenine dinucleotide phosphate (NADP⁺), reduced nicotinamide adenine dinucleotide phosphate (NADPH), 1-methylnicotinamide chloride, NaBH₄ and 1M BH₃-THF were purchased from Sigma-Aldrich and were used without purification. Boric acid, phosphate buffer saline (1 \times , 10 \times , 20 \times), DMEM (Corning, New York, USA), and RPMI 1640 (Corning, New York, USA) culture medium were purchased from Fischer Scientific. Sodium chloride (NaCl) and ODQ (1H-[1,2,4]oxadiazolo[4,3-a]-quinoxalin-1-one) were purchased from VWR. Hydrogen peroxide (35%, H₂O₂) was purchased from Oakwood Chemicals. *N*-Methylpyridine and methylated DABCO were synthesized using literature procedures.^{91, 92} Lithium phosphate buffer was made using phosphoric acid and lithium hydroxide. Pure CO gas was purchased from Airgas Company.

2.4.2 UV-Vis Analysis

Absorption spectra were measured and observed at 340 nm (NADH) and 260 nm (NAD⁺) on Varian Cary 100 Bio UV–visible spectrophotometer (UV-Vis) using a 1-mL cuvette. Standard curves for NADH and NADPH were established to calculate the approximate concentration of NADH produced in each reaction (Fig 2 (and Fig. S2). The reactions were either incubated at higher concentrations, specified for each experiment as described in the main text, and then diluted with PBS to 100-200 μ M to maintain an absorbance under 1.0 au or conducted at 100-200 μ M.

For reactions conducted at higher concentrations (e.g., 2 mM CORM-A1: 2 mM NAD^+), CORM-A1 was weighed and the solid was placed into a glass vial. The necessary volume to obtain the reported concentration of CORM-A1 was added through a solution of NAD^+ or NADP^+ . The glass vial was then incubated at 37 °C using a water bath and diluted to 1-mL at each designated time point. For reactions conducted at 100-200 μM , CORM-A1 was weighed and the solid was directly added to solution in cuvette (heated to 37 °C) and reaction was monitored. *Hence, a stock solution of CORM-A1 was not used in any UV-Vis experiments, since the CORM-A1 solid was directly added to all solutions.*

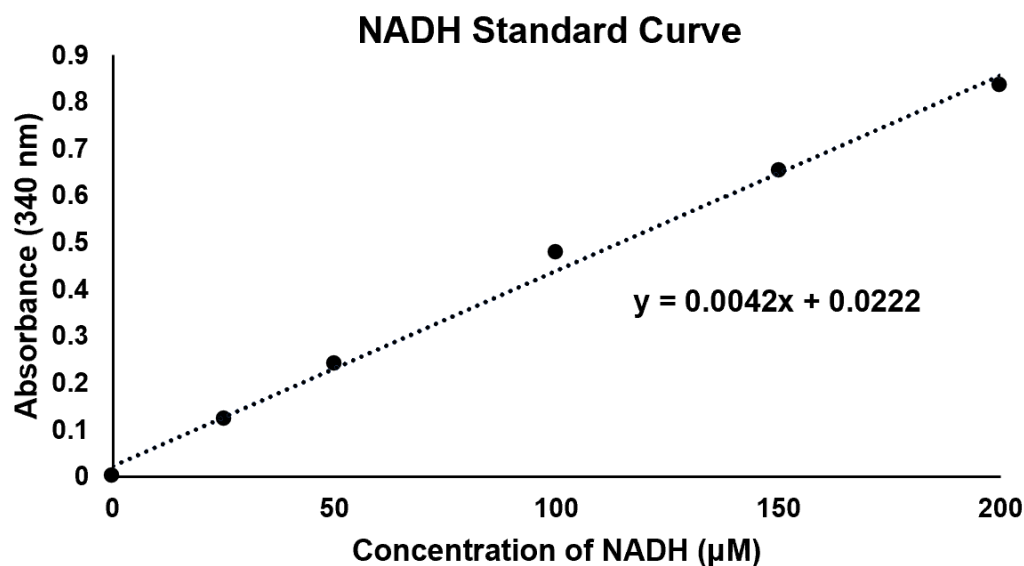


Figure S 2-1. A. NADH Standard Curve in PBS

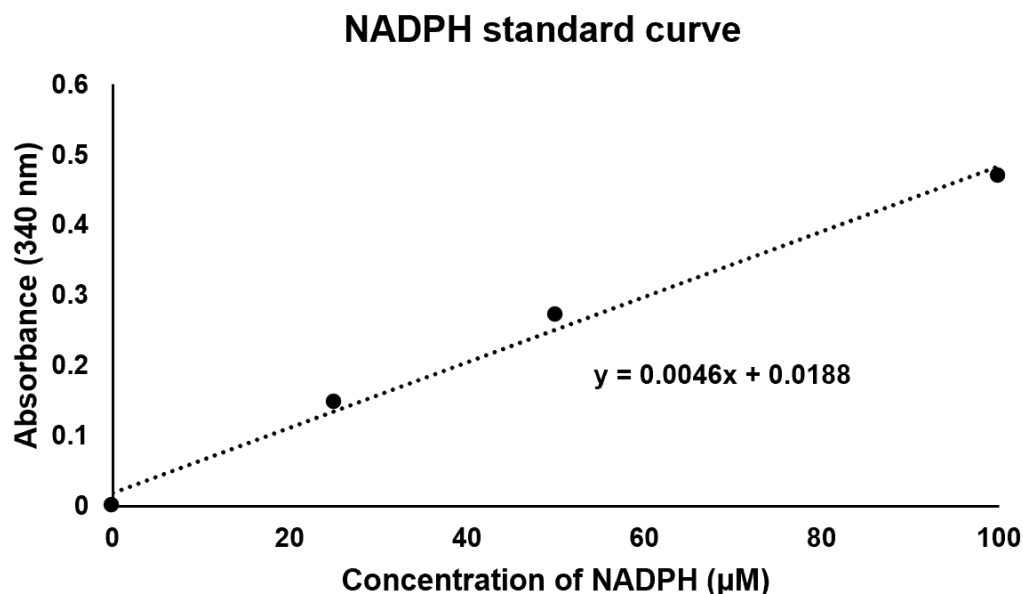


Figure S 1-1 B. NADPH Standard Curve in PBS

2.4.3 LC-MS/MS Analysis

LC-MS/MS Data was obtained using an API 3200 triple quadrupole mass spectrometer coupled with an Agilent 1200 series HPLC and UV-DAD spectrometer. Methods used a reversed-phase analytical column (Kromasil 100-3.5-C18) and electrospray ionization source in a negative mode with positive polarity. Selected ion mode was used for the detection of ions at m/z 662 and 540 for NAD^+ and m/z 664, 408, and 397 for NADH. A 10- μL sample solution was delivered through automatic injection to the HPLC. The mobile phase was ACN and 0.1% formic acid (in water) used for gradient elution from 0-95-0% over 15 min at 500 $\mu\text{L}/\text{min}$ flow rate. The CDL temperature was 200 $^{\circ}\text{C}$ and the heat block temperature was 250 $^{\circ}\text{C}$. Nebulizing gas flow was 4.5 L/min. NAD^+ : DP=50; EP=-10; CE=-26; CXP=-5; IS=4500; CAP=12; TEM=250; NADH: DP=-50; EP=-10; CE=-50; CXP=-5; IS=-4500.

General Protocol. Using a microbalance, NAD^+ , NADH, CORM-A1, boric acid, and NaBH_4 were weighed and dissolved to create stock solutions in HPLC grade water (filtered and

degassed via Barnstead NanoPure, pH: 5.5). Each were diluted using degassed and filtered water to desired concentrations. Solutions of $\text{BH}_3\text{-THF}$ were measured via pipette and prepared in anhydrous THF solvent. For reactions, equal volumes of NAD^+ (either 4 mM or 2 mM) and boron-based compounds (either 4 mM or 20 mM) were added to HPLC-specific vials and incubated at 37 °C for either 15 or 30 minutes. For 1:1 molar ratio, 4 mM of each were added in equal volume to give a final concentration of 2 mM. For 10:1 molar ratio, 2 mM of NAD^+ and 20 mM of a boron-based compound were added in equal volume to give final concentrations of 1 mM and 10 mM, respectively. The ratio of NADH and NAD^+ is calculated by using AUC provided by the LC-MS, which included negligible background noise or impurity in the multi-reaction monitoring (MRM) spectra detecting for NADH, making up <2% of NADH achievable in reactions (Fig. S3b, S4b, S5b).

2.4.4 *B NMR Analysis*

^{11}B NMR spectra were recorded on Bruker-400 spectrometers (128 MHz for ^{11}B NMR). 100 mM CORM-A1 in D_2O and reaction of CORM-A1 and NAD^+ at 3:1 (100mM:33.3mM) and 1:1 (100mM:100mM) ratios are seen at the end of the SI in figure S19.

2.4.5 *Quantitative CO Analysis*

An Agilent 7820A GC System equipped with a methanizer-FID (CH4izer, Restek, USA) was used to quantify CO release yield of CORM-A1. Because of CORM-A1's originally reported fast CO release, along with our data describing degrading stock solutions of CORM-A1, it is important to emphasize *that stock solutions of CORM-A1 were not be used in any GC experiments*. Instead, CORM-A1 was weighed using a microbalance, and the solid was then sealed in a gas tight headspace glass vial. The designated solution, including solvent and added reagent (e.g. NAD^+ , NADP^+ , etc.), was then added to sealed vial via a syringe. Using a gas tight syringe, 100 μL of the

headspace of 6-mL (actually 8.8-mL) Supelco headspace vials were sampled and transferred to the injector port maintained at 150 °C. Helium was used as the carrier gas with a flow rate of 30 mL/min. Gaseous components of the headspace were separated by passing through a packed column with 80/100 5A molecular sieve solid support, L × I.D. 2m × 0.53 mm (Restek). The column was heated at 100 °C for 5 min then 250 °C for 10 min while the detector was held at 300 °C. To calculate the CO release yield from CORM-A1, a standard curve was established using pre-made CO gas of 10, 20, 50, 100, and 10,000 ppm (Figure S2a). Over the course of the study, the catalyst in the methanizer required replacement and another standard curve was generated under the same condition (Figure S2b) after catalyst replacement to ensure the system suitability. The AUC observed was used in a linear equation to solve for concentration of CO released from CORM-A1. CO yield was calculated using Equation S1.

2.4.5.1 CO Gas Standard Curve

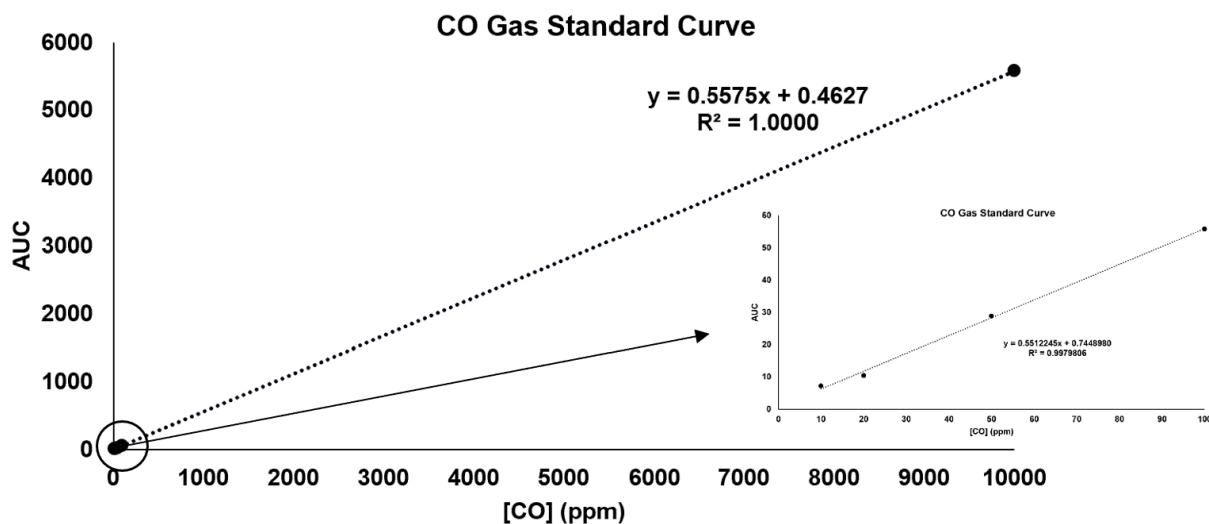


Figure S 2-2 A. CO standard curve using 100 µL injections

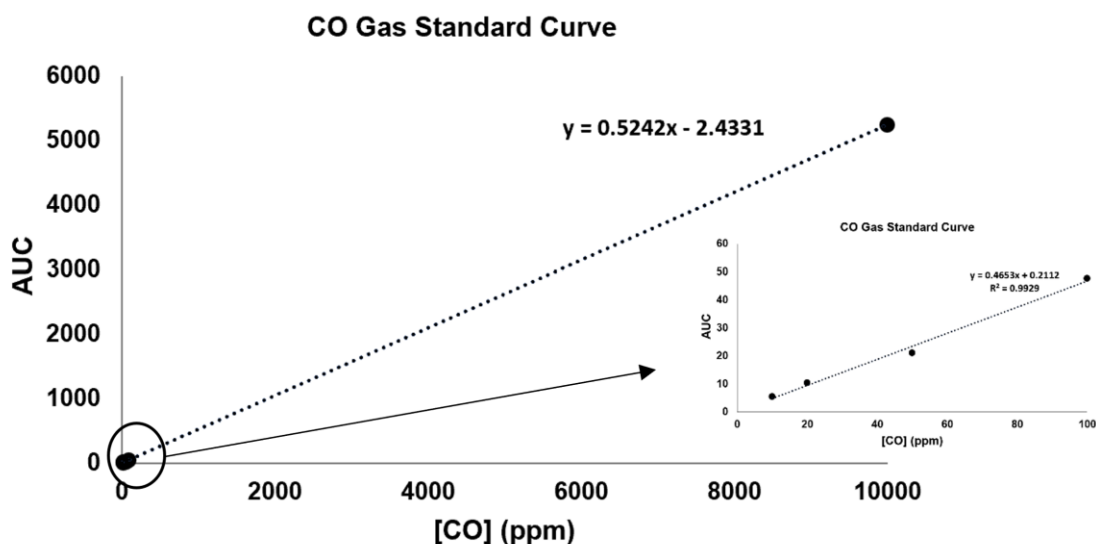


Figure S 1-2 B. CO standard curve (after catalyst replacement) using 100 μ L injections

$$CO \text{ (PPM)} = \frac{AUC}{\text{slope}} \text{ (simplified by using } CO \text{ (PPM)} = AUC \times 2)$$

$$CO \text{ (mol)} = \frac{(CO \text{ (PPM)} \times 10^{-6}) \times L \text{ headspace}}{22.4}$$

$$CO \text{ Yield \%} = \left(\frac{\text{mol of CO experimental}}{\text{mol of CO theoretical}} \right) \times 100$$

Equation 2-1. Equations used to calculate CO yield from CORM-A1. L headspace is calculated by subtracting the amount of solvent added from the total volume of the vial (8.8-mL)

2.4.5.2 CO Production from 1 mM CORM-A1 in 100 mM PBS at RT

Table S 2-1. CO Production from 1 mM CORM-A1 in 100mM PBS at room temperature

Entry	[CORM-A1]	Solvent	Added Reagent:	Initial CO Yield %	Total CO Yield %
				(15 min)	(20+ h)
S1	1 mM	10 \times PBS (at RT)	---	13 \pm 3.2	54 \pm 4.0

2.4.6 Reaction of 1-methylnicotinamide (1 mM) and CORM-A1 (5 mM) or NaBH₄ (10 mM) in PBS

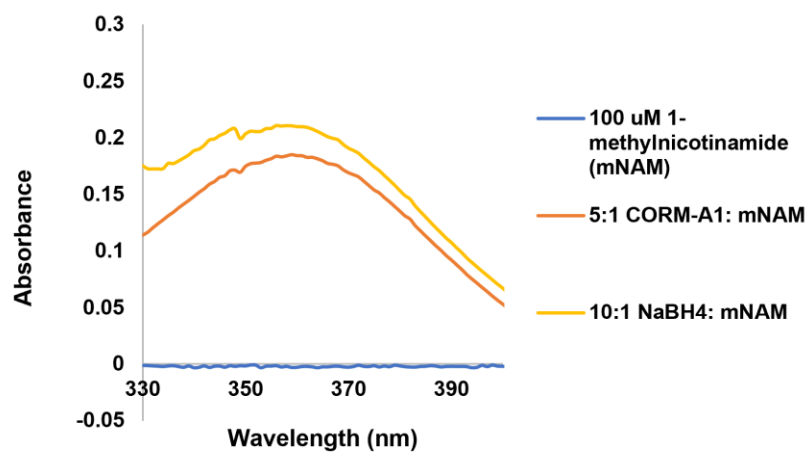


Figure S 2-3. Reactions of 1-methylnicotinamide (1 mM) and CORM-A1 (5 mM) or NaBH₄ (10 mM) in PBS, monitored by UV-Vis after 10-fold dilution of the reaction solution. PBS sample shown to represent no change in absorbance from the blank and mNAM control.

3 ANALYSIS OF COMMERCIALY AVAILABLE CARBON MONOXIDE DONOR, CORM-401

This chapter is mainly based on my publications: Bauer, N. et al. *Med Chem Res.* **2024**, X, X;
Bauer, N. et al. *Biochem Pharmacol.* **2023**, 214, 115642.

3.1 Introduction

In this chapter, we characterize CORM-401 for its CO-donating ability under various conditions relevant to studying CO biology. First, with regard to the “intrinsic” CO-release ability of CORM-401 and factors that could influence such ability, we found significant effects of added reagents such as thiol, peroxide, and dithionite on CO-release yields and rate. The variable nature of CO release from CORM-401 indicates the need for predetermining CO production yield and rate under the same conditions before biology experiments. Second, because of the commercial availability of CORM-401 in DMSO stock solution, we characterized its stability in such a preparation and found significantly diminished CO-release capacity of CORM-401 after exposing to DMSO or aqueous solution. Third, because carboxyhemoglobin (COHb) is an important indicator of the ability for a CO donor to supply CO in animal model work, we characterized the property for CORM-401 to elevate COHb. Fourth, quality assurance of such a metal complex is important to ensure consistency in results. Our findings indicate that the unstable nature of CORM-401 presents a quality assurance issue for end users. All these combined with the previously reported chemical reactivity of CORM-401 could lead to intractable scenarios in obtaining meaningful results using CORM-401 that can be reasonably attributed to CO in biology experiments.

3.2 Results and Discussion

In the interest in focusing the studies on aspects that directly impact the utility of CORM-401 in studying CO biology, we plan to address the following issues with rationales and analysis described in each relevant section: (1) the intrinsic ability for CORM-401 to produce CO in PBS or water without added reagents such as a nucleophilic or a redox-active compound, (2) the effect of added thiol or oxidizing agents on the CO release properties of CORM-401, (3) whether the CO-releasing ability of CORM-401 translates into elevating blood carboxyhemoglobin (COHb) level, (4) whether CORM-401 is stable in DMSO, a commonly used solvent in making stock solutions; and (5) what end users can do for quality assurance. Studies are performed using the gold-standard GC method with a flame-ionization detector (FID) coupled with a methanizer for highly sensitive detection. Below we describe our individual studies together with discussions of the implications of our findings.

3.2.1 CO Production using GC

*Table 3-1. CO production from 1 mM and 100 μ M CORM-401 in PBS or unbuffered water detected via GC-FID (n=3). * $P \leq 0.05$ vs CORM-401 in PBS (1 mM and 100 μ M) via one-tailed, equal variance t-test*

[CORM-401]	Solution/Added Reagent	Moles of CO produced per mol of CORM at 15 min	Moles of CO produced per mol of CORM at 60 min	Moles of CO produced per mol of CORM at 120 min
1 mM	PBS, pH 7.4	0.33 ± 0.13	0.65 ± 0.20	0.84 ± 0.20
100 μM	PBS, pH 7.4	0.19 ± 0.09	0.39 ± 0.18	0.72 ± 0.20
1 mM	Unbuffered water	0.25 ± 0.05	0.53 ± 0.04	0.81 ± 0.02
100 μM	Unbuffered water	0.24 ± 0.08	0.67 ± 0.17	1.14 ± 0.12 *
1 mM	Citrate buffer, pH 10	0.36 ± 0.10	0.72 ± 0.06	0.99 ± 0.22
1 mM	Citrate buffer, pH 6	0.37 ± 0.03	0.69 ± 0.09	0.93 ± 0.10

The intrinsic ability for CORM-401 to produce CO in PBS and water. In the current study, we used GC-FID and chose a time point of 2 h for the experiments, although CORM-401 continues to slowly release CO beyond 10 h. At this time, it is important to note the gaseous nature of CO and its rapid exchange with the environment. As such, release rates by donors that are slower than the exchange rate of CO with the environment will have very little practical meaning in the context of CO concentration in solution. In our pharmacokinetic studies, we have observed peak COHb levels of about 1 h in mouse models using various CO prodrugs.³² Therefore, we chose the 2-h time point for studies. Specifically, 1 mM CORM-401 incubated at 37 °C in PBS (pH 7.4) released 0.84 moles of CO per mole of CORM-401 within 2 hours (Table 1). Under the same conditions, 100 µM CORM-401 released 0.72 mole of CO per mol of CORM-401. Along a similar line, solutions of CORM-401 in unbuffered water (~pH 5.5) released 0.81 mole CO at 1 mM of CORM-401 and 1.1 moles of CO at 100 µM of CORM-401 within 2 hours. To examine whether pH affects CO production from CORM-401, 1 mM CORM-401 was incubated in citrate buffer at pH 6 and pH 10 at 37 °C. No significant variation from solutions in PBS pH 7.4 was observed (Table 1). Thus, the release yields are similar in aqueous solutions despite the difference in pH and presence of buffer. However, such numbers contrast previous reports that CORM-401 only releases 0.33 moles of CO within 4 hours. Specifically, CORM-401 has been previously reported to only release 0.33 mol of CO per mol of CORM when detected using GC.^{93, 94} These results are different from the CO production quantified using the myoglobin assay in the original publication, where CORM-401 was reported to produce approximately 10-fold more CO, or 3.2 equivalents of CO.⁹³ Such discrepancy was explained by invoking the idea that CO “re-backbonds” to the metal core after release if there is no “scavenging” agent (myoglobin) (Figure 1).

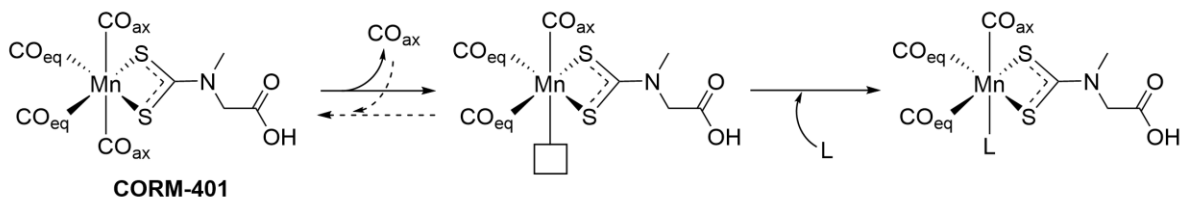


Figure 3-1. Previously proposed CO release and “re-backbonding” mechanism⁹⁵

Because this “re-backbond” proposition was central to the original explanation of experimental discrepancies, we are interested in examining this issue in depth. The idea of “re-backbonding” in essence describes a binding equilibrium. Whether “re-backbonding” would affect the quantitative determination of CO production depends on the K_d of this “re-backbonding” equilibrium. In doing this analysis, it is important to note two factors: CO’s solubility in an aqueous solution and the concentrations (in ppm) in the headspace for CO quantitation. The solubility under 1 atm of CO is known to be *ca.* 1 mM.⁹⁶ In our experiments, we normally end up with samples in the range of 100-1000 ppm CO in the head space, which correspond to about 100 nM to 1 mM of CO in solution when calculated using Henry’s law. On one hand, it is clear that the “re-backbonding” equilibrium would have a K_d far higher than that of Mb for CO (29 nM)⁹⁶ if Mb indeed out-competed CORM-401 for CO binding as stated in the original publication. This establishes the lower boundary of the K_d (the higher boundary for affinity) for “re-backbonding.” To assess whether this proposed “re-backbonding” equilibrium would affect CO quantification, we build on the finding described in the previous paragraph that CORM-401 releases about 0.8 mol equivalent of CO within 2 h. Then we incubated CORM-401 in varying concentrations in PBS, leading to varying CO levels in the headspace (100-1000 ppm). This is to assess whether contents in the range of 100-1000 ppm would have suppressive effects on CO release because of “re-backbonding.” Again, 1000 ppm corresponds to *ca.* 1 mM of CO in solution. If the “re-backbonding” process had a K_d close to or

lower than 1 mM, we would expect to see a significant suppressive effect on CO release. Specifically, we used 100, 250, 500, 750, and 1000 μM concentrations of CORM-401. At the 2-h point, the CO yields from these various experiments were the same, although the CO concentration in the headspace varied from 300-1000 ppm. Such results mean the originally proposed “re-backbonding” had no effect on CO release into the headspace when tested up to 1000 ppm. Such results further indicate that even if “re-backbonding” indeed happens, it would have a K_d far higher than 1 mM and would have no effect on CO quantifications as long as the CO contents in the headspace is below 1000 ppm. We should note that in our extensive work with CORM-401, we never had the need to go above 1000 ppm in CO contents in the headspace. Therefore, for all practical purpose, the originally proposed “re-backbonding” has no effect on CO quantification using GC. However, our results do not allow us to conclude whether “re-backbonding” happens at a higher CO concentration. Therefore, it is our interpretation that discrepancy between the original GC experiments and the original myoglobin assay was more likely due to the difference in chemical conditions (dithionite) than “re-backbonding.” Conceivably, “re-backbonding” might happen, but at a significantly higher CO concentration than what was observed under the experimental conditions used.

Table 3-2. CO production from CORM-401 in PBS detected via GC-FID (n=3).

[CORM-401]	[CO] in headspace (ppm)[†]	Corresponding [CO] in solution (μM)	CO Yield
100 μM	554 \pm 96	0.55 \pm 0.10	0.72 \pm 0.21
250 μM	403 \pm 82	0.40 \pm 0.08	0.89 \pm 0.02
500 μM	567 \pm 85	0.57 \pm 0.09	0.81 \pm 0.11
750 μM	808 \pm 280	0.81 \pm 0.28	0.79 \pm 0.04
1000 μM	917 \pm 293	0.92 \pm 0.29	0.88 \pm 0.16

[†]Because CO release occurs immediately after dissolution, we did not use sequential dilution method for preparing the CORM-401 solution. Instead, experiments were conducted by weighing out certain amount of CORM-401. Solvent volume was adjusted to give the desired concentration. As such, concentration does not correlate with the absolute quantity used for a given experiment. This is why [CO] in headspace does not correlate with CORM-401 concentration in solution.

Overall, CORM-401 is able to release slightly less than 1 molar equivalent of CO within 2 hours without assistance by either a strong nucleophile or an oxidizing agent (next sections). This release stoichiometry does not seem to be affected by the presence of buffer, seems to be independent of the initial concentrations of CORM-401 or the final CO concentrations in the headspace (ppm). The last point indicates that within the concentrations examined, a proposed “re-backbonding” mechanism has minimal or no effect on CO release.

Stock solution stability. There are literature reports of using CORM-401 stock solutions of CORM-401 in aqueous solution. The preceding discussion highlights that CORM-401 in aqueous solution is not stable and stock solutions should not be prepared in this manner to avoid significant experimental variations. Another important area of discussion is the stability of CORM-401 in DMSO. CORM-401 is commercially available in a pre-dissolved DMSO solution. Though there has been a report stating CORM-401 being stable in DMSO,⁹⁷ the lack of reported experimental evidence led us to investigate whether dissolution in DMSO compromises the ability for CORM-401 to release CO. Therefore, we measured whether CORM-401 releases CO in DMSO. By using the same GC method, CORM-401 (10 mM) in DMSO was found to produce 0.34 mol of CO per mol of CORM-401 in 10 minutes and approximately 1 mol of CO within 60 minutes at room temperature. After dilution to 1 mM in PBS and further incubation for an additional 30 min at 37 °C, only an additional 0.08 mol of CO was detected. These results suggest that CORM-401 is not stable in DMSO and stock solutions should not be prepared this way because of DMSO’s ability to compromise CORM-401’s ability to donate CO. Due to the lack of stability in both aqueous solution and DMSO, the data discussed in the following sections were obtained using samples prepared with solid CORM-401 and not stock solutions (see footnote of Table 2).

Effects of added thiol or oxidizing agents on the CO release properties of CORM-401.

We studied the effects of an oxidant H_2O_2 for several reasons. First, CO has been reported to induce elevated levels of reactive oxygen species (ROS).⁹⁸ Second, redox signaling has been proposed as a key mechanism for the action of CO.⁹⁸ Third, CORM-401 has been reported to degrade H_2O_2 in a non-catalytic manner.⁶³ Fourth, earlier studies using the myoglobin assay has shown accelerated CO release from CORM-401 in the presence of oxidants, where increasing concentrations of H_2O_2 (5-20 μM) showed a concentration-dependent CO release from 20 μM solutions of CORM-401.⁹⁴ For all these reasons, the interplay between ROS and the CO release property of CORM-401 needs to be probed. Herein, we use the most stable and abundant form of ROS, H_2O_2 , as a representative. Specifically, CORM-401 was incubated with H_2O_2 in different ratios. In the presence of 100 μM H_2O_2 , 1 mM CORM-401 in PBS showed an facilitated CO production, producing 1.35 moles of CO per 1 mol of CORM within 2 hours (Table 3). Along the same line, 100 μM CORM-401 in the presence of 100 μM H_2O_2 had a more significant facilitation, releasing 3.7 equivalents of CO per 1 mole of CORM within 2 hours. Such results strongly indicate that H_2O_2 triggers the release of the second and third equivalents of CO from CORM-401. We also conducted sequential release experiments to probe the effect of H_2O_2 . Specifically, 1 mM CORM-401 was allowed to release approximately 1 mol equivalent of CO (through incubation at 37 °C in PBS for 2 hours). Following this, the solution was bubbled with N_2 for at least 5 minutes to displace the remaining CO in solution. Solutions were then diluted to 100 mM using H_2O_2 , resulting in equivalent molar ratio of 100 μM CORM-401 and 100 μM H_2O_2 . Upon exposure to H_2O_2 , CORM-401 released an additional 2.25 moles of CO within 2 hours after bubbling with N_2 . In solutions further diluted with PBS, CORM-401 continued to release CO slowly, producing an additional 0.55 moles of CO in the second 2-h period of incubation after bubbling with N_2 . These results correspond to a separate

sample of CORM-401 releasing approximately 1.6 moles of CO after around 300 minutes without bubbling N₂. To ensure the solution was capable of releasing the maximal amount of CO, H₂O₂ was added after 2 hours, resulting in a CO production of an additional 2.25 equivalents of CO.

Overall, the combined results suggest that the release of the first CO in solution is “spontaneous” without the need for assistance, except water. The release of the second and third can be triggered by H₂O₂. Further, CO “re-backbonding” to the Mn core of CORM-401 after its initial CO release was not observed. Along this line, the release from CORM-401 can be considered in two categories. The first is spontaneous release under physiological conditions and the second is stimulus-induced release, seen with H₂O₂, DMSO, and thiols (next section). The second, stimulus-induced release, is seen throughout the data presented in this paper and contributes significantly to variations in CO release from CORM-401 depending on specific experimental conditions. Although we did not comprehensively characterize all the possible stimulus-induced triggers of CORM-401, the results presented clearly emphasize the need for examining various factors when CORM-401 is used for a given set of biological experiments.

*Table 3-3. CO production from 1 mM and 100 μ M CORM-401 in 100 μ M H₂O₂ detected via GC-FID (n=3). * $P \leq 0.05$, ** $P \leq 0.01$ vs CORM-401 in PBS (1 mM and 100 μ M) via one-tailed, equal variance t-test*

[CORM-401]	Solution/Added Reagent	Moles of CO produced per mol CORM at 15 min	Moles of CO produced per mol CORM at 60 min	Moles of CO produced per mol CORM at 120 min
1 mM	100 μ M H ₂ O ₂	0.84 \pm 0.13 *	1.17 \pm 0.12 *	1.35 \pm 0.13 *
100 μM	100 μ M H ₂ O ₂	1.64 \pm 0.15 **	3.64 \pm 0.20 **	3.70 \pm 0.14 **

Effects of Thiol Species. We next studied the effects of thiol species on the CO release properties of CORM-401 because of the now well-known complications of dithionite as a nucleophile in the myoglobin assay. Further, because there is a large number of biologically

relevant thiol species, sensitivity of CORM-401 toward thiols could make a great deal of difference in terms of its ability to donate CO. We first examined simple thiol species including GSH and cysteine. In the presence of 100 μM GSH, 100 μM CORM-401 produced 2.7 moles of CO per 1 mol of CORM within two hours. In contrast, 1 mM CORM-401 only produced 1.1 moles of CO in the presence of 100 μM of a thiol species (Table 4). The presence of cysteine showed a similar effect, where in the presence of 100 μM cysteine, 100 μM CORM-401 released 1.8 moles of CO and 1 mM CORM-401 released 1.0 moles of CO per 1 mole of CORM. Such results suggest that biological thiols can trigger the release of the second and third CO from CORM-401.

All the results suggest that there are multiple factors that can affect the ability and quantity for CORM-401 to release CO. Dosage considerations need to rely on knowledge of concentrations of ROS and thiol species.

*Table 3-4. CO production from 1 mM and 100 μM CORM-401 in 100 μM GSH or cysteine detected via GC-FID (n=3). * $P \leq 0.05$, ** $P \leq 0.01$ vs CORM-401 in PBS (1 mM and 100 μM) via one-tailed, equal variance t-test*

[CORM-401]	Solution/Added Reagent	Moles of CO produced per mol CORM at 15 min	Moles of CO produced per mol CORM at 60 min	Moles of CO produced per mol CORM at 120 min
1 mM	100 μM GSH	0.42 ± 0.05	0.68 ± 0.19	1.09 ± 0.09
100 μM	100 μM GSH	0.42 ± 0.04	1.5 ± 0.17 **	2.58 ± 0.2 **
1 mM	100 μM cysteine	0.46 ± 0.08	0.89 ± 0.08	1.21 ± 0.1 *
100 μM	100 μM cysteine	0.46 ± 0.10 *	1.42 ± 0.15 **	2.29 ± 0.15 **

Effect of Proteins. We also examined the effect of two proteins, albumin and myoglobin, because of albumin's high abundance and myoglobin's role in CO binding. Further, these proteins all have nucleophilic functional groups. We found that myoglobin, without the addition of a reducing agent, is capable of slightly increasing CO production from CORM-401. When incubated at 1 mM with 100 μM myoglobin in PBS for 2 hours, CORM-401 produced 1.02 moles of CO per 1 mole of CORM-401 (Table 5). This remained consistent at lower concentrations, where 100 μM

CORM-401 produced 0.95 moles of CO per 1 mole of CORM-401 under the same conditions. These results suggest that myoglobin itself may also play a role in facilitating CO release. Further, these results explain the slightly increased COHb levels found with CORM-401, detailed in a later section, in comparison to the CO yield quantified using GC. To probe whether the increased effect was due to the presence of a protein, we looked at CO production from CORM-401 in the presence of albumin. In the presence of 100 μ M albumin, 1 mM CORM-401 produced 0.99 moles of CO per 1 mole of CORM, which was a slight increase in comparison to PBS solutions. Interestingly, the presence of albumin incubated with lower concentrations of CORM-401 (100 μ M) led to opposite results. In the presence of 100 μ M albumin, 100 μ M CORM-401 showed significantly decreased CO production, producing only 0.40 moles of CO per 1 mol of CORM after 2 hours. These results suggest that CORM-401 interacts with biologically relevant proteins that alter its CO production. Because albumin is present in the blood at mM concentrations (0.5-0.7 mM),⁹⁹ this pronounced impediment of CO release by albumin at a 1:1 ratio add another significant convoluting factor in estimating CO dosage when CORM-401 is used *in vivo*.

*Table 3-5. CO production from 1 mM and 100 μ M CORM-401 in 100 μ M myoglobin (Mb) or albumin detected via GC-FID (n=3). * $P \leq 0.05$ vs CORM-401 in PBS (1 mM and 100 μ M) via one-tailed, equal variance t-test*

[CORM-401]	Solution/Added Reagent	Moles of CO produced per mol CORM at 15 min	Moles of CO produced per mol CORM at 60 min	Moles of CO produced per mol CORM at 120 min
1 mM	100 μ M Mb	0.44 \pm 0.07	0.81 \pm 0.07	1.02 \pm 0.09
100 μM	100 μ M Mb	0.45 \pm 0.04 *	0.74 \pm 0.03 *	0.95 \pm 0.07
1 mM	100 μ M albumin	0.5 \pm 0.12	0.88 \pm 0.1	0.99 \pm 0.14
100 μM	100 μ M albumin	0.13 \pm 0.10	0.30 \pm 0.08	0.40 \pm 0.07

3.2.2 *CO-releasing ability of CORM-401 translates into hemoglobin binding*

In this study, we used whole mouse blood samples and incubated them with CORM-401 and CO gas. Each was measured to produce a theoretical maximum of 740 μM of CO, assuming each CORM produces 1 mol equivalent and a theoretical upper limit COHb level of 8% (See SI). The basal level of COHb was $0.23 \pm 0.3\%$. When 740 μM CO gas was incubated with mouse blood for 2 hours, the maximal COHb level experimentally observed was $5.77 \pm 0.4\%$ (Table 6). This is used as the benchmark of CO (0.37 μmoles) that can be captured when analyzing the COHb level arising from incubation with each CORM. When 740 μM CORM-401 was incubated with mouse blood for 2 hours, the maximum COHb level was $5.17 \pm 0.5\%$. In comparison to the COHb produced when the blood was incubated with CO gas, CORM-401 led to a ratio of 0.896 (%COHb CORM-401/%COHb CO gas). This number is generally consistent with the CO release stoichiometry by CORM-401 as described in Table 1. Such results indicate that the CO released from CORM-401 can be captured by hemoglobin, as expected.

As previously discussed, the other three commercially available CORMs have been reported to have similar issues with lack of CO release (CORM-2 and CORM-3) or idiosyncratic CO production (CORM-A1). Since the CO production of these CORMs has been well-characterized outside of using the myoglobin assay, we did comparative experiments with CORM-3 and CORM-A1 to further demonstrate that CO production quantified using GC corresponds to %COHb levels in whole blood samples. CORM-A1 was originally reported to have a $t_{1/2}$ of 21 minutes at 37 °C in PBS, pH 7.4.¹⁰⁰ Our lab has recently reported the redox activity and idiosyncratic CO production of CORM-A1,¹⁰¹ in which we reported that 20 μM -100 mM of CORM-A1 in unbuffered water releases up to 33% over 20+ hours. With such background information, we incubated 740 μM CORM-A1 for 2 hours with mouse blood and observed a maximum of $2.30 \pm 0.07\%$ COHb (Table

6). This is a lower COHb level compared with CORM-401 and pure CO gas and is consistent with what one would have expected based on CORM-A1's CO production stoichiometry detected by GC.¹⁰¹

Table 3-6. Maximum %COHb in mouse blood in vitro achieved within 2 h when incubated with CORM-3, CORM-401, CORM-A1, or CO gas. The ratio to CO gas is calculated by %COHb CORM/%COHb CO gas.

	None	740 mM CO Gas	740 mM CORM-401	740 mM CORM-A1	740 mM CORM-3
%COHb	0.23 ± 0.29	5.77 ± 0.36	5.17 ± 0.47	2.3 ± 0.07	0.57 ± 0.29
%COHb CORM/%COHb CO gas	0.040	1	0.896	0.399	0.099

We also conducted similar experiments with CORM-3, which has been reported not to raise COHb. The biological effects of CORM-3 has been attributed to CO based on “its ability to actively deliver CO to the tissue without raising systemic CO concentration.”¹⁰² The concept of direct transfer of CO was said as the way for CO to engage with a biological target without increasing COHb levels.¹⁰³ Here, we present that the reason CORM-3 does not raise COHb is likely because it does not deliver a meaningful amount of CO. CORM-3 was originally reported to release 1 mol of CO per 1 mole of CORM, with a $t_{1/2}$ ranging from 4-18 minutes.¹⁰⁴ It has since been reported that these kinetics were reliant on the presence of sodium dithionite.^{105, 106} A comprehensive table of all different conditions tested in the CO production from CORM-3 is shown in a previously mentioned review.³⁶ In 2011, Santos-Silva and coworkers reported that using GC-TCD, no CO production was detected from 10 mM CORM-3 in various solutions, including H₂O, PBS (pH 7.4), RMPI-10%FBS, and sheep plasma.¹⁰⁷ Other labs have also reported using GC-TCD as a reliable method for quantifying CO production from CORMs.¹⁰⁸ In a recent report from our lab, 50 μ M CORM-2 and CORM-3 released 1.3% and 0.6% CO, respectively,

when quantified using GC-FID.¹⁰⁹ Our lab has specifically found that using GC-FID, 1 mM CORM-3 has a CO yield $\leq 2\%$ over 24 hours incubated at 37 °C in PBS, pH 7.4 (Table 7). We also found that 1 mM CORM-3 has similarly low CO yields ($\leq 2\%$) over 24 hours incubated at 37 °C in both unbuffered water and biological media (DMEM, 10% FBS) (Table 7). These results correspond with the COHb levels obtained *in vitro*. When 740 μM CORM-3 was incubated with mouse blood for 3 hours, the maximum COHb level was found to be $0.57 \pm 0.29\%$ (Table 6). This is within statistical errors of the baseline. In another related study aimed at examining the ability for CO to induced HO-1 expression, we conducted similar studies with the same finding of miniscule amount of CO production from CORM-2 and CORM-3. Such results are consistent with the inability for CORM-3 to increase COHb. Furthermore, the proposition of direct transfer of CO from CORM-3 without the ability to increase COHb is actually a similar question as that of “re-backbonding” for CORM-401. Short of any suggestion for quantum-tunneling¹¹⁰ or even a special proximity effect as one would see in an enzymatic or intramolecular reaction,¹¹¹⁻¹¹³ “transferring” a ligand from one host to another is fundamentally a basic question of binding equilibrium. Therefore, one needs to consider the known affinity of CO for various hemoprotein targets. For example, the K_d of Hb for CO in the artery is 0.7-1.7 nM.⁹⁶ Very few known hemoproteins have affinity higher than this, except for neuroglobin (0.2 nM).⁹⁶ Therefore, if Hb does not have a high enough affinity for CO to allow for “its transfer” from CORM-3, very few other hemoproteins are expected to be in a thermodynamically favorable position to accept CO from CORM-3. All these point to the inability for CORM-3 to produce CO as the reason that it does not elevate COHb level.

Table 3-7. CO production of 1 mM CORM-3 in different solvent detected via GC-FID (n=3)

Solvent	Initial CO Yield (2 h)	Total CO Yield (24 h)
PBS, pH 7.4	$1.5 \pm 0.04\%$	$2 \pm 0.14\%$
Unbuffered water	$2 \pm 0.74\%$	$2 \pm 0.68\%$
DMEM, 10%FBS	$1.8 \pm 0.04\%$	$2 \pm 0.12\%$

To further examine the ability for CORM-401 to elevate COHb at the molecular level, a “hemoglobin assay” was performed to observe the ability of CORM-401 to shift ferrous stabilized oxyhemoglobin (OxyHb) to carboxyhemoglobin (COHb). As a control, Hb was reduced using $\text{Na}_2\text{S}_2\text{O}_4$ and then bubbled with pure CO gas, leading to the disappearance of the OxyHb peak at 577 nm along with the appearance of a peak at 569 nm (COHb) (Figure 2A). When 75 mM CORM-401 was incubated with approximately 78.9 mM Hb (calculated using literature molar absorptivity¹¹⁴) in the absence of dithionite, a significant depression of the 577 nm peak was observed, though OxyHb was still present (Figure 2A). When an additional molar equivalent of CORM-401 was added to the same sample and incubated for 90 minutes, only a slight further wavelength shift towards COHb was observed (Figure 2B). To probe whether additional dithionite could further promote CO production from the CORM-401 solutions, $\text{Na}_2\text{S}_2\text{O}_4$ was added. A significant increase of the peak at 568 nm (COHb) was observed, further supporting the notion that CO release from CORM-401 is enhanced in the presence of $\text{Na}_2\text{S}_2\text{O}_4$. Although a significant shift to COHb was seen, this only represented up to 77% COHb (Figure 2C). The increase in %COHb after the addition of $\text{Na}_2\text{S}_2\text{O}_4$ over time was observed (Figure 2C), which reached 82% COHb after 15 minutes when CORM-401 was in molar equivalent and 90% COHb when CORM-401 was in molar excess in comparison to Hb concentration. The increase in overall %COHb seen in the 1:2 reaction (Figure 2C) comes from the higher concentration of CORM-401 used, allowing for more CO to be released after addition of $\text{Na}_2\text{S}_2\text{O}_4$. All the results support the ability for CORM-401 to lead to an increase of COHb level and the pronounced effects of sodium dithionite in facilitating CO release from CORM-401. Such results are also consistent with the finding that it is not “re-backbonding” that led to the discrepancy in CO release yield in the original publication, as

described earlier. It is indeed the difference in whether dithionite is present to impact CO release yield.

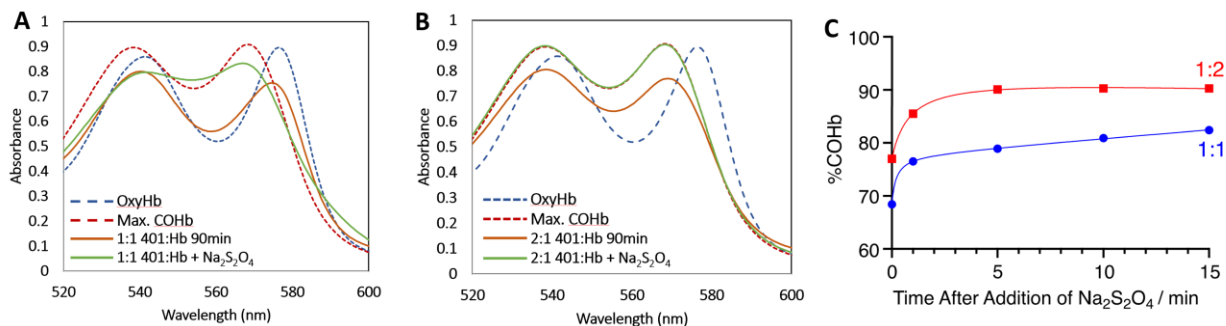


Figure 3-2. **A.** UV-vis spectra of OxyHb and COHb (78.9 μ M) and UV-vis spectra of 1:1 reaction between CORM-401 and Hb, with and without Na₂S₂O₄. **B.** UV-vis spectra of 2:1 reaction between CORM-401 and Hb, with and without Na₂S₂O₄. **C.** %COHb Yield calculated using Hb assay from 25 mM and 150 mM CORM-401, respectively

3.2.3 EPR Characterization of CORM-401

In order to determine the manganese oxidation states of CORM-401, the EPR spectra of CORM-401 were measured. Commercially available CORM-401 was dissolved in PBS, immediately transformed to an EPR tube, and frozen by liquid nitrogen. As shown in Figure 3A, the EPR signals with hyperfine structures ($g = 2$) of Mn(II) was observed at the temperature of 77 K.¹¹⁵ However, in CORM-401, the manganese atom should be in Mn(I) state.⁹³ Previous reports by Ford and coworkers have shown that similar Mn(I)-CO complexes are EPR silent before CO release.²³ Therefore, we anticipated an EPR silent spectrum for CORM-401 at a pure state. Our results indicate the presence of a of Mn (II) in the sample and thus the presence of impurity. Along the same line, the EPR signals of Mn(II) states increased when the sample was incubated at 37 °C for 120 minutes (Figure 3B), the same time point where the GC indicated the release of almost 1 mol CO from CORM-401 (Table 1). Further, we found that incubation with excess Na₂S₂O₄ further

increased the EPR signal intensity of Mn (II) in the sample (Figure 3B). As noted earlier, such incubation allows for production of 2-3 equivalents of CO. Both results suggest that upon CO release, a Mn (II) complex is likely formed from CORM-401. Other manganese species were not observed in our experiment method. We bubbled pure CO gas into the sample of 400 μ M CORM-401 solution after 120-minute incubation to confirm if CO could “re-backbond” to the metal core after CO release. As shown in Figure 3C, no meaningful change in the EPR signal was observed, further indicating that it is unlikely that CORM-401 shifts between the 18e- and 16e- states and re-back-bonds CO, as previously reported.⁹⁴ It is understood that full structural studies of the issues involved require much more work and are beyond the scope of this study. The issue most relevant to this study is that commercially available CORM-401, either in solution or as solid, are unstable and contain Mn(II) impurities of unknown amount and unknown structure, immediately after sample preparation and frozen at liquid N₂ temperature. There does not seem to be a way to readily assess the quality of CORM-401 by end users who do not have the specialized equipment needed.

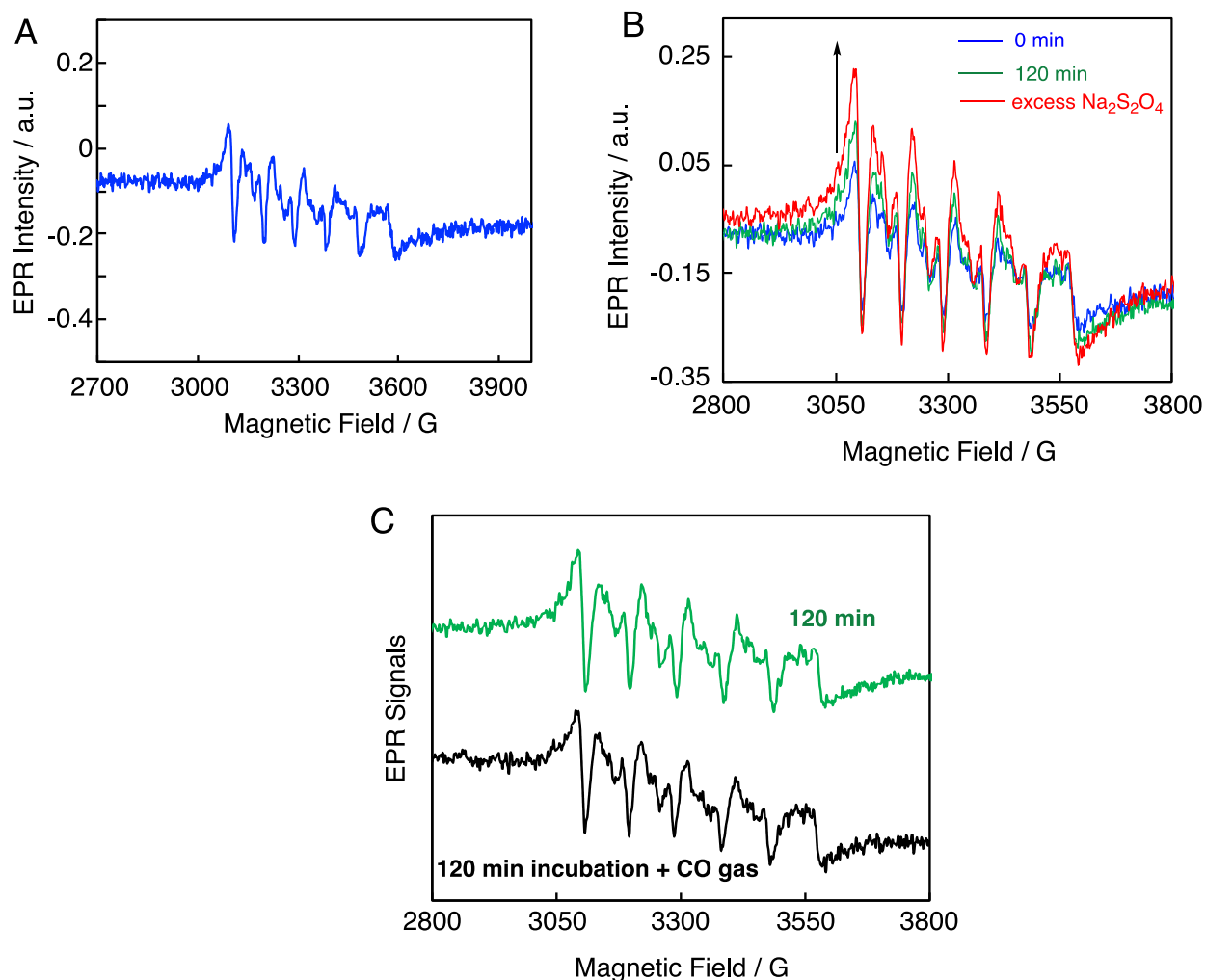


Figure 3-3. X-Band EPR spectra of CORM-401 solutions ($400\ \mu\text{M}$). A. CORM-401 dissolved in PBS at RT (blue); B. CORM-401 dissolved in PBS, incubated at $37\ ^\circ\text{C}$ for 120 min (green), and in PBS with excess $\text{Na}_2\text{S}_2\text{O}_4$ for 5 min incubation at $37\ ^\circ\text{C}$ (red) and C. CORM-401 dissolved in PBS incubated at $37\ ^\circ\text{C}$ for 120 min, then bubbled with excess CO gas (black). The EPR conditions were shown in SI.

3.3 Conclusion

The results presented bring to light major factors to consider in using CORM-401 to study the pharmacological and biological effects of CO. Through quantification of CO

production from CORM-401 in the absence of $\text{Na}_2\text{S}_2\text{O}_4$ using the gold standard GC-FID and COHb levels, we report that CORM-401 has variable CO production. Our results show that although CORM-401 does release more CO than CORM-2 and CORM-3, as previously reported, its CO production is altered in the presence of biologically relevant reagents, such as H_2O_2 , myoglobin, albumin, GSH, and cysteine. Further, there are already literature reports of the chemical reactivity issues from CORM-401⁶³ and the lack of adequate negative controls.³⁶ Such findings mean that biology experiments need to be carefully designed and controlled, including, at the minimum, predetermining the CO production under the same conditions used, addressing the chemical reactivity issues, and validating appropriate negative controls. Furthermore, through comparison with other CORMs, CORM-3 and CORM-A1, and COHb levels, we confirm that GC-FID is a useful direct method to quantify CO production from CO donors. The results presented here demonstrate that CO quantified using GC generally corresponds to the CO measured using COHb. Additional factors to consider in using CORM-401 to study CO biology include its chemical reactivity with DMSO and the presence of a significant amount of Mn(II) immediately after solution preparation, which is not consistent with pure CORM-401. We hope that the studies described will help researchers in fully considering possible interfering factors in contemplating using CORM-401 as a CO surrogate in studying CO biology. The same applies to the development of other CO donors for the same purpose. Factors that need to be considered include tractable chemical composition and chemical reactivity, reliable and well-defined CO production property in terms of both rate and yield, availability of adequate controls with well-understood chemical compositions reflecting the true nature of the product after CO release, tractable biological activity of the negative controls, and the ability to conduct quality assurance tests by end users.

3.4 Experimental

3.4.1 General Information

All reagents and solvents were of reagent grade from commercial suppliers (such as Sigma-Aldrich, among others). Absorption spectra were measured and observed on Shimadzu UV-1900i UV–visible spectrophotometer (UV-Vis). Gas chromatography studies were performed on an Agilent 7820A system equipped with flame ionization detector (FID) coupled with a methanizer (CH4izer, Restek, USA). Column: Packed; 80/100 5A molecular sieve solid support, $L \times I.D.$ 2m \times 0.53 mm (Restek). Carrier gas: Helium (Airgas). Gas tanks (Helium, H₂, CO, and Air) were purchased from Airgas. Electron paramagnetic resonance was conducted on a Bruker EMXplus EPR spectrometer at the University of Georgia in Athens, GA. Carboxyhemoglobin levels (COHb) were determined using an ITC AVOXimeter 4000. CD-1 mice (25–30 g) were purchased from Charles River Laboratories (Wilmington, MA, USA), and were fed with food and drinking water ad libitum. Animals were maintained in accordance with the Guide for the Care and Use of Laboratory Animals of the National Institute of Health. All the animal protocols were approved by the Institutional Animal Care and Use Committee of Georgia State University (IACUC protocol: A21055). Mice (male) were anesthetized with 2% isoflurane/oxygen and blood (about 1ml) was collected via cardiac puncture and transferred to a tube containing 40-unit heparin. CORM-401, CORM-A1, CORM-3, GSH, cysteine, myoglobin from horse heart, hemoglobin A₀ ferrous-stabilized human were purchased from Sigma-Aldrich and were used without purification. Phosphate buffer saline (1 \times) and Dulbecco's modified Eagle's medium (DMEM, Corning) supplemented with 10% fetus bovine serum (FBS, Corning) and 1% penicillin/streptomycin (PNS). were purchased from Fischer Scientific. Hydrogen peroxide (35%, H₂O₂) was purchased from Oakwood Chemicals. Pure CO gas was purchased from Airgas Company.

3.4.2 UV-vis Analysis

Absorption spectra were measured and observed at 577 nm (OxyHb) and 569 nm (COHb) on Shimadzu UV-1900i UV–visible spectrophotometer (UV-Vis) using a 1-mL cuvette. For the “hemoglobin assay” degassed PBS was added to the sealed container of ferrous-stabilized hemoglobin to produce 25 μ M. 1 mL of the solution was run in the UV to obtain the baseline OxyHb and COHb levels. This sample was then sequentially incubated with $\text{Na}_2\text{S}_2\text{O}_4$ and CO Gas, respectively, to obtain the maximum deoxyHb and COHb levels. Another 6 mL of the solution was added to a sealed vial containing CORM-401. 1 mL was removed from the vial to run the following sample: 1:1 Hb:401 at 90 minutes. After each of these samples were run, $\text{Na}_2\text{S}_2\text{O}_4$ was added; the sample was run again to observe if $\text{Na}_2\text{S}_2\text{O}_4$ promoted CO production from 401. Then CO gas was bubbled through, and the sample was run again to observe the maximum obtainable COHb level for that sample. After this, additional equivalent of CORM-401 was added to the remaining solution to produce a 1:2 Hb:401 reaction. After this was incubated at 37 °C for 90 minutes, the sequential $\text{Na}_2\text{S}_2\text{O}_4$ and CO gas steps were also taken. All CORM-401 solution used was freshly prepared. A stock solution of CORM-401 was not used in any UV-Vis experiments, since CORM-401 solid was directly added to all solutions.

3.4.3 Quantitative CO Analysis

An Agilent 7820A GC System equipped with a methanizer-FID (CH4izer, Restek, USA) was used to quantify CO release yield of CORM-401, -A1, and -3. Because of CORM-401’s originally reported fast CO release, it is important to emphasize *that stock solutions of CORM-401, -A1, or -3 were not be used in any GC experiments*. Instead, CORMs were weighed using a microbalance, and the solid was then sealed in a gas tight headspace glass vial. The designated solution, including solvent and added reagent (e.g. GSH, cysteine, H_2O_2 , etc.) was then added to

sealed vial via a syringe. Using a gas tight syringe, 100 μL of the headspace of 6-mL (actually 8.8-mL) Supelco headspace vials were sampled and transferred to the injector port maintained at 150 $^{\circ}\text{C}$. Helium was used as the carrier gas with a flow rate of 30 mL/min. Gaseous components of the headspace were separated by passing through a packed column with 80/100 5A molecular sieve solid support, $\text{L} \times \text{I.D.}$ 2m \times 0.53 mm (Restek). The column was heated at 100 $^{\circ}\text{C}$ for 5 min then 250 $^{\circ}\text{C}$ for 10 min while the detector was held at 300 $^{\circ}\text{C}$. To calculate the CO release yield from CORMs, a standard curve was established using pre-made CO gas of 10, 20, 50, 100, and 10,000 ppm (Figure S1a). The AUC observed was used in a linear equation to solve for concentration of CO released from CORMs. CO yield was calculated using Equation S1.

3.4.3.1 CO Gas Standard Curve

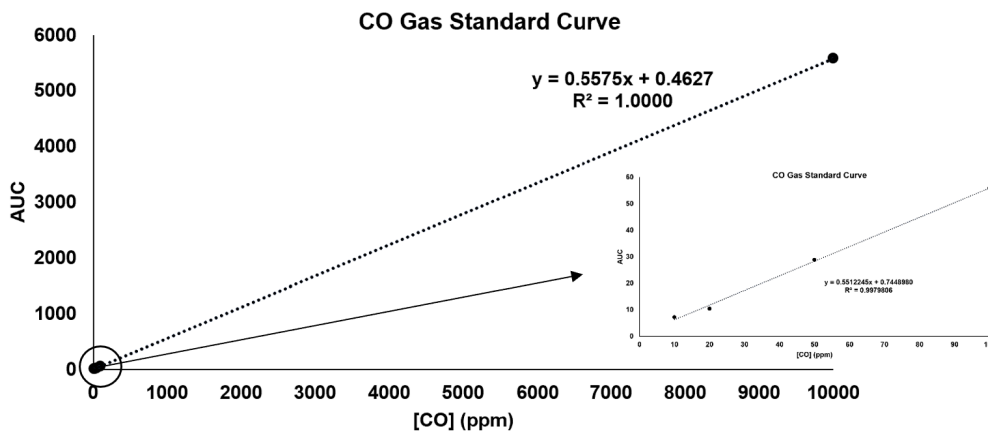


Figure S 3-1. CO standard curve using 100 μL injections

$$\text{CO (PPM)} = \frac{\text{AUC}}{\text{slope}} \quad (\text{simplified by using } \text{CO (PPM)} = \text{AUC} \times 2)$$

$$\text{CO (mol)} = \frac{(\text{CO (PPM)} \times 10^{-6}) \times \text{L headspace}}{22.4}$$

$$CO\ Yield\% = \left(\frac{\text{mol of CO experimental}}{\text{mol of CO theoretical}} \right) \times 100$$

Equation 3-1. Equations used to calculate CO yield from CORMs. L headspace is calculated by subtracting the amount of solvent added from the total volume of the vial (8.8-mL)

3.4.4 CO-oximetry

Ability to increase COHb in whole blood samples was monitored using a CO-oximeter (AVOXimeter 4000, Avox Systems, New York, NY, USA). The CO-oximetry measurements were made following the manufacturer's protocol and were validated by performing the specified quality control protocol. The whole blood samples were taken from mice and incubated with either CO gas or solids of CORM-401, CORM-A1, or CORM-3 to produce a theoretical concentration of 740 μM CO, assuming each CORM released 1 mol equivalent of CO. Each sample was gently shaken at 37 °C for up to 2 hours. The baseline COHb level was obtained under the same conditions in the absence of any added reagent. A theoretical %COHb level was calculated to be 8% COHb. We used the %COHb obtained by CO gas (5.77%) to determine the ratios since this is the maximum %COHb we would expect a CORM to be able to achieve. The CO gas sample was prepared by adding 8.13 μL pure CO gas into a gas tight vial containing 500 μL whole mouse blood. The CO gas sample may be lower than the theoretical due to competition of oxygen, formation of MetHb, or other common interferences. Amongst all the samples, the average total hemoglobin (tHb) content for each sample was 15 g/dL.

3.4.5 EPR

X-band (~9.6 GHz) EPR spectra were recorded using a Bruker EMXplus CW EPR spectrometer and all EPR experiments were conducted at the EPR Facility at the University of Georgia in Athens, Georgia via a fee-for-service arrangement. All samples were prepared at room temperature and either frozen using liquid nitrogen right away or incubated at 37 °C, as designated

in the main text, and then frozen using liquid nitrogen. All samples were stored in liquid nitrogen between preparation and data collection. Experimental parameters:

Microwave Frequency	9.35 GHz
Temperature	77 K
Microwave Power	2 mW
Modulation Amplitude	4 Gauss
Modulation Frequency	100 kHz
Conversion time	4.00 ms

4 DESIGN OF CARBON MONOXIDE DONOR FOR CARBONYLATION REACTIONS

This chapter is mainly based on my publications: De La Cruz LK, **Bauer N**, et al. *Organic Letters*. **2022**, 24 (27), 4902-4907

4.1 Introduction

Transition metal-catalyzed carbonylation, pioneered by Heck and co-workers,¹¹⁶ is a one-step route to directly introduce molecular complexity in organic synthesis enabling access to a wide range of carbonyl containing intermediates.¹¹⁷ Widespread application of carbonylation in small-scale laboratory setting is hindered by the inherent toxicity and thus storage and handling issues associated with CO gas tanks. Development of bench-stable, solid or liquid reagents that replace the direct use of CO gas is an active research area. CO surrogates developed thus far include a wide array of compounds ranging from low molecular weight compounds such as CO₂,¹¹⁸ formic acid and its derivatives,¹¹⁹ chloroform,¹²⁰ oxalyl chloride,¹²¹ acyl chlorides,¹²² oxalic acid,¹²³ paraformaldehyde and methanol^{124, 125} to more complex compounds such as metal carbonyls,¹²⁶ aldehydes,^{127, 128} silacarboxylic acids,¹²⁹ and 9-methyl-fluorene-9-carbonyl chloride,¹²² among many others. Although, these surrogates provide advantages over the use of CO gas, additional reagents are required to initiate CO release. In most instances, spatial separation of the CO surrogate from the carbonylation reaction is necessary since reaction conditions for CO release are incompatible with the carbonylation chemistry. Current approaches involve thermal activation or transition metal-mediated CO release in one vessel, run in parallel with a secondary vessel where carbonylation takes place (**Fig 1A**). There are several CO surrogates that can be used in one-pot systems. However, their applicability is most often limited to highly specific reaction conditions.

One major hurdle is the inaccessibility of alkyl halides as substrates for transition metal-catalyzed carbonylation reactions. Carbonylation of alkyl halides is challenging due to its inherently slow oxidative addition step coupled with increased propensity to undergo isomerization via β -elimination.¹³⁰ Through a radical pathway, previously challenging substrates such as non-activated alkyl halides and bulky nucleophiles have been made more accessible for carbonylation reactions.¹³¹⁻¹³⁴

Herein, we describe the design and synthesis of a high-content CO donor that utilizes low-power blue LED as a clean, remote trigger for CO release. This photo-activated CO donor performs as a versatile CO surrogate that can be used under various conventional Pd-catalyzed carbonylation reactions. Its utility is further exemplified in carbonylation reactions employing light to access usually restrictive, less-reactive alkyl halide and bulky nucleophile substrates (**Fig 1B**).¹³¹⁻¹³³ In these examples, the same blue light that activates the CO donor also assists in the catalysis. The polymeric version of this photo-activated donor extends its utility to include suitability in fully aqueous systems which could be an entry point for further biological applications.

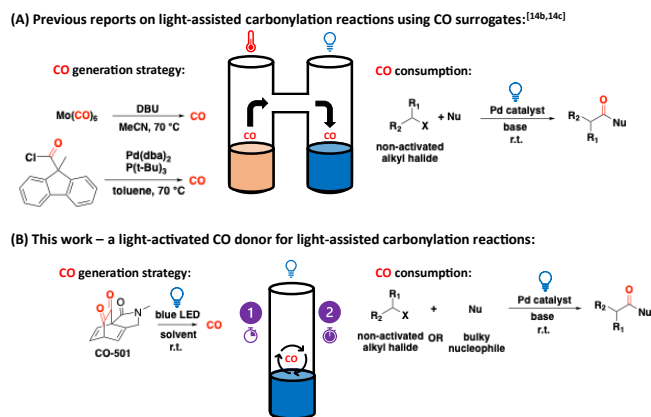


Figure 4-1. (A) For light-assisted carbonylation reactions using CO surrogates, a two-chamber reaction vessel is needed. (B) Photoactivated CO donor simplifies set-up and protocol.

4.1.1 Preliminary Work Conducted by Dr. Ladie Kimberly De La Cruz

We based our design on the photo-labile chemistry of bridged 1,2-diketones. Aromatic 1,2-diketone photoprecursors of polyacenes have been previously shown to extrude the diketone moiety as two equivalents of CO.^{135, 136} Photobisdecarbonylation under visible light is partially driven by extending and conjugating the isolated aromatic rings originally present in the precursor. We sought to synthesize an aliphatic version of the bridged 1,2-diketone and test if this will still result in extrusion of two equivalents of CO under visible light irradiation. To construct the aliphatic 1,2-diketone moiety, literature precedents describe an intermolecular Diels-Alder reaction between 1,2-quinones and strained alkyne partners,¹³⁷ which requires tedious synthesis. A simplified synthesis (3-4 steps) via an intramolecular approach starting from the cheap and readily available catechol, 2,3-dihydroxybenzoic acid was carried out to prepare the photoactivated CO donor, **CO-501 (Figure 2)**. Amidation to a propargylic amine installs an alkyne intramolecular to the latent quinone group formed after oxidation of the catechol moiety. The diene of the benzoquinone reacts via a Diels-Alder reaction with the tethered alkyne. Echoing our earlier findings,^{57, 138} tethering a regular alkyne intramolecular to its dienone partner obviated the need for a strained alkyne to drive the Diels-Alder reaction.

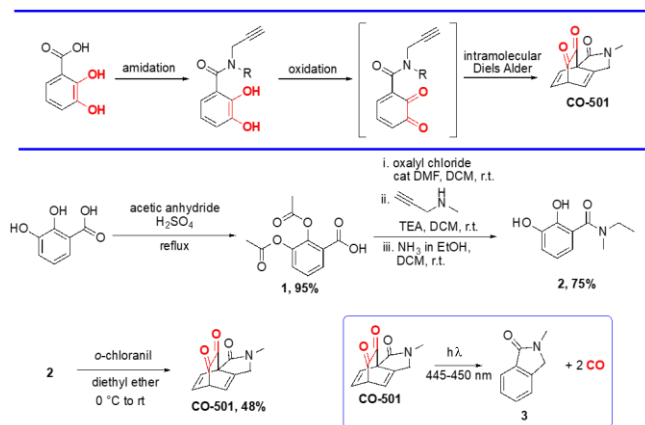


Figure 4-2. Strategy to prepare **CO-501** that undergoes photochemical transformation to release two equivalents of CO and by-product **3**.

The UV-Vis spectrum of **CO-501** shows two absorption bands. The absorption between 420 to 500 nm with λ_{max} of 441 nm corresponds to the $n\text{-}\pi^*$ transition of the carbonyl groups. Irradiation for 5 minutes with blue LED (440-445 nm) led to the gradual disappearance of the absorption at this wavelength (**Fig 3A**). Under ambient light, **CO-501** remains stable (**Fig 3B**) for at least a few hours. $^1\text{H-NMR}$ study reveals that upon irradiation all three alkene protons (a, b, d) and bridgehead proton (c) are converted to aromatic protons (g-j) accompanied by the disappearance of complex splitting due to the diastereotopic methylene protons (e and e') consistent with the formation of photoproduct **3** (**Fig 3C**). Likewise, ^{13}C NMR shows disappearance of two carbonyl carbons (α and β) and downfield shift of the two bridgehead carbons (γ and c) to the aromatic region. Furthermore, GC-TCD headspace analysis of **CO-501** confirmed unloading of two equivalents of CO (27 mol wt% CO) upon exposure to blue LED. These characterization studies validate the possible use of **CO-501** as a CO surrogate for carbonylation reactions.

In aqueous systems, 1,2-diketones are readily and reversibly hydrated.¹³⁹ Liao and co-workers reported that hydration prevents 1,2-diketones from releasing CO, and that micellar structures¹³⁶

and hydrophobic moieties such as *tert*-butyl groups¹⁴⁰ can circumvent the hydration problem. **CO-501** also undergoes hydration. However, instead of abolishing its CO releasing capability, hydration merely slows down the process. The diketone $n\text{-}\pi^*$ transition at 441 nm present in DMSO also disappears in the presence of water while another peak appears at ~380 nm. This suggests that one of the carbonyl groups is hydrated, leaving one ketone group intact. NMR studies show that the hydration equilibrium favors the hydrated form in DMSO:water solutions. Upon extended irradiation with LED (440-445 nm) for around 65 min, the hydrated products were converted to compounds with spectra corresponding to that of by product **3**. Reversibility of the hydration was further confirmed when resuspension in DMSO of a lyophilized 1:1 DMSO- d_6 :D₂O solution gave an NMR spectrum corresponding to that of intact **CO-501**. CO yield is also dependent on water ratio. At 50% DMSO, only 0.8 eq of CO was recovered after 5 minutes of irradiation. Increasing the irradiation time to 30 min increased CO recovery up to 1.5 eq. Further increase in water content up to 98% water in DMSO led to a yield of 1.2 eq of CO after irradiation for 30 min, representing a slight decrease in CO production. These findings indicate that these 1,2-diketones are compatible with applications in aqueous systems. Nevertheless, irradiation time of **CO-501** will need to be adjusted accordingly to achieve maximal CO yield.

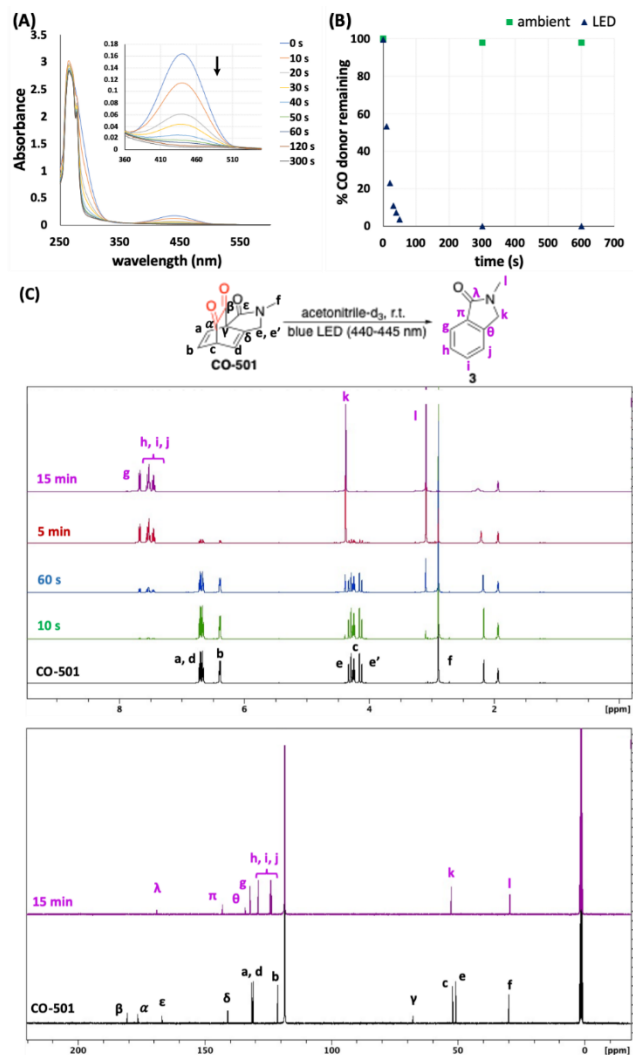
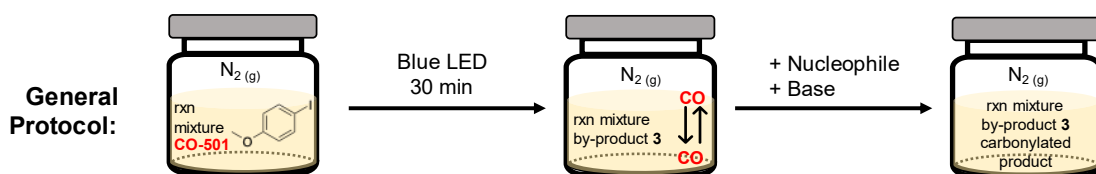
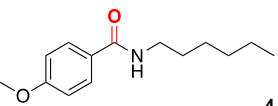
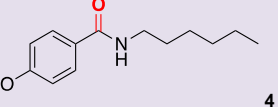
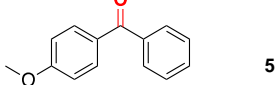
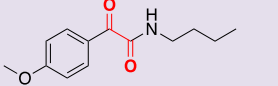
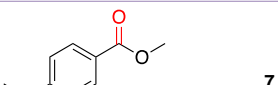
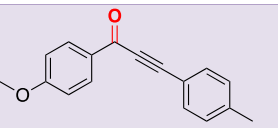


Figure 4-3. A) UV-Vis spectrum **CO-501** (1 mM in DMSO) upon exposure to blue LED light. (B) **CO-501** is stable under ambient light but releases CO when exposed to blue LED. (C) NMR studies confirming conversion of **CO-501** to photoproduct **3**

4.2 Results and Discussion

Table 4-1. Proof-of-concept studies on the applicability of **CO-501** as a CO surrogate for various carbonylation reactions (≈ 0.1 mmol scale) under different reaction conditions. $\# \approx 1$ mmol scale.



Carbonylative Reactions	Reaction Partner/Nucleophile	Catalyst/Ligand	Base	Solvent	Temp (°C)	Product	%yield, isolated
Aminocarbonylation ¹²²	hexan-1-amine	$Pd(dba)_2$, PPh_3	Et_3N	dioxane	80	 4	89 (98) [#]
Aminocarbonylation ¹³³	hexan-1-amine	$Pd(PPh_3)_4$	K_2CO_3	MeTHF:H ₂ O	r.t.	 4	82
Carbonylative Suzuki-Miyaura ¹⁴¹	phenylboronic acid	$Pd_2(dba)_3$	K_2CO_3	anisole	100	 5	80
Double Carbonylation ¹⁴²	butan-1-amine	$Pd(t-Bu_3P)_2$	DBU	THF	r.t.	 6	77
Alkoxy carbonylation ¹⁴³	methanol	$Pd(OAc)_2$, Xantphos	Et_3N	acetonitrile	80	 7	56
Carbonylative Sonogashira ¹⁴⁴	4-ethynyltoluene	$PdCl_2$, Xantphos	Et_3N	dioxane	80	 8	79

Due to the vicinal carbonyl moieties, 1,2-diketones such as **CO-501** are rendered more susceptible to attack by nucleophiles. Control experiments indicate when all reaction components are added together with the CO donor, no carbonylated products are observed (**Table S1**). This could be explained by the reaction of **CO-501** with the base and/or amine nucleophiles that are usually added in excess. In the presence of triethylamine and hexylamine, CO yield is decreased and completely abolished, respectively (**Fig S10**). Because of this, use of donors with electrophilic

centers would need physical separation of the CO generating reaction from the carbonylation reaction.

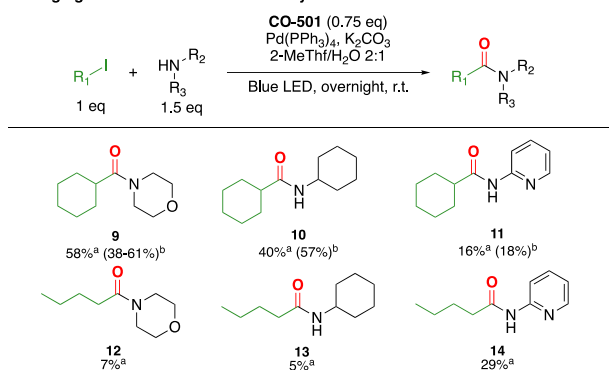
The use of commercially available two-chamber gas reactors have been shown to be effective in employing most of the CO surrogates.¹⁴⁵ Here, because CO generation is light-activated, instead of spatial separation, we utilize light as an external trigger to temporally enrich the reaction vessel with CO before the addition of reaction components that may inactivate the donor. Indeed, we find that chronological separation of the CO generation process and the carbonylation reaction allowed the use of **CO-501** in various carbonylative reactions under a wide range of reaction conditions (**Table 1**). We carried out the reactions in various vessel volumes ranging from 6-20 mL vials and in 50-mL round-bottom flasks for larger scale reactions (**Fig S12**) and found **CO-501** and this protocol to be widely applicable.

Because **CO-501** releases two equivalents of CO, sub-stoichiometric amount of the donor is needed to provide more than one equivalent of CO to the reaction mixture. The low-power visible light needed for the reaction coupled with the fast kinetics associated with the photo-bisdecarbonylation of **CO-501** provides CO within 30 minutes of irradiation without instigating possible cross photoreaction of 1,2-diketones¹⁴⁶ with other components of the reaction mixture. Results also indicate that photoproduct **3** is a stable, benign by-stander that does not interfere with the carbonylation process.

Up to this point we showed that **CO-501** is a CO donor that can be used in conventional Pd-catalyzed carbonylation reactions. Next, we demonstrate that the photolysis conditions to release CO from **CO-501** is compatible with the conditions needed for light-assisted carbonylation of challenging substrates. In prior works utilizing CO surrogates for light-mediated carbonylation, a two-chamber set-up is required to accommodate the different reaction conditions employed for

CO generation and light-assisted carbonylation reactions.^{132, 133} Here, we show that **CO-501** can be used in a simplified, one-pot reaction set-up that is convenient for light-mediated carbonylation reactions. Cyclohexyl iodide and butyl iodide with either primary or secondary amine nucleophiles were carbonylated under these reaction conditions (**Figure 4**). Carbonylation with the bulky nucleophile 2,6-diisopropylaniline was also shown to be compatible with **CO-501** and the protocol (**Figure 4**).

(A) Challenging Substrate - Non-activated alkyl halides^[14c]



(B) Challenging Substrate - Bulky Nucleophile^[14a]

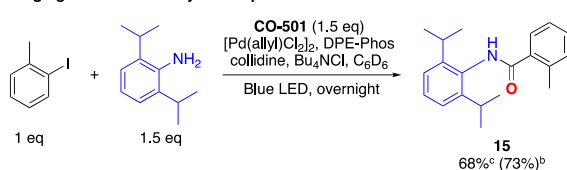


Figure 4-4. Light-activated CO surrogate for light-assisted carbonylation reactions of challenging substrates. (A) non-activated alkyl iodides (B) bulky nucleophile. (^aisolated yield, ^bliterature yield, ^cNMR yield)

4.3 Conclusion

In summary, the photo-activated CO donor **CO-501** delivers CO upon activation by low power blue LED light. To the best of our knowledge, these are the first photo-activated, one-pot CO donors that have been demonstrated to be applicable under different carbonylation reaction conditions. More specifically, the use of this light-activated donor has been demonstrated to be compatible with blue light-assisted carbonylation reactions of un-activated alkyl halides. Further,

there have been literature reports of various ways of synthesizing catechols (precursors to the CO donors described) with demonstrated ability to accommodate isotopic labeling using either C-13 or O-18 or both.^[26a-c] Such methods make it possible to synthesize isotopically labeled CO donors.

4.4 Experimental

4.4.1 General

All reagents and solvents were used as received without further purification. Starting materials and solvents were purchased from Sigma-Aldrich, VWR International, or Oakwood Chemicals. Analytical-grade solvents were used for all reactions except for moisture-sensitive reactions, in which anhydrous solvents were used. Thin layer chromatography was performed on glass-backed silica gel TLC plates (250 μm) using mixtures of hexanes/ethyl acetate as eluent, and using either UV light, iodine powder, or potassium permanganate stain for visualization. Column chromatography was done using Silica Flash P60 silica gel (230-400 mesh). ^1H - and ^{13}C -NMR spectra were recorded on Bruker-400 spectrometers (400 MHz and 100 MHz, respectively). Chemical shifts were reported in ppm relative to residual solvent peaks (δ 77.26 for ^1H , 77.1 for ^{13}C , $\text{CHCl}_3/\text{CDCl}_3$) and (δ 2.49 for ^1H , and 39.1 for ^{13}C , $\text{DMSO}/\text{DMSO}-d_6$). Data are reported as follows: bs= broad singlet, s= singlet, d= doublet, t= triplet, q= quartet, m= multiplet, dd= doublet of doublets, ddd= doublet of doublet of doublets, ddt= doublet of doublets of triplets, td= triplet of doublets; coupling constants in Hz; integration. Accurate mass measurements were performed by the Mass Spectrometry Facilities at Georgia State University. For spectrophotometric studies, Varian Cary 100-Bio was used as UV-Vis spectrophotometer. Agilent 7820A with TCD detector was used for CO quantification.

4.4.2 Synthesis of CO-501

Compound **1**¹⁴⁷: To a solution of 2,3-dihydroxybenzoic acid (340 mg, 2.2 mmol) in acetic anhydride (650 μ L, 6.8 mmol) was added five drops of H₂SO₄. The reaction mixture was heated under reflux for 2 h. After cooling to room temperature, iced water was added, and the reaction was stirred for a few minutes. The precipitate was filtered to give an off-white solid (323 mg, 95%). ¹H NMR (CDCl₃): δ 7.99 (1H, m), 7.44 (1H, m), 7.36 (1H, t, J = 8.0 Hz), 2.34 (3H, s), 2.33 (3H, s). ¹³C NMR (CDCl₃): δ 169.2, 168.6, 168.4, 143.8, 143.3, 129.7, 129.0, 126.4, 124.1, 20.7. HRMS (ESI) calculated for C₁₁H₁₀O₆ [M+Na]⁺: m/z 261.0375, found 261.0368.

Compound **2**: To a solution of **2** (304 mg, 1.3 mmol) in anhydrous DCM was added oxalyl chloride (240 μ L, 2.8 mmol) followed by DMF (3 drops). The reaction mixture was stirred at room temperature. Gas evolution was observed. After 1 h, the solvent was removed *in vacuo*, then the crude acid chloride was redissolved in DCM while cooling in an ice-water bath. Triethylamine (400 μ L, 2.0 mmol) was added dropwise followed by the addition of the *N*-methylpropargylamine (130 μ L, 1.2 mmol) dropwise. The reaction mixture was removed from ice-bath and allowed to run at room temperature for 1.5 h. The solvent was removed *in vacuo* and the crude product was loaded into a column and eluted using DCM. The isolated compound was dissolved in ammonia in ethanol (2.0 M, 4.8 mL, 9.6 mmol) and stirred overnight. The mixture was concentrated under rotary evaporation and loaded into a silica gel column using 15:3 hexane: ethyl acetate as the eluent to give a white solid (256 mg, 75% over three steps). ¹H NMR (CDCl₃): δ 6.97-6.94 (2H, m), 6.76 (1H, t, J = 8.0 Hz), 4.26 (2H, m), 3.20 (3H, s), 2.36 (1H, m). ¹³C NMR (CDCl₃): δ 171.6, 146.0, 145.9, 119.3, 119.2, 117.8, 117.4, 78.1, 73.2, 60.5, 21.1. HRMS (ESI) calculated for C₁₁H₁₁NO₃ [M+Na]⁺: m/z 228.0637, found 228.0640.

CO-501: To **2** (300 mg, 1.5 mmol) dissolved in diethyl ether was added *o*-chloranil (378 mg, 1.5 mmol) while stirring at -78 °C for 30 min. Then the reaction mixture was removed from the dry ice-acetone bath and stirred at room temperature. After 30 min, ether was removed through rotary evaporation and residue was loaded into a column and eluted using 4:1 dichloromethane: ethyl acetate to give a bright yellow solid (144 mg, 48%). ¹H NMR (DMSO-*d*₆): δ 6.65-6.73 (2H, m), 6.38-6.40 (1H, dt, *J* = 6.1, 2.1 Hz), 4.11-4.33 (2H, qd,), 4.23-4.26 (1H, td, *J* = 6.0, 1.8 Hz), 2.89 (3H, s). ¹³C NMR (DMSO-*d*₆): δ 180.6, 176.4, 166.8, 140.9, 131.3, 130.8, 121.2, 67.7, 52.0, 50.8, 29.9. HRMS (ESI) calculated for C₁₁H₉NO₃ [M+Na]⁺: *m/z* 226.0480, found 226.0488. Decomposition temperature of 106 °C (started to decolorize without melting)

Large scale synthesis of **CO-501: 2** (1220 mg), *o*-chloranil (1610 mg). Bright yellow solid (633 mg, 52%).

Alternative Procedure to compound **2**:

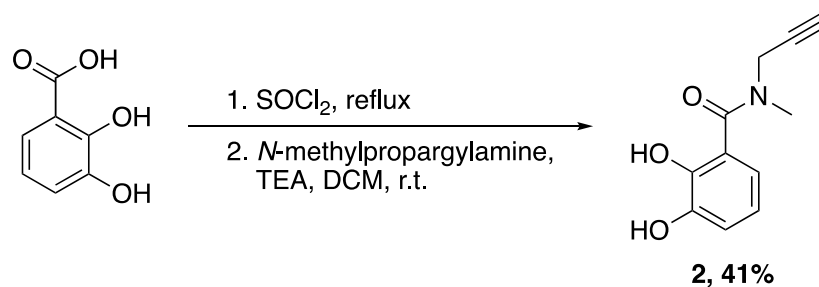


Figure S 4-1. Alternative procedure to obtain intermediate 2

2,3-Dihydroxybenzoic acid (2 g, 13 mmol) was suspended in SOCl₂ (8 mL, 110 mmol) and then heated at reflux for 3 h. After cooling to room temperature, reaction mixture was concentrated

by rotary evaporation to give a slight yellow solid. The crude product was dissolved in DCM followed by slow addition of triethylamine (2.8 mL, 20 mmol) and *N*-methylpropargylamine (1.6 mL, 19.2 mmol). After stirring overnight, reaction mixture was concentrated in the rotary evaporator to give a sticky yellow residue. Residue was redissolved in dichloromethane, washed with 1M HCl and brine, and concentrated in the rotary evaporator. The residue was loaded into a column using 25:1 dichloromethane: ethyl acetate as eluent (1.09 g, 41%).

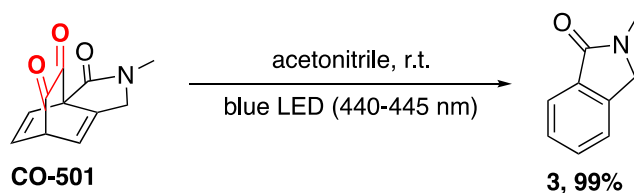


Figure S 4-2. **CO-501** is converted to photoproduct **3** after blue LED irradiation

Synthesis of photoproduct 3

CO-501 (52.3 mg, 0.26 mmol) was dissolved in acetonitrile and exposed to blue LED for 1 h. The solution gradually turned from bright yellow to colorless. After completion of reaction based on TLC, the reaction mixture was concentrated in the rotary evaporator, loaded into a column, and eluted using 3:1 dichloromethane: ethyl acetate to give a white solid (37.6 mg, 99%). ¹H NMR (ACN-d₃): δ 7.68 (1H, d, *J* = 7.5 Hz), 7.58-7.51 (2H, m), 7.46 (1H, t, *J* = 7.8 Hz), 4.38 (2H, s), 3.10 (3H, s). ¹³C NMR (ACN-d₃): δ 168.8, 142.9, 133.9, 132.0, 128.7, 124.0, 123.6, 52.5, 29.4. HRMS (ESI) calculated for C₉H₉NO₁₀ [M+Na]⁺: *m/z* 170.0582, found 170.0587.

4.4.3 General Protocol

Alkyl/aryl halide, Pd source, ligand, and **CO-501/502** are weighed into a reaction vessel then sealed. Air is removed by vacuum and replaced with N₂ via a balloon; such actions are repeated three times. Non-nucleophilic solvent is added and N₂ balloon is removed. Reaction vessel is exposed to blue LED for 30 min at 3 cm distance. Remaining reagents (nucleophile, base, and nucleophilic solvent) are added directly or dissolved in additional solvent through a syringe. Then, reaction is allowed to proceed.

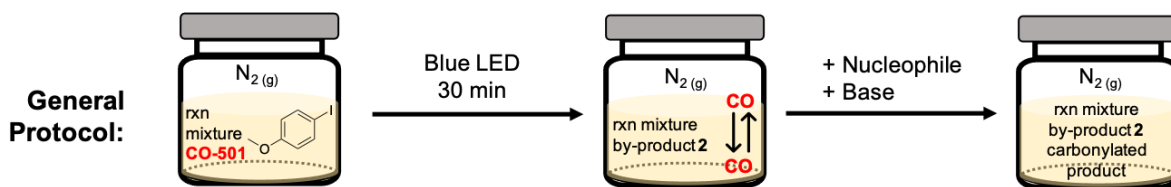


Figure S 4-3. General protocol temporally separating CO generation and carbonylation reaction

4.4.4 Reaction Vessel

Most of the reaction vessels used in this paper are crimp top vials (either 6-mL or 20-mL) sealed using aluminum septum caps. A large scale set-up using a 50-mL round bottom flask with a rubber septum was also used.

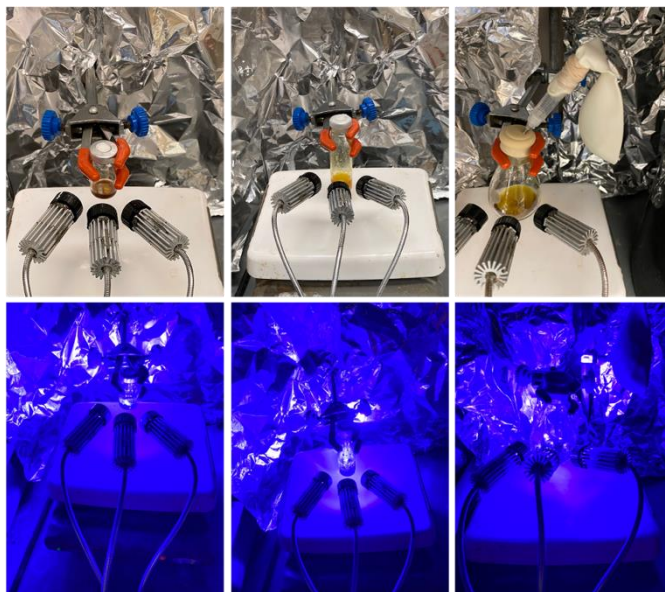


Figure S 4-4. Reaction vessels: 1st column – 6-mL vial (0.1 mmol scale); 2nd column – 20-mL vial (0.1 mmol to 0.6 mmol scale); 3rd column: 50-mL reaction flask (1 mmol scale) with attached empty balloon to allow for expansion of gas at higher temperature.

4.4.5 Proof-of-concept- CO-501 as a CO source for various carbonylative reactions

4.4.5.1 Carbonylative Amidation

a. Carbonylative Amidation, reaction condition 1 – compound **4**.¹²²

4-Methoxyiodobenzene (26.6 mg, 0.11 mmol), Pd(dba)₂ (3.8 mg, 6.6 μ mol), PPH₃ (16.2 mg, 14.9 μ mol), and **CO-501** (16.2 mg, 0.08 mmol) were weighed into a 6-mL crimp top vial and sealed. After evacuation of air and replacement with N₂, anhydrous dioxane was added (0.5 mL). Then vial was exposed to blue LED for 30 min at 3-cm distance. Then, 6-aminohexane (0.03 mL, 0.23 mmol), and triethylamine (0.03 mL, 0.21 mmol) were added, and the reaction mixture stirred at 80 °C overnight. Dioxane was removed by rotary evaporation and the residue was loaded into a column and eluted using 5:1 hexane: ethyl acetate to give a faintly yellow solid (23.8 mg, 89%).
¹H NMR (CDCl₃): δ 7.72 (2H, d, J = 8.7 Hz), 6.89 (2H, d, J = 8.7 Hz), 6.24 (1H, bs), 3.82 (3H, s),

3.40 (2H, q, $J =$), 1.54-1.61 (2H, m), 1.29-1.38 (6H, m), 0.86-0.89 (3H, m). ^{13}C NMR (CDCl_3): δ 167.1, 162.1, 128.7, 127.3, 113.8, 55.5, 40.2, 31.6, 29.8, 26.8, 22.7, 14.1.

b. Carbonylative Amidation, reaction condition 1 (1 mmol scale) – compound **4**:¹²²

4-Methoxyiodobenzene (233.1 mg, 0.996 mmol), $\text{Pd}(\text{dba})_2$ (29.7 mg, 0.052 mmol), PPh_3 (29.6 mg, 0.113 mmol), and **CO-501** (152.2 mg, 0.75 mmol) were weighed into a 50-mL reaction flask. Then, the flask was sealed using a rubber septum. Air was evacuated and replaced with N_2 via a balloon three times. Under N_2 balloon, anhydrous dioxane (10 mL) was added via syringe. Then the N_2 balloon was replaced by an empty balloon. The vial was exposed to blue LED light for 30 min at 3 cm distance. Then, 6-aminohexane (0.3 mL, 2.28 mmol) and Et_3N (0.3 mL, 2.28 mmol) were added via syringe. The reaction was stirred at 80°C for 25 h. Solvent was removed by rotary evaporation. Product was isolated through column chromatography (5:1 hexane: ethyl acetate) to give a faintly tan-orange solid (229.4 mg, 98%).

c. Carbonylative Amidation, reaction condition 2 – compound **4**:¹³³

4-Methoxyiodobenzene (26.4 mg, 0.11 mmol), $\text{Pd}(\text{PPh}_3)_4$ (7.7 mg, 6.6 μmol), and **CO-501** (16.4 mg, 0.081 mmol) were weighed into a 6-mL crimp top vial and sealed. After evacuation of air and replacement with N_2 , 2-methyltetrahydrofuran was added (0.3 mL). Then vial was exposed to blue LED for 30 min at 3 cm distance. Then, 6-aminohexane (0.5 mL, 0.38 mmol), and K_2CO_3 (15 mg, 0.11 mmol) dissolved in deionized water (0.2 mL) were added, and the reaction mixture stirred at room temperature overnight under continuous blue LED irradiation. Solvent was removed by rotary evaporation and the residue was loaded into a column and eluted using 5:1 hexane: ethyl acetate to give a faintly yellow solid (21.6 mg, 82%).

4.4.5.2 Carbonylative Suzuki Miyaura

d. Carbonylative Suzuki-Miyaura – compound **5**:¹⁴¹

4-Methoxyiodobenzene (0.12 mmol), Pd₂(dba)₃ (1 mol%), phenylboronic acid (0.12 mmol), and **CO-501** (0.275 mmol), and K₂CO₃ (0.33 mmol) were weighed into a 20-mL crimp top vial. The vial was sealed using aluminum septum caps. Air inside the vial is evacuated and replaced with N₂ via a balloon three times. Under N₂ balloon, anhydrous anisole (1.0 mL) was added via syringe, followed by removal of the balloon. The vial was exposed to blue LED light for 30 min at 3 cm distance. Vial was then placed in an oil bath and stirred at 100 °C for 20 h. Reaction was filtered through celite and washed with ethyl acetate. Compound was dry loaded onto flash column (10:1 hexane: ethyl acetate) to give a faintly yellow solid (19.8 mg, 80%). ¹H NMR (CDCl₃): δ 7.83 (2H, m), 7.75 (2H, t), 7.56 (1H, t), 7.46 (2H, t), 6.96 (2H, q), 3.88 (3H, s); ¹³C NMR (CDCl₃): δ 195.7, 163.3, 138.4, 132.7, 132.0, 130.3, 129.9, 128.3, 113.7, 55.6.

4.4.5.3 Double Carbonylation

e. Double Carbonylation – compound **6**:¹⁴²

4-Methoxyiodobenzene (0.13 mmol), Pd(t-BuP)₂ (0.004 mmol), and **CO-501** (0.192 mmol) were weighed into a 20-mL crimp top vial. The vial was sealed using aluminum septum caps. Air inside the vial is evacuated and replaced with N₂ via a balloon three times. Under N₂ balloon, dry tetrahydrofuran (1.0 mL) was added via syringe, followed by removal of the balloon. The vial was exposed to blue LED light for 30 min at 3 cm distance. Then, n-butylamine (0.30 mmol) and DBU (0.33 mmol) were added via syringe. The reaction was stirred at room temperature for 24 h. Solvent was removed by rotary evaporation. Product was isolated through column chromatography (hexane: ethyl acetate) to give a white solid (19.3 mg, 77%). ¹H NMR

(CDCl₃): δ 8.41 (2H, d), 7.12 (1H, s), 6.94 (2H, d), 3.87 (3H, s), 3.37 (2H, q), 1.59 (2H, m), 1.40 (2H, q), 0.95 (3H, t); ¹³C NMR (CDCl₃): δ 186.0, 164.9, 162.5, 134.1, 126.7, 114.0, 77.5, 76.8, 55.7, 39.3, 31.5, 20.2, 13.8.

4.4.5.4 Alkoxyacylation

f. Alkoxyacylation – compound **7**:¹⁴³

4-Methoxyiodobenzene (24 mg, 0.103 mmol), Pd(OAc)₂ (1.2 mg, 5 μ mol), Xantphos (2.8 mg, 5 μ mol), and **CO-501** (16.5 mg, 0.081 mmol) were weighed into a 20-mL crimp top vial. The vial was sealed using aluminum septum caps. Air inside the vial is evacuated and replaced with argon via a balloon three times. Under argon balloon, dry acetonitrile (1.0 mL) was added via syringe, followed by removal of the balloon. The vial was exposed to blue LED light for 30 min at 3 cm distance. Then, Et₃N (250 μ L, 1.81 mmol) and MeOH (50 μ L, 1.07 mmol) were added via syringe. The reaction was stirred at 80 °C for 17 h. Solvent was removed by rotary evaporation. Product was isolated through column chromatography (25:1 hexane: ethyl acetate) to give an off-white solid (9.9 mg, 56%). ¹H NMR (CDCl₃): δ 7.99 (q, 2H), 6.91 (q, 2H), 3.89 (s, 3H), 3.85 (s, 3H); ¹³C NMR (CDCl₃): δ 167.0, 163.5, 131.7, 125.9, 122.8, 113.7, 90.3, 55.6, 52.0.

4.4.5.5 Carbonylative Sonogashira

g. Carbonylative Sonogashira – compound **8**:¹⁴⁴

4-Methoxyiodobenzene (30 mg, 0.13 mmol), 1-ethynyl-4-methylbenzene **40** (40 μ L, 0.256 mmol), PdCl₂ (2.8 mg, 0.016 mmol), Xantphos (4.0 mg, 7 μ mol), and **CO-501** (19.6 mg, 0.097 mmol) were weighed into a 20-mL crimp top vial. The vial was sealed using aluminum septum caps. Air inside the vial is evacuated and replaced with N₂ via a balloon three times. Under N₂

balloon, dry dioxane (1.0 mL) was added via syringe, followed by removal of the balloon. The vial was exposed to blue LED light for 30 min at 3 cm distance. Then, Et₃N (55 μ L, 0.384 mmol) were added via syringe. The reaction was stirred at 80 °C for 24 h. Solvent was removed by rotary evaporation. Product was isolated through column chromatography (hexane: ethyl acetate) to give a yellow-orange solid (25.1 mg, 79%). ¹H NMR (CDCl₃): δ 8.22 (d, 2H), 7.57 (d, 2H), 7.23 (q, 2H), 7.00 (d, 2H), 3.91 (d, 3H), 2.40 (q, 3H); ¹³C NMR (CDCl₃): δ 176.9, 164.5, 141.4, 133.1, 132.0, 130.5, 129.6, 117.3, 114.0, 93.1, 86.9, 55.7, 21.9.

4.4.6 *Light-assisted Carbonylation using CO-501 as a CO Source*

4.4.6.1 *Non-activated Alkyl Halide*

Compound **9**:¹³³

Iodocyclohexane (30.2 mg, 0.14 mmol), Pd(PPh₃)₄ (7.9 mg, 6.8 μ mol), and **CO-501** (21.5 mg, 0.11 mmol) were weighed into a 6-mL crimp top vial and sealed. After evacuation of air and replacement with N₂, 2-methyltetrahydrofuran was added (0.3 mL). Then vial was exposed to blue LED for 30 min at 3 cm distance. Then, morpholine (0.05 mL, 0.38 mmol) and K₂CO₃ (15 mg, 0.11 mmol) dissolved in deionized water (0.2 mL) were added, and the reaction mixture was stirred at room temperature overnight under continuous blue LED irradiation. Solvent was removed by rotary evaporation and the residue was loaded into a column and eluted using 10:3 hexane: ethyl acetate to give a white solid (17.8 mg, 58%). ¹H NMR (CDCl₃): δ 3.48-3.642 (8H, m), 2.37-2.44 (1H, m), 1.77-1.80 (2H,m), 1.67-1.70 (2H, m), 1.46-1.56 (2H, m), 1.20-1.30 (4H, m); ¹³C NMR (CDCl₃): δ 174.8, 67.1, 67.0, 46.0, 42.0, 40.3, 29.4, 25.9.

Compound **10**:¹³³

Iodocyclohexane (123.8 mg, 0.59 mmol), Pd(PPh₃)₄ (40.1 mg, 35 μ mol), and **CO-501** (93 mg, 0.45 mmol) were weighed into a 6-mL crimp top vial and sealed. After evacuation of air and replacement with N₂, 2-methyltetrahydrofuran was added (2 mL). Then vial was exposed to blue LED for 30 min at 3 cm distance. Then, aminocyclohexane (0.1 mL, 0.92 mmol) and K₂CO₃ (84 mg, 0.61 mmol) dissolved in deionized water (1 mL) were added, and the reaction mixture was stirred at room temperature overnight under continuous blue LED irradiation. Solvent was removed by rotary evaporation and the residue was loaded into a column and eluted using 5:1 hexane: ethyl acetate to give a white solid (49.7 mg, 40%). ¹H NMR (CDCl₃): δ 3.42 (1H, d), 3.67-3.77 (1H, m), 1.96-2.03 (1H, m), 1.73-1.88 (6H, m), 1.55-1.69 (4H, m), 1.27-1.43 (4H, m), 1.02-1.25 (6H, m); ¹³C NMR (CDCl₃): δ 175.3, 47.8, 45.7, 33.3, 29.8, 25.8, 25.6, 25.0.

Compound **11**:¹³²

Iodocyclohexane (49.9 mg, 0.24 mmol), Pd(PPh₃)₄ (13.9 mg, 12 μ mol), and **CO-501** (36.9 mg, 0.18 mmol) were weighed into a crimp top vial. The vial was sealed using aluminum septum caps. Air inside the vial is evacuated and replaced with N₂ via a balloon three times. Under N₂ balloon, 2-methyltetrahydrofuran (1.0 mL) was added via syringe, followed by removal of the balloon. The vial was exposed to blue LED light for 30 min at 3 cm distance. Then, 2-aminopyridine (75.9 mg, 0.81 mmol) and K₂CO₃ (36.9 mg, 0.28 mmol) in 0.5 mL deionized water were added via syringe. The reaction was stirred at room temperature overnight under continuous blue LED irradiation. Solvent was removed by rotary evaporation. Product was isolated through column chromatography (hexane: ethyl acetate) to give a faintly yellow solid (7.6 mg, 16%). ¹H NMR (CDCl₃): δ 1.27 (4H, m), 1.53 (2H, m), 1.69 (1H, q), 1.81 (2H, m), 1.97 (3H, d), 2.25 (1H,

m), 7.01 (1H, q), 7.69 (1H, m), 8.26 (3H, t); ^{13}C NMR (CDCl_3): δ 25.71, 25.77, 29.61, 46.60, 114.25, 119.72, 138.57, 147.72, 151.78, 174.99

Compound **12**:¹³²

Iodobutane (47.2 mg, 0.26 mmol), $\text{Pd}(\text{PPh}_3)_4$ (16.5 mg, 14 μmol), and **CO-501** (42.8 mg, 0.211 mmol) were weighed into a crimp top vial. The vial was sealed using aluminum septum caps. Air inside the vial is evacuated and replaced with N_2 via a balloon three times. Under N_2 balloon, 2-methyltetrahydrofuran (1.0 mL) was added via syringe, followed by removal of the balloon. The vial was exposed to blue LED light for 30 min at 3 cm distance. Then, morpholine (80 μL , 0.91 mmol) and K_2CO_3 (43.3 mg, 0.31 mmol) in 0.5 mL deionized water were added via syringe. The reaction was stirred at room temperature overnight under continuous blue LED irradiation. Solvent was removed by rotary evaporation. Product was isolated through column chromatography (hexane: ethyl acetate) to give a faintly yellow solid (2.3 mg, 5%). ^1H NMR (CDCl_3): δ 0.92 (3H, t), 1.36 (2H, q), 1.60 (2.37, m), 2.30 (2H, t), 3.46 (2H, t), 3.62 (6H, m); ^{13}C NMR (CDCl_3): δ 14.02, 22.71, 27.49, 32.99, 41.99, 46.20, 66.83, 67.11, 172.05

Compound **13**:¹³²

Iodobutane (56.3 mg, 0.31 mmol), $\text{Pd}(\text{PPh}_3)_4$ (20.1 mg, 17 μmol), and **CO-501** (45.2 mg, 0.22 mmol) were weighed into a crimp top vial. The vial was sealed using aluminum septum caps. Air inside the vial is evacuated and replaced with N_2 via a balloon three times. Under N_2 balloon, 2-methyltetrahydrofuran (1.0 mL) was added via syringe, followed by removal of the balloon. The vial was exposed to blue LED light for 30 min at 3 cm distance. Then, cyclohexylamine (110 μL , 0.96 mmol) and K_2CO_3 (43.4 mg, 0.31 mmol) in 0.5 mL deionized water were added via syringe. The reaction was stirred at room temperature overnight under continuous blue LED irradiation.

Solvent was removed by rotary evaporation. Product was isolated through column chromatography (hexane: ethyl acetate) to give a faintly yellow solid (4.2 mg, 7%). ^1H NMR (CDCl_3): δ 0.91 (4H, m), 1.13 (4H, m), 1.38 (4H, m), 1.66 (6H, m), 1.92 (2H, m), 2.15 (2H, t), 3.78 (1H, m), 5.30 (1H, s); ^{13}C NMR (CDCl_3): δ 13.83, 22.39, 24.88, 25.55, 27.98, 29.70, 33.29, 36.86, 48.01, 172.17

Compound **14**:¹³²

Iodobutane (57.4 mg, 0.31 mmol), $\text{Pd}(\text{PPh}_3)_4$ (23.1 mg, 20 μmol), and **CO-501** (53.2 mg, 0.26 mmol) were weighed into a crimp top vial. The vial was sealed using aluminum septum caps. Air inside the vial is evacuated and replaced with N_2 via a balloon three times. Under N_2 balloon, 2-methyltetrahydrofuran (1.0 mL) was added via syringe, followed by removal of the balloon. The vial was exposed to blue LED light for 30 min at 3 cm distance. Then, 2-aminopyridine (100.0 mg, 1.06 mmol) and K_2CO_3 (53.2 mg, 0.43 mmol) in 0.5 mL deionized water were added via syringe. The reaction was stirred at room temperature overnight under continuous blue LED irradiation. Solvent was removed by rotary evaporation. Product was isolated through column chromatography (hexane: ethyl acetate) to give a faintly yellow solid (16.2 mg, 29%). ^1H NMR (CDCl_3): δ 0.93 (3H, t), 1.39 (2H, m), 1.70 (2H, m), 2.39 (2H, t), 7.03 (1H, m), 7.68 (1H, m), 8.24 (2H, t), 8.60 (1H, s); ^{13}C NMR (CDCl_3): δ 13.90, 22.44, 27.55, 37.60, 114.33, 119.74, 138.59, 147.71, 151.74, 172.10.

4.4.6.2 *Bulky Nucleophile*

Compound **15**:¹³¹

2-Iodotoluene (16.9 mg, 0.08 mmol), $[\text{Pd}(\text{allyl})\text{Cl}_2]_2$ (4.6 mg, 13 μmol), Bis[(2-diphenylphosphino)phenyl] ether, DPE-Phos (7.4 mg, 14 μmol), **CO-501** (21.3 mg, 0.10 mmol),

tetrabutylammonium chloride, Bu₄NCl (21.7 mg, 78 μmol), and benzyl benzoate (8.8 mg, 41 μmol) were weighed into a 6-mL crimp top vial and sealed. After evacuation of air and replacement with N₂, C₆D₆ was added (0.5 mL). Then vial was exposed to blue LED for 30 min at 3 cm distance. Then, 2,6-di-*tert*-butylaniline (0.02 mL, 0.11 mmol), and collidine (0.02 mL, 0.15 mmol) were added, and the reaction mixture stirred at room temperature overnight under continuous blue LED irradiation. NMR yield was calculated based on 2-iodotoluene as limiting reactant and benzyl benzoate as standard.

5 CONCLUSION

During my time in my PhD, I have worked on many projects, all of which focused on the end goal of progressing different areas of the CO field. In the realm of synthetic organic chemistry, my efforts were used towards demonstrating the wide-applicability of a photo-activated CO surrogate developed in our lab for one-pot Pd-catalyzed and light mediated carbonylation reactions. In the realm of medicinal chemistry, my work has been broad, ranging from development of CO prodrugs, working with CO probes, and highlighting new potential for CO in neuromodulation and cognition. The therapeutic potential of endogenous and exogenous carbon monoxide has been well studied over the last four decades, and in my time, I have become incredibly passionate about the significance and value of the promising future of CO as a broadly applicable therapeutic. Through this, I learned that the field is being convoluted and held back by a 20-year detour involving the commercially available CO-releasing molecules (CORMs). These CORMs have led many research directions astray, including introducing brand-new mechanisms for “CO”, such as antibacterial properties and induction of HO-1, that have later been shown to be completely CO-independent. My work specifically has holistically brought together the foundational issues and unreliability with the commercially available CORMs including a lack of idiosyncratic CO production, CO-independent chemical and biological activity, and lack of good negative controls of the carrier. More specifically, we have reported the idiosyncratic CO production and redox activity of CORM-A1, as well as the variable CO production and impure commercial samples of CORM-401, for the first time.

Along this line I make one final point: the original reports of the CORMs do not demonstrate malintent, rather just a small oversight that led to a 20-year snowball effect. The contention comes from the continued use and promotion of the CORMs from prominent researchers and more

importantly, commercial vendors, despite the plethora of papers outlining the serious implications of using CORMs without proper controls. At this time, it can no longer be attributed to accidental misinterpretation of results or understandable human error, which is completely normal within the realm of research. Rather, the continued ignorance of the issues at hand seemingly indicates interests outside of robust research, but at the consequence of leading young researchers down the wrong path and holding the CO field back from progressing and reaching the shared goal of defining CO as a broadly applicable therapeutic. I hope that my time and energy spent during my PhD tenure only has one impact: to clear up the convolution and help future researchers down the right path in developing strong, robust data to support the use of CO as a therapeutic. Finally:

In science, there is no absolute truth, only ever-evolving theories and evidence.

However, scientific research is a tireless pursuit of truth, undeterred by mistakes or failures, all in the best interest of scientific progress.

REFERENCES

1. Sjostrand, T., Endogenous formation of carbon monoxide in man. *Nature* **1949**, *164*, 580.
2. De La Cruz, L. K. C.; Wang, B., Carbon Monoxide Production: In Health and in Sickness. In *Carbon Monoxide in Drug Discovery: Basics, Pharmacology, and Therapeutic Potential*, Wang, B.; Otterbein, L. E., Eds. John Wiley and Sons, Hoboken, New Jersey: 2022; pp 302-318.
3. Engstedt, L., Endogenous formation of carbon monoxide in hemolytic disease; with special regard to quantitative comparisons to other hemolytic indices. *Acta Med Scand Suppl* **1957**, *332*, 1-63.
4. Coburn, R. F.; Forster, R. E.; Kane, P. B., Considerations of the physiological variables that determine the blood carboxyhemoglobin concentration in man. *J Clin Invest* **1965**, *44* (11), 1899-910.
5. Coburn, R. F.; Williams, W. J.; Forster, R. E., Effect of Erythrocyte Destruction on Carbon Monoxide Production in Man. *J Clin Invest* **1964**, *43*, 1098-103.
6. Wang, B.; Otterbein, L. E., *Carbon Monoxide in Drug Discovery: Basics, Pharmacology, and Therapeutic Potential*. First ed.; John Wiley and Sons: Hoboken, New Jersey, 2022.
7. De La Cruz, L. K.; Yang, X.; Menshikh, A.; Brewer, M.; Lu, W.; Wang, M.; Wang, S.; Ji, X.; Cachuela, A.; Yang, H.; Gallo, D.; Tan, C.; Otterbein, L.; De Caestecker, M.; Wang, B., Adapting decarbonylation chemistry for the development of prodrugs capable of *in vivo* delivery of carbon monoxide utilizing sweeteners as carrier molecules. *Chem. Sci.* **2021**, *12* (31), 10649-10654.
8. Correa-Costa, M.; Gallo, D.; Csizmadia, E.; Gomperts, E.; Lieberum, J.-L.; Hauser, C. J.; Ji, X.; Wang, B.; Câmara, N. O. S.; Robson, S. C.; Otterbein, L. E., Carbon monoxide protects the kidney through the central circadian clock and CD39. *PNAS* **2018**, *115* (10), E2302-E2310.
9. Zheng, Y.; Ji, X.; Yu, B.; Ji, K.; Gallo, D.; Csizmadia, E.; Zhu, M.; Choudhury, M. R.; De La Cruz, L. K. C.; Chittavong, V.; Pan, Z.; Yuan, Z.; Otterbein, L. E.; Wang, B., Enrichment-triggered prodrug activation demonstrated through mitochondria-targeted delivery of doxorubicin and carbon monoxide. *Nat. Chem.* **2018**, *10* (7), 787-794.
10. Zuckerbraun, B. S.; Billiar, T. R.; Otterbein, S. L.; Kim, P. K. M.; Liu, F.; Choi, A. M. K.; Bach, F. H.; Otterbein, L. E., Carbon Monoxide Protects against Liver Failure through Nitric Oxide-induced Heme Oxygenase 1. *J. Exp. Med.* **2003**, *198* (11), 1707-1716.
11. Kyokane, T.; Norimizu, S.; Taniai, H.; Yamaguchi, T.; Takeoka, S.; Tsuchida, E.; Naito, M.; Nimura, Y.; Ishimura, Y.; Suematsu, M., Carbon monoxide from heme catabolism protects against hepatobiliary dysfunction in endotoxin-treated rat liver. *Gastroenterology* **2001**, *120* (5), 1227-1240.

12. Nakao, A., Immunomodulatory effects of inhaled carbon monoxide on rat syngeneic small bowel graft motility. *Gut* **2003**, 52 (9), 1278-1285.
13. Neto, J. S.; Nakao, A.; Kimizuka, K.; Romanosky, A. J.; Stolz, D. B.; Uchiyama, T.; Nalesnik, M. A.; Otterbein, L. E.; Murase, N., Protection of transplant-induced renal ischemia-reperfusion injury with carbon monoxide. *Am. J. Physiol.* **2004**, 287 (5), F979-F989.
14. Brugger, J.; Schick, M. A.; Brock, R. W.; Baumann, A.; Muellenbach, R. M.; Roewer, N.; Wunder, C., Carbon monoxide has antioxidative properties in the liver involving p38 MAP kinase pathway in a murine model of systemic inflammation. *Microcirculation* **2010**.
15. Wang, B.; Du, Y.-C. N., The anti-metastasis effect of low-dose carbon monoxide. *Ann. Pancr. Cancer* **2023**, 6, 1.
16. Zhang, T.; Zhang, G.; Chen, X.; Chen, Z.; Tan, A. Y.; Lin, A.; Zhang, C.; Torres, L. K.; Bajrami, S.; Zhang, T.; Zhang, G.; Xiang, J. Z.; Hissong, E. M.; Chen, Y.-T.; Li, Y.; Du, Y.-C. N., Low-dose carbon monoxide suppresses metastatic progression of disseminated cancer cells. *Cancer Lett.* **2022**, 546, 215831.
17. Bauer, N.; Liu, D.; Nguyen, T.; Wang, B., Unraveling the Interplay of Dopamine, Carbon Monoxide, and Heme Oxygenase in Neuromodulation and Cognition. *ACS Chemical Neuroscience* **2024**.
18. Wang, R., Resurgence of carbon monoxide: an endogenous gaseous vasorelaxing factor. *Can. J. Physiol. Pharmacol.* **1998**, 76 (1), 1-15.
19. Motterlini, R.; Clark, J.; Foresti, R.; Sarathchandra, P.; Mann, B.; Green, C., Carbon Monoxide-Releasing Molecules. *Circ. Res.* **2002**, 90 (2), e17-e24.
20. Motterlini, R.; Otterbein, L. E., The therapeutic potential of carbon monoxide. *Nat. Rev.* **2010**, 9 (9), 728-743.
21. Romao, C. C.; Blattler, W. A.; Seixas, J. D.; Bernardes, G. J., Developing drug molecules for therapy with carbon monoxide. *Chem Soc Rev* **2012**, 41 (9), 3571-83.
22. Romanski, S.; Stamellou, E.; Jaraba, J. T.; Storz, D.; Krämer, B. K.; Hafner, M.; Amslinger, S.; Schmalz, H. G.; Yard, B. A., Enzyme-triggered CO-releasing molecules (ET-CORMs): evaluation of biological activity in relation to their structure. *Free Radic Biol Med* **2013**, 65, 78-88.
23. Barrett, J. A.; Li, Z.; Garcia, J. V.; Wein, E.; Zheng, D.; Hunt, C.; Ngo, L.; Sepunaru, L.; Iretskii, A. V.; Ford, P. C., Redox-mediated carbon monoxide release from a manganese carbonyl-implications for physiological CO delivery by CO releasing moieties. *R Soc Open Sci* **2021**, 8, 211022.

24. Kawahara, B.; Sen, S.; Mascharak, P. K., Reaction of carbon monoxide with cystathionine β -synthase: implications on drug efficacies in cancer chemotherapy. *Future Med Chem* **2020**, *12*, 325-337.
25. Belcher, J. D.; Gomperts, E.; Nguyen, J.; Chen, C.; Abdulla, F.; Kiser, Z. M.; Gallo, D.; Levy, H.; Otterbein, L. E.; Vercellotti, G. M., Oral carbon monoxide therapy in murine sickle cell disease: Beneficial effects on vaso-occlusion, inflammation and anemia. *PLOS ONE* **2018**, *13*, e0205194.
26. Šťacková, L.; Russo, M.; Muchová, L.; Orel, V.; Vitek, L.; Šťacko, P.; Klán, P., Cyanine-Flavonol Hybrids for Near-Infrared Light-Activated Delivery of Carbon Monoxide. *Chemistry* **2020**, *26*, 13184-13190.
27. Abeyrathna, N.; Washington, K.; Bashur, C.; Liao, Y., Nonmetallic carbon monoxide releasing molecules (CORMs). *Org Biomol Chem* **2017**, *15*, 8692-8699.
28. Soboleva, T.; Berreau, L. M., 3-Hydroxyflavones and 3-Hydroxy-4-oxoquinolines as Carbon Monoxide-Releasing Molecules. *Molecules* **2019**, *24*.
29. Xing, L.; Wang, B.; Li, J.; Guo, X.; Lu, X.; Chen, X.; Sun, H.; Sun, Z.; Luo, X.; Qi, S.; Qian, X.; Yang, Y., A Fluorogenic ONOO(-)-Triggered Carbon Monoxide Donor for Mitigating Brain Ischemic Damage. *J Am Chem Soc* **2022**, *144*, 2114-2119.
30. Wang, D.; Viennois, E.; Ji, K.; Damera, K.; Draganov, A.; Zheng, Y.; Dai, C.; Merlin, D.; Wang, B., A click-and-release approach to CO prodrugs. *Chem. Commun.* **2014**, *50* (100), 15890-15893.
31. Ji, X.; Wang, B., Strategies toward Organic Carbon Monoxide Prodrugs. *Acc Chem Res* **2018**, *51*, 1377-1385.
32. Yang, X.; Lu, W.; Wang, M.; Tan, C.; Wang, B., "CO in a pill": Towards oral delivery of carbon monoxide for therapeutic applications. *J Control Release* **2021**, *338*, 593-609.
33. Yang, X. X.; Ke, B. W.; Lu, W.; Wang, B. H., CO as a therapeutic agent: discovery and delivery forms. *Chin J Nat Med* **2020**, *18*, 284-295.
34. Johnston, H. M.; Kueh, J. T. B.; Hartley, R. H.; Bland, A. R.; Payne, F. M.; Harrison, J. C.; Sammut, I. A.; Larsen, D. S., Utilising fluorescent reporters to probe the mode of action of norbornen-7-one CO releasing molecules. *Org Biomol Chem* **2022**, *20*, 5812-5819.
35. Min, Q.; Ni, Z.; You, M.; Liu, M.; Zhou, Z.; Ke, H.; Ji, X., Chemiexcitation-Triggered Prodrug Activation for Targeted Carbon Monoxide Delivery. *Angew Chem Int Ed Engl* **2022**, *61*, e202200974.
36. Bauer, N.; Yuan, Z.; Yang, X.; Wang, B., Plight of CORMs: the unreliability of four commercially available CO-releasing molecules, CORM-2, CORM-3, CORM-A1, and CORM-401, in studying CO biology. *Biochem. Pharmacol.* **2023**, *214*, 115642.

37. Liu, D.; Yang, X.; Wang, B., Sensing a CO-Releasing Molecule (CORM) Does Not Equate to Sensing CO: The Case of DPHP and CORM-3. *Anal. Chem.* **2023**.
38. Wu, L.; Wang, R., Carbon Monoxide: Endogenous Production, Physiological Functions, and Pharmacological Applications. *Pharmacol. Rev.* **2005**, 57 (4), 585-630.
39. Coburn, R. F., The carbon monoxide body stores. *Ann N Y Acad Sci.* **1970**, 174, 11-22.
40. Wang, B.; Otterbein, L., *Carbon Monoxide in Drug Discovery: Basics, Pharmacology, and Therapeutic Potential*. First ed.; John Wiley and Sons: Hoboken, New Jersey, 2022.
41. Motterlini, R.; Clark, J. E.; Foresti, R.; Sarathchandra, P.; Mann, B. E.; Green, C. J., Carbon Monoxide-Releasing Molecules. *Circ. Res.* **2002**, 90 (2), 17e-24.
42. Jimenez, J.; Chakraborty, I.; Dominguez, A.; Martinez-Gonzalez, J.; Sameera, W. M. C.; Mascharak, P. K., A Luminescent Manganese PhotoCORM for CO Delivery to Cellular Targets under the Control of Visible Light. *Inorg. Chem.* **2018**, 57 (4), 1766-1773.
43. Pierri, A. E.; Huang, P.-J.; Garcia, J. V.; Stanfill, J. G.; Chui, M.; Wu, G.; Zheng, N.; Ford, P. C., A photoCORM nanocarrier for CO release using NIR light. *Chem. Commun.* **2015**, 51 (11), 2072-2075.
44. Romão, C. C.; Blättler, W. A.; Seixas, J. D.; Bernardes, G. J. L., Developing drug molecules for therapy with carbon monoxide. *Chem. Soc. Rev.* **2012**, 41 (9), 3571-3583.
45. Anderson, S. N.; Richards, J. M.; Esquer, H. J.; Benninghoff, A. D.; Arif, A. M.; Berreau, L. M., A Structurally-Tunable 3-Hydroxyflavone Motif for Visible Light-Induced Carbon Monoxide-Releasing Molecules (CORMs). *ChemistryOpen* **2015**, 4 (5), 590-594.
46. Poloukhine, A.; Popik, V. V., Highly Efficient Photochemical Generation of a Triple Bond: Synthesis, Properties, and Photodecarbonylation of Cyclopropanones. *J. Org. Chem.* **2003**, 68 (20), 7833-7840.
47. Abeyrathna, N.; Washington, K.; Bashur, C.; Liao, Y., Nonmetallic carbon monoxide releasing molecules (CORMs). *Org. Biomol. Chem.* **2017**, 15 (41), 8692-8699.
48. Palao, E.; Slanina, T.; Muchová, L.; Šolomek, T.; Vitek, L.; Klán, P., Transition-Metal-Free CO-Releasing BODIPY Derivatives Activatable by Visible to NIR Light as Promising Bioactive Molecules. *J. Am. Chem. Soc.* **2016**, 138 (1), 126-133.
49. Min, Q.; Ni, Z.; You, M.; Liu, M.; Zhou, Z.; Ke, H.; Ji, X., Chemiexcitation-Triggered Prodrug Activation for Targeted Carbon Monoxide Delivery. *Angew. Chem. Int. Ed.* **2022**, 61 (26).
50. Sun, Y.; Neary, W. J.; Burke, Z. P.; Qian, H.; Zhu, L.; Moore, J. S., Mechanically Triggered Carbon Monoxide Release with Turn-On Aggregation-Induced Emission. *J. Am. Chem. Soc.* **2022**, 144 (3), 1125-1129.

51. Alghazwat, O.; Talebzadeh, S.; Oyer, J.; Copik, A.; Liao, Y., Ultrasound responsive carbon monoxide releasing micelle. *Ultrason. Sonochem.* **2021**, 72, 105427.
52. Stamellou, E.; Storz, D.; Botov, S.; Ntasis, E.; Wedel, J.; Sollazzo, S.; Krämer, B. K.; van Son, W.; Seelen, M.; Schmalz, H. G.; Schmidt, A.; Hafner, M.; Yard, B. A., Different design of enzyme-triggered CO-releasing molecules (ET-CORMs) reveals quantitative differences in biological activities in terms of toxicity and inflammation. *Redox Biol.* **2014**, 2, 739-748.
53. Heinemann, S. H.; Hoshi, T.; Westerhausen, M.; Schiller, A., Carbon monoxide – physiology, detection and controlled release. *Chem. Commun.* **2014**, 50 (28), 3644-3660.
54. Aucott, B. J.; Ward, J. S.; Andrew, S. G.; Milani, J.; Whitwood, A. C.; Lynam, J. M.; Parkin, A.; Fairlamb, I. J. S., Redox-Tagged Carbon Monoxide-Releasing Molecules (CORMs): Ferrocene-Containing [Mn(CN)(CO)₄] Complexes as a Promising New CORM Class. *Inorg. Chem.* **2017**, 56 (9), 5431-5440.
55. Steiger, C.; Lühmann, T.; Meinel, L., Oral drug delivery of therapeutic gases — Carbon monoxide release for gastrointestinal diseases. *J. Control. Release* **2014**, 189, 46-53.
56. Yang, X.; Lu, W.; Hopper, C. P.; Ke, B.; Wang, B., Nature's marvels endowed in gaseous molecules I: Carbon monoxide and its physiological and therapeutic roles. *Acta Pharm. Sin. B.* **2021**, 11 (6), 1434-1445.
57. Ji, X.; Wang, B., Strategies toward Organic Carbon Monoxide Prodrugs. *Acc. Chem. Res.* **2018**, 51 (6), 1377-1385.
58. Kueh, J. T. B.; Stanley, N. J.; Hewitt, R. J.; Woods, L. M.; Larsen, L.; Harrison, J. C.; Rennison, D.; Brimble, M. A.; Sammut, I. A.; Larsen, D. S., Norborn-2-en-7-ones as physiologically-triggered carbon monoxide-releasing prodrugs. *Chem. Sci.* **2017**, 8 (8), 5454-5459.
59. De La Cruz, L. K.; Yang, X.; Menshikh, A.; Brewer, M.; Lu, W.; Wang, M.; Wang, S.; Ji, X.; Cachuela, A.; Yang, H.; Gallo, D.; Tan, C.; Otterbein, L.; De Caestecker, M.; Wang, B., Adapting decarbonylation chemistry for the development of prodrugs capable of *in vivo* delivery of carbon monoxide utilizing sweeteners as carrier molecules. *Chem. Sci.* **2021**, 12 (31), 10649-10654.
60. Motterlini, R.; Sawle, P.; Bains, S.; Hammad, J.; Alberto, R.; Foresti, R.; Green, C. J., CORM-A1: a new pharmacologically active carbon monoxide-releasing molecule. *FASEB J.* **2005**, 19 (2), 1-24.
61. Kaczara, P.; Sitek, B.; Przyborowski, K.; Kurpinska, A.; Kus, K.; Stojak, M.; Chlopicki, S., Antiplatelet Effect of Carbon Monoxide Is Mediated by NAD⁺ and ATP Depletion. *Arterioscler. Thromb. Vasc. Biol.* **2020**, 40 (10), 2376-2390.
62. Kaczara, P.; Przyborowski, K.; Mohaissen, T.; Chlopicki, S., Distinct Pharmacological Properties of Gaseous CO and CO-Releasing Molecule in Human Platelets. *Int. J. Mol. Sci.* **2021**, 22 (7), 3584.

63. Yuan, Z.; Yang, X.; Wang, B., Redox and catalase-like activities of four widely used carbon monoxide releasing molecules (CO-RMs). *Chem. Sci.* **2021**, *12* (39), 13013-13020.
64. Yuan, Z.; Yang, X.; Ye, Y.; Tripathi, R.; Wang, B., Chemical Reactivities of Two Widely Used Ruthenium-Based CO-Releasing Molecules with a Range of Biologically Important Reagents and Molecules. *Anal. Chem.* **2021**, *93* (12), 5317-5326.
65. Southam, H. M.; Smith, T. W.; Lyon, R. L.; Liao, C.; Trevitt, C. R.; Middlemiss, L. A.; Cox, F. L.; Chapman, J. A.; El-Khamisy, S. F.; Hippler, M.; Williamson, M. P.; Henderson, P. J. F.; Poole, R. K., A thiol-reactive Ru(II) ion, not CO release, underlies the potent antimicrobial and cytotoxic properties of CO-releasing molecule-3. *Redox Biol.* **2018**, *18*, 114-123.
66. Nielsen, V. G., Ruthenium, Not Carbon Monoxide, Inhibits the Procoagulant Activity of Atheris, Echis, and Pseudonaja Venoms. *Int. J. Mol. Sci.* **2020**, *21* (8), 2970.
67. Gessner, G.; Sahoo, N.; Swain, S. M.; Hirth, G.; Schönherr, R.; Mede, R.; Westerhausen, M.; Brewitz, H. H.; Heimer, P.; Imhof, D.; Hoshi, T.; Heinemann, S. H., CO-independent modification of K⁺ channels by tricarbonyldichlororuthenium(II) dimer (CORM-2). *Eur. J. Pharmacol.* **2017**, *815*, 33-41.
68. Seixas, J. D.; Santos, M. F. A.; Mukhopadhyay, A.; Coelho, A. C.; Reis, P. M.; Veiros, L. F.; Marques, A. R.; Penacho, N.; Gonçalves, A. M. L.; Romão, M. J.; Bernardes, G. J. L.; Santos-Silva, T.; Romão, C. C., A contribution to the rational design of Ru(CO)₃Cl₂L complexes for in vivo delivery of CO. *Dalton Trans.* **2015**, *44* (11), 5058-5075.
69. Southam, H. M.; Williamson, M. P.; Chapman, J. A.; Lyon, R. L.; Trevitt, C. R.; Henderson, P. J. F.; Poole, R. K., 'Carbon-Monoxide-Releasing Molecule-2 (CORM-2)' Is a Misnomer: Ruthenium Toxicity, Not CO Release, Accounts for Its Antimicrobial Effects. *Antioxidants* **2021**, *10* (6), 915.
70. Aki, T.; Unuma, K.; Noritake, K.; Kurahashi, H.; Funakoshi, T.; Uemura, K., Interaction of carbon monoxide-releasing ruthenium carbonyl CORM-3 with plasma fibronectin. *Toxicol. In Vitro* **2018**, *50*, 201-209.
71. Aki, T.; Unuma, K.; Noritake, K.; Hirayama, N.; Funakoshi, T.; Uemura, K., Formation of high molecular weight p62 by CORM-3. *PLOS ONE* **2019**, *14* (1), e0210474.
72. Almeida, A. S.; Soares, N. L.; Vieira, M.; Gramsbergen, J. B.; Vieira, H. L. A., Carbon Monoxide Releasing Molecule-A1 (CORM-A1) Improves Neurogenesis: Increase of Neuronal Differentiation Yield by Preventing Cell Death. *PLOS ONE* **2016**, *11* (5), e0154781.
73. Almeida, A. S.; Soares, N. L.; Sequeira, C. O.; Pereira, S. A.; Sonnewald, U.; Vieira, H. L. A., Improvement of neuronal differentiation by carbon monoxide: Role of pentose phosphate pathway. **2018**, *17*, 338-347.

74. Avigad, G., Reduction of nicotinamide adenine dinucleotides by sodium cyanoborohydride. *Biochim Biophys Acta* **1979**, 571 (1), 171-174.
75. Eisner, U.; Kuthan, J., Chemistry of dihydropyridines. *Chem. Rev.* **1972**, 72 (1), 1-42.
76. Rover, L.; Fernandes, J. C. B.; Neto, G. d. O.; Kubota, L. T.; Katekawa, E.; Serrano, S. I. H. P., Study of NADH Stability Using Ultraviolet–Visible Spectrophotometric Analysis and Factorial Design. *Anal. Biochem.* **1998**, 260 (1), 50-55.
77. Cantó, C.; Menzies, J.; Keir; Auwerx, J., NAD⁺ Metabolism and the Control of Energy Homeostasis: A Balancing Act between Mitochondria and the Nucleus. *Cell Metabolism* **2015**, 22 (1), 31-53.
78. Nielsen, V. G., The anticoagulant effect of *Apis mellifera* phospholipase A2 is inhibited by CORM-2 via a carbon monoxide-independent mechanism. *J. Thromb. Thrombolysis* **2020**, 49 (1), 100-107.
79. Lane, C. F., Reduction of organic compounds with diborane. *Chem. Rev.* **1976**, 76 (6), 773-799.
80. Zaidlewicz, M.; Brown, H. C.; Neelamkavil, S. F., Borane–Tetrahydrofuran. In *Encyclopedia of Reagents for Organic Synthesis*, **2008**.
81. McMurry, J., *Organic Chemistry*. 9th ed.; Cengage Learning: 2015.
82. Lewis, D., *Advanced Organic Chemistry*. Illustrated ed.; Oxford University Press: 2015.
83. Brown, H. C.; Heim, P.; Yoon, N. M., Selective reductions. XV. Reaction of diborane in tetrahydrofuran with selected organic compounds containing representative functional groups. *J. Am. Chem. Soc.* **1970**, 92 (6), 1637-1646.
84. Klein, M.; Neugebauer, U.; Schmitt, M.; Popp, J., Elucidation of the CO-Release Kinetics of CORM-A1 by Means of Vibrational Spectroscopy. *ChemPhysChem* **2015**, 17 (7), 985-993.
85. Lu, W.; Yang, X.; Wang, B., Carbon monoxide signaling and soluble guanylyl cyclase: Facts, myths, and intriguing possibilities. *Biochem. Pharmacol.* **2022**, 200, 115041.
86. Magierowska, K.; Magierowski, M.; Hubalewska-Mazgaj, M.; Adamski, J.; Surmiak, M.; Sliwowski, Z.; Kwiecien, S.; Brzozowski, T., Carbon Monoxide (CO) Released from Tricarbonyldichlororuthenium (II) Dimer (CORM-2) in Gastroprotection against Experimental Ethanol-Induced Gastric Damage. *PLOS ONE* **2015**, 10 (10), e0140493.
87. Foresti, R.; Hammad, J.; Clark, J. E.; Johnson, T. R.; Mann, B. E.; Friebe, A.; Green, C. J.; Motterlini, R., Vasoactive properties of CORM-3, a novel water-soluble carbon monoxide-releasing molecule. *Br. J. Pharmacol.* **2004**, 142 (3), 453-460.
88. Zheng, Y.; Yu, B.; Ji, K.; Pan, Z.; Chittavong, V.; Wang, B., Esterase-Sensitive Prodrugs with Tunable Release Rates and Direct Generation of Hydrogen Sulfide. *Angew. Chem. Int. Ed.* **2016**, 55 (14), 4514-4518.

89. Hardy, K. R.; Thom, S. R., Pathophysiology and Treatment of Carbon Monoxide Poisoning. *J. Toxicol.* **1994**, *32* (6), 613-629.
90. Shimazu, T., Half-life of Blood Carboxyhemoglobin. *Chest.* **2001**, *119* (2), 661-662.
91. Hofmann, T.; Held, S.; Lang, R.; Somoza, V. Pyrimidinium derivatives for use in the treatment or prevention of diabetes. WO 2010/055170 A1, 2010.
92. Sreeperumbuduru, R. S.; Abid, Z. M.; Claunch, K. M.; Chen, H.-H.; McGillivray, S. M.; Simanek, E. E., Synthesis and antimicrobial activity of triazine dendrimers with DABCO groups. *RSC Adv.* **2016**, *6* (11), 8806-8810.
93. Crook, S. H.; Mann, B. E.; Meijer, A. J. H. M.; Adams, H.; Sawle, P.; Scapens, D.; Motterlini, R., [Mn(CO)₄{S₂CNMe(CH₂CO₂H)}], a new water-soluble CO-releasing molecule. *Dalton Trans.* **2011**, *40* (16), 4230-4235.
94. Fayad-Kobeissi, S.; Ratovonantenaina, J.; Dabiré, H.; Wilson, J. L.; Rodriguez, A. M.; Berdeaux, A.; Dubois-Randé, J.-L.; Mann, B. E.; Motterlini, R.; Foresti, R., Vascular and angiogenic activities of CORM-401, an oxidant-sensitive CO-releasing molecule. *Biochem pharmacol* **2016**, *102*, 64-77.
95. Vummaleti, S. V. C.; Branduardi, D.; Masetti, M.; De Vivo, M.; Motterlini, R.; Cavalli, A., Theoretical Insights into the Mechanism of Carbon Monoxide (CO) Release from CO-Releasing Molecules. *Chem. Eur. J.* **2012**, *18* (30), 9267-9275.
96. Yuan, Z.; De La Cruz, L. K.; Yang, X.; Wang, B., Carbon Monoxide Signaling: Examining Its Engagement with Various Molecular Targets in the Context of Binding Affinity, Concentration, and Biologic Response. *Pharm. Rev.* **2022**, *74* (3), 825.
97. Babu, D.; Leclercq, G.; Motterlini, R.; Lefebvre, R. A., Differential Effects of CORM-2 and CORM-401 in Murine Intestinal Epithelial MODE-K Cells under Oxidative Stress. *Front Pharmacol* **2017**, *8*, 31.
98. Piantadosi, C. A., Carbon monoxide, reactive oxygen signaling, and oxidative stress. *Free Radic. Biol. Med.* **2008**, *45* (5), 562-569.
99. Tatlidil, D.; Ucuncu, M.; Akdogan, Y., Physiological concentrations of albumin favor drug binding. *Phys. Chem. Chem. Phys.* **2015**, *17* (35), 22678-22685.
100. Motterlini, R.; Sawle, P.; Bains, S.; Hammad, J.; Alberto, R.; Foresti, R.; Green, C. J., CORM-A1: a new pharmacologically active carbon monoxide-releasing molecule. *FASEB J.* **2005**, *19*, 1-24.
101. Bauer, N.; Yang, X.; Yuan, Z.; Wang, B., Reassessing CORM-A1: redox chemistry and idiosyncratic CO-releasing characteristics of the widely used carbon monoxide donor. *Chem. Sci.* **2023**, *14* (12), 3215-3228.
102. Guo, Y.; Stein, A. B.; Wu, W.-J.; Tan, W.; Zhu, X.; Li, Q.-H.; Dawn, B.; Motterlini, R.; Bolli, R., Administration of a CO-releasing molecule at the time of reperfusion

- reduces infarct size in vivo. *Am. J. Physiol. Heart Circ. Physiol.* **2004**, 286 (5), H1649-H1653.
103. Santos-Silva, T.; Mukhopadhyay, A.; D. Seixas, J.; J.L. Bernardes, G.; C. Romao, C.; J. Romao, M., Towards Improved Therapeutic CORMs: Understanding the Reactivity of CORM-3 with Proteins. *Cur. Med Chem* **2011**, 18 (22), 3361-3366.
 104. Clark, J. E.; Naughton, P.; Shurey, S.; Green, C. J.; Johnson, T. R.; Mann, B. E.; Foresti, R.; Motterlini, R., Cardioprotective Actions by a Water-Soluble Carbon Monoxide-Releasing Molecule. *Circ. Res.* **2003**, 93 (2), 2e-8.
 105. McLean, S.; Mann, B. E.; Poole, R. K., Sulfite species enhance carbon monoxide release from CO-releasing molecules: implications for the deoxymyoglobin assay of activity. *Anal Biochem* **2012**, 427 (1), 36-40.
 106. Klein, M.; Neugebauer, U.; Gheisari, A.; Malassa, A.; Jazzazi, T. M. A.; Froehlich, F.; Westerhausen, M.; Schmitt, M.; Popp, J., IR Spectroscopic Methods for the Investigation of the CO Release from CORMs. *J. Phys. Chem.* **2014**, 118 (29), 5381-5390.
 107. Santos-Silva, T.; Mukhopadhyay, A.; Seixas, J. D.; Bernardes, G. J. L.; Romão, C. C.; Romão, M. J., CORM-3 Reactivity toward Proteins: The Crystal Structure of a Ru(II) Dicarbonyl-Lysozyme Complex. *J. Am. Chem. Soc.* **2011**, 133 (5), 1192-1195.
 108. Rimmer, R. D.; Richter, H.; Ford, P. C., A Photochemical Precursor for Carbon Monoxide Release in Aerated Aqueous Media. *Inorg Chem* **2010**, 49 (3), 1180-1185.
 109. Yang, X.; Mao, Q.; Wang, B., Question of CO's Ability to Induce HO-1 Expression in Cell Culture: A Comparative Study Using Different CO Sources. *ACS Chem. Biol.* **2024**, 19 (3), 725-735.
 110. Garashchuk, S.; Gu, B.; Mazzuca, J., Calculation of the Quantum-Mechanical Tunneling in Bound Potentials. *J. Theor. Chem.* **2014**, 2014, 1-11.
 111. Bruice, T. C.; Lightstone, F. C., Ground State and Transition State Contributions to the Rates of Intramolecular and Enzymatic Reactions. *Acc Chem Res* **1999**, 32 (2), 127-136.
 112. Dong, R.; Yang, X.; Wang, B.; Ji, X., Mutual leveraging of proximity effects and click chemistry in chemical biology. *Med. Res. Rev.* **2023**, 43 (2), 319-342.
 113. Jencks, W., *Catalysis in Chemistry and Enzymology*. Dover Publications, Inc: 1987.
 114. Meng, F.; Alayash, A. I., Determination of extinction coefficients of human hemoglobin in various redox states. *Anal Biochem* **2017**, 521, 11-19.
 115. Bard, J. R.; Holman, J. T.; Wear, J. O., An Electron Paramagnetic Resonance Study of Mn(II)-Chloro Complex Formation in N,N-Dimethylformamide. *Zeitschrift für Naturforschung B* **1969**, 24 (8), 989-993.
 116. Schoenberg, A.; Bartoletti, I.; Heck, R. F., Palladium-catalyzed carboalkoxylation of aryl, benzyl, and vinylic halides. *J. Org. Chem.* **1974**, 39 (23), 3318-3326.

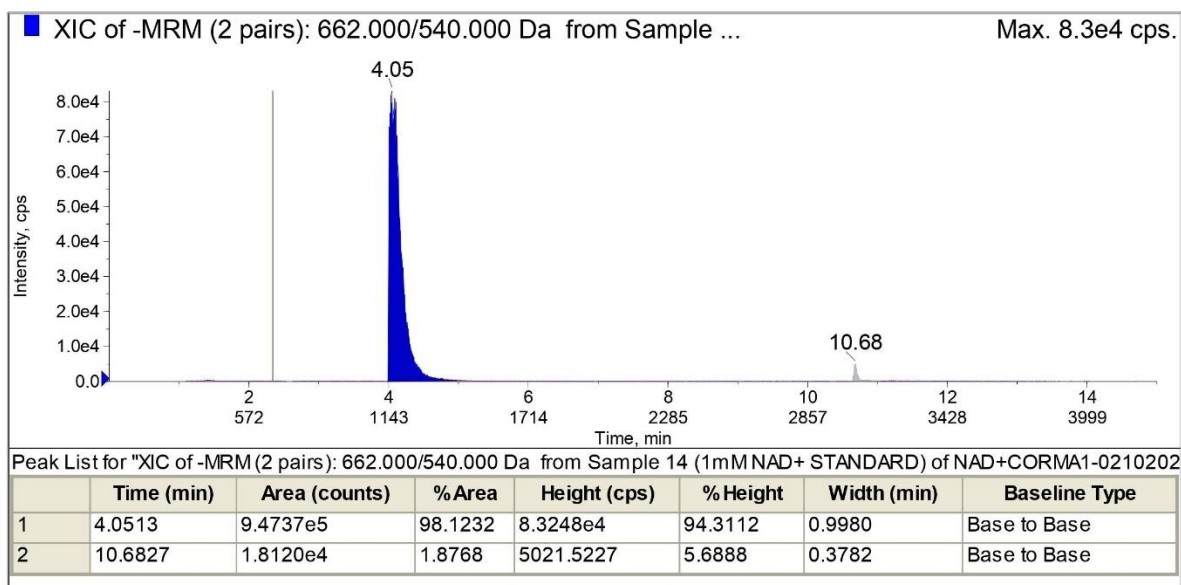
117. Peng, J.-B.; Geng, H.-Q.; Wu, X.-F., The Chemistry of CO: Carbonylation. *Chem* **2019**, 5 (3), 526-552.
118. Ren, X.; Zheng, Z.; Zhang, L.; Wang, Z.; Xia, C.; Ding, K., Rhodium-Complex-Catalyzed Hydroformylation of Olefins with CO₂ and Hydrosilane. *Angew. Chem. Int. Ed. Engl.* **2017**, 56 (1), 310-313.
119. Morimoto, T.; Kakiuchi, K., Evolution of Carbonylation Catalysis: No Need for Carbon Monoxide. *Angew. Chem. Int. Ed. Engl.* **2004**, 43 (42), 5580-5588.
120. Grushin, V. V.; Alper, H., Novel palladium-catalyzed carbonylation of organic halides by chloroform and alkali. *Organometallics* **1993**, 12 (10), 3846-3850.
121. Hansen, S. V. F.; Ulven, T., Oxalyl Chloride as a Practical Carbon Monoxide Source for Carbonylation Reactions. *Org. Lett.* **2015**, 17 (11), 2832-2835.
122. Hermange, P.; Lindhardt, A. T.; Taaning, R. H.; Bjerglund, K.; Lupp, D.; Skrydstrup, T., Ex Situ Generation of Stoichiometric and Substoichiometric 12CO and 13CO and Its Efficient Incorporation in Palladium Catalyzed Aminocarbonylations. *J. Am. Chem. Soc.* **2011**, 133 (15), 6061-6071.
123. Shao, C.; Lu, A.; Wang, X.; Zhou, B.; Guan, X.; Zhang, Y., Oxalic acid as the in situ carbon monoxide generator in palladium-catalyzed hydroxycarbonylation of arylhalides. *Org. Biomol. Chem.* **2017**, 15 (23), 5033-5040.
124. Liu, Q.; Yuan, K.; Arockiam, P.-B.; Franke, R.; Doucet, H.; Jackstell, R.; Beller, M., Regioselective Pd-Catalyzed Methoxycarbonylation of Alkenes Using both Paraformaldehyde and Methanol as CO Surrogates. *Angew. Chem. Int. Ed. Engl.* **2015**, 54 (15), 4493-4497.
125. Natte, K.; Dumrath, A.; Neumann, H.; Beller, M., Palladium-Catalyzed Carbonylations of Aryl Bromides using Paraformaldehyde: Synthesis of Aldehydes and Esters. *Angew. Chem. Int. Ed. Engl.* **2014**, 53 (38), 10090-10094.
126. Kaiser, N. F.; Hallberg, A.; Larhed, M., In situ generation of carbon monoxide from solid molybdenum hexacarbonyl. A convenient and fast route to palladium-catalyzed carbonylation reactions. *J. Comb. Chem.* **2002**, 4 (2), 109-111.
127. Morimoto, T.; Fuji, K.; Tsutsumi, K.; Kakiuchi, K., CO-Transfer Carbonylation Reactions. A Catalytic Pauson–Khand-Type Reaction of Enynes with Aldehydes as a Source of Carbon Monoxide. *J. Am. Chem. Soc.* **2002**, 124 (15), 3806-3807.
128. Ueda, T.; Konishi, H.; Manabe, K., Palladium-Catalyzed Reductive Carbonylation of Aryl Halides with N-Formylsaccharin as a CO Source. *Angew. Chem. Int. Ed. Engl.* **2013**, 52 (33), 8611-8615.
129. Friis, S. D.; Taaning, R. H.; Lindhardt, A. T.; Skrydstrup, T., Silacarboxylic Acids as Efficient Carbon Monoxide Releasing Molecules: Synthesis and Application in

- Palladium-Catalyzed Carbonylation Reactions. *J. Am. Chem. Soc.* **2011**, *133* (45), 18114-18117.
130. Sumino, S.; Fusano, A.; Fukuyama, T.; Ryu, I., Carbonylation Reactions of Alkyl Iodides through the Interplay of Carbon Radicals and Pd Catalysts. *Acc. Chem. Res.* **2014**, *47* (5), 1563-1574.
 131. Torres, G. M.; Liu, Y.; Arndtsen, B. A., A dual light-driven palladium catalyst: Breaking the barriers in carbonylation reactions. *Science* **2020**, *368* (6488), 318-323.
 132. Roslin, S.; Odell, L. R., Palladium and visible-light mediated carbonylative Suzuki–Miyaura coupling of unactivated alkyl halides and aryl boronic acids. *Chem. Comm.* **2017**, *53* (51), 6895-6898.
 133. Sardana, M.; Bergman, J.; Ericsson, C.; Kingston, L. P.; Schou, M.; Dugave, C.; Audisio, D.; Elmore, C. S., Visible-Light-Enabled Aminocarbonylation of Unactivated Alkyl Iodides with Stoichiometric Carbon Monoxide for Application on Late-Stage Carbon Isotope Labeling. *J. Org. Chem.* **2019**, *84* (24), 16076-16085.
 134. Sargent, B. T.; Alexanian, E. J., Palladium-Catalyzed Alkoxy carbonylation of Unactivated Secondary Alkyl Bromides at Low Pressure. *J. Am. Chem. Soc.* **2016**, *138* (24), 7520-7523.
 135. Mondal, R.; Okhrimenko, A. N.; Shah, B. K.; Neckers, D. C., Photodecarbonylation of α -Diketones: A Mechanistic Study of Reactions Leading to Acenes. *J. Phys. Chem. B* **2008**, *112* (1), 11-15.
 136. Peng, P.; Wang, C.; Shi, Z.; Johns, V. K.; Ma, L.; Oyer, J.; Copik, A.; Igarashi, R.; Liao, Y., Visible-light activatable organic CO-releasing molecules (PhotoCORMs) that simultaneously generate fluorophores. *Org. Biomol. Chem.* **2013**, *11* (39), 6671-6674.
 137. Escorihuela, J.; Das, A.; Looijen, W. J. E.; van Delft, F. L.; Aquino, A. J. A.; Lischka, H.; Zuilhof, H., Kinetics of the Strain-Promoted Oxidation-Controlled Cycloalkyne-1,2-quinone Cycloaddition: Experimental and Theoretical Studies. *J. Org. Chem.* **2018**, *83* (1), 244-252.
 138. Ji, X.; Zhou, C.; Ji, K.; Aghoghovbia, R. E.; Pan, Z.; Chittavong, V.; Ke, B.; Wang, B., Click and Release: A Chemical Strategy toward Developing Gasotransmitter Prodrugs by Using an Intramolecular Diels–Alder Reaction. *Angew. Chem. Int. Ed. Engl.* **2016**, *55* (51), 15846-15851.
 139. Poziomek, E. J.; Kronenberg, M. E.; Havinga, E., Chemical consequences of the hydration of 1,2-diketones. *Recl. Trav. Chim. Pays-Bas* **1966**, *85* (8), 791-792.
 140. Elgattar, A.; Washington, K. S.; Talebzadeh, S.; Alwagdani, A.; Khalil, T.; Alghazwat, O.; Alshammri, S.; Pal, H.; Bashur, C.; Liao, Y., Poly(butyl cyanoacrylate) nanoparticle containing an organic photoCORM. *Photochem. Photobiol. Sci.* **2019**, *18* (11), 2666-2672.

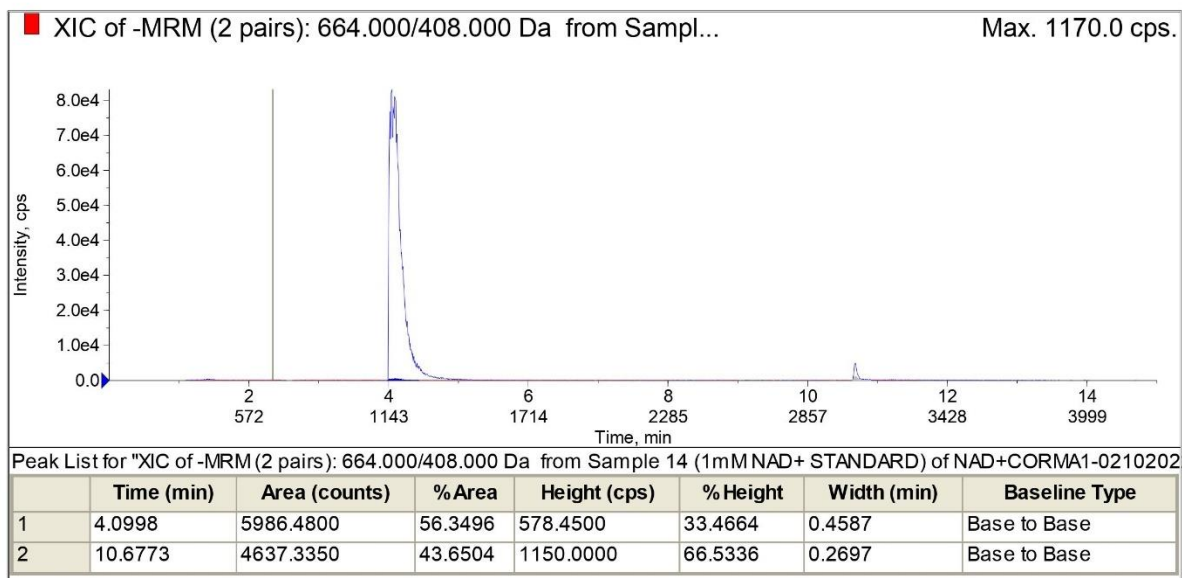
141. Li, H.; Yang, M.; Qi, Y.; Xue, J., Ligand-Free Pd-Catalyzed Carbonylative Cross-Coupling Reactions under Atmospheric Pressure of Carbon Monoxide: Synthesis of Aryl Ketones and Heteroaromatic Ketones. *Eur. J. Org. Chem.* **2011**, 2011 (14), 2662-2667.
142. Iizuka, M.; Kondo, Y., Remarkable ligand effect on the palladium-catalyzed double carbonylation of aryl iodides. *Chem. Comm.* **2006**, (16), 1739-1741.
143. Martinelli, J. R.; Watson, D. A.; Freckmann, D. M. M.; Barder, T. E.; Buchwald, S. L., Palladium-Catalyzed Carbonylation Reactions of Aryl Bromides at Atmospheric Pressure: A General System Based on Xantphos. *J. Org. Chem.* **2008**, 73 (18), 7102-7107.
144. Neumann, K. T.; Laursen, S. R.; Lindhardt, A. T.; Bang-Andersen, B.; Skrydstrup, T., Palladium-Catalyzed Carbonylative Sonogashira Coupling of Aryl Bromides Using Near Stoichiometric Carbon Monoxide. *Org. Lett.* **2014**, 16 (8), 2216-2219.
145. Friis, S. D.; Lindhardt, A. T.; Skrydstrup, T., The Development and Application of Two-Chamber Reactors and Carbon Monoxide Precursors for Safe Carbonylation Reactions. *Acc. Chem. Res.* **2016**, 49 (4), 594-605.
146. Huang, C.; Zheng, M.; Xu, J.; Zhang, Y., Photo-Induced Cycloaddition Reactions of α -Diketones and Transformations of the Photocycloadducts. *Molecules* **2013**, 18 (3), 2942-2966.
147. Albrecht, M.; Baumert, M.; Winkler, H. D. F.; Schalley, C. A.; Fröhlich, R., Hierarchical self-assembly of metallo-dendrimers. *Dalton Transactions* **2010**, 39 (31), 7220-7222.

APPENDICES

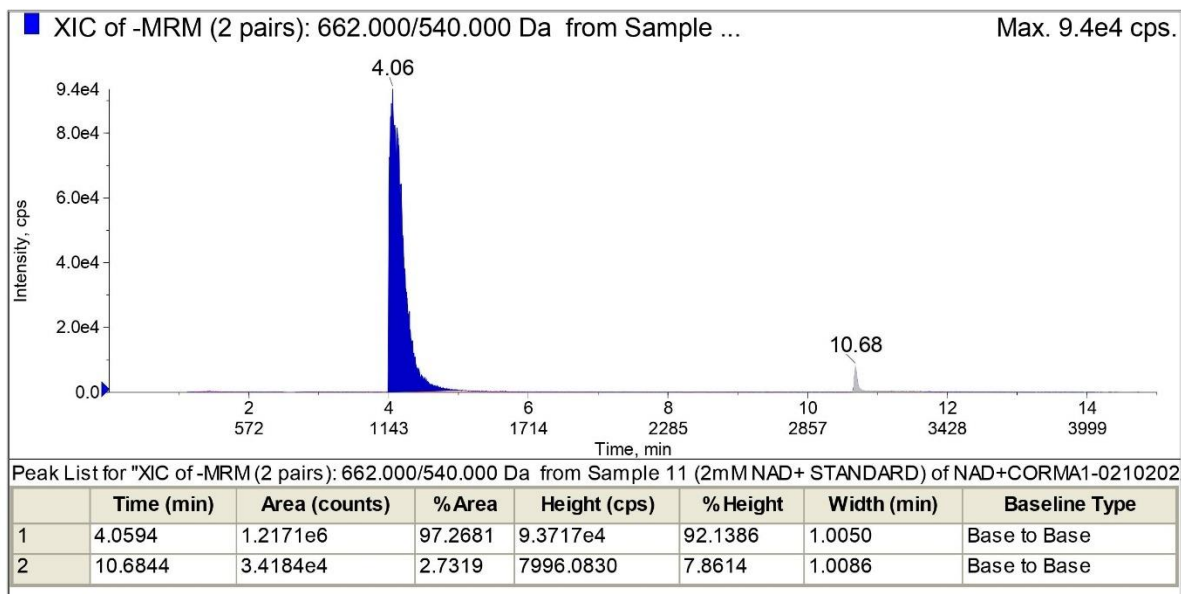
Appendix A: LC-MS Chromatographs for Chapter 1



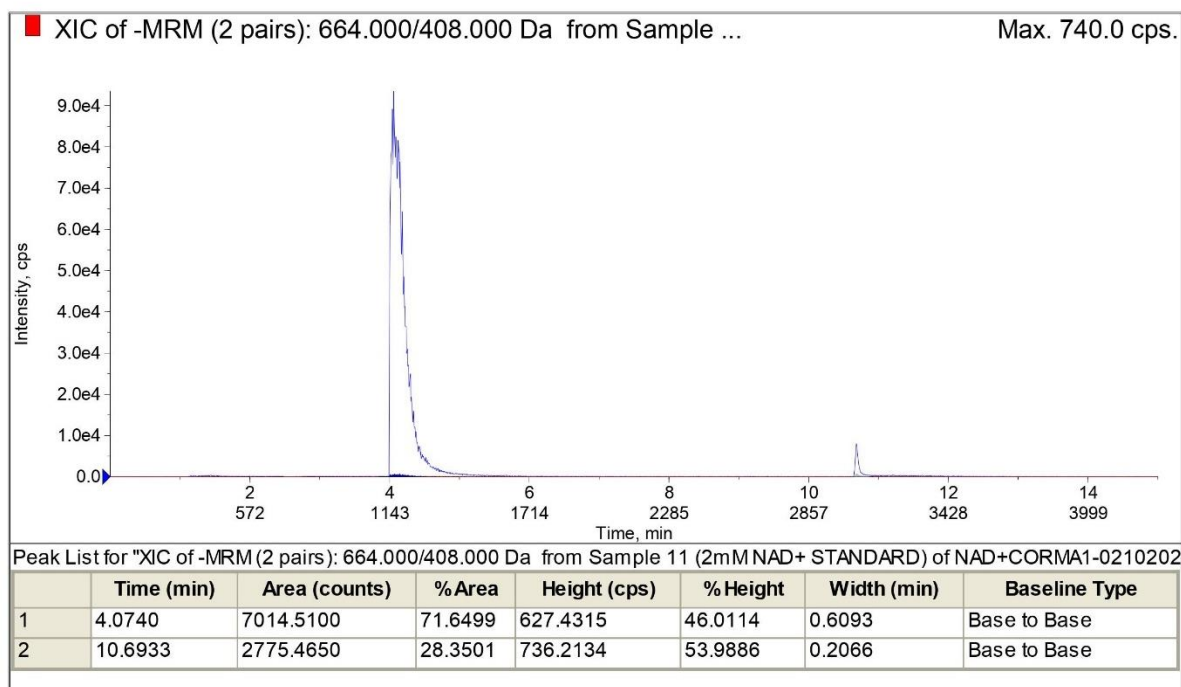
XIC of 1mM NAD⁺ standard in water detecting for NAD⁺



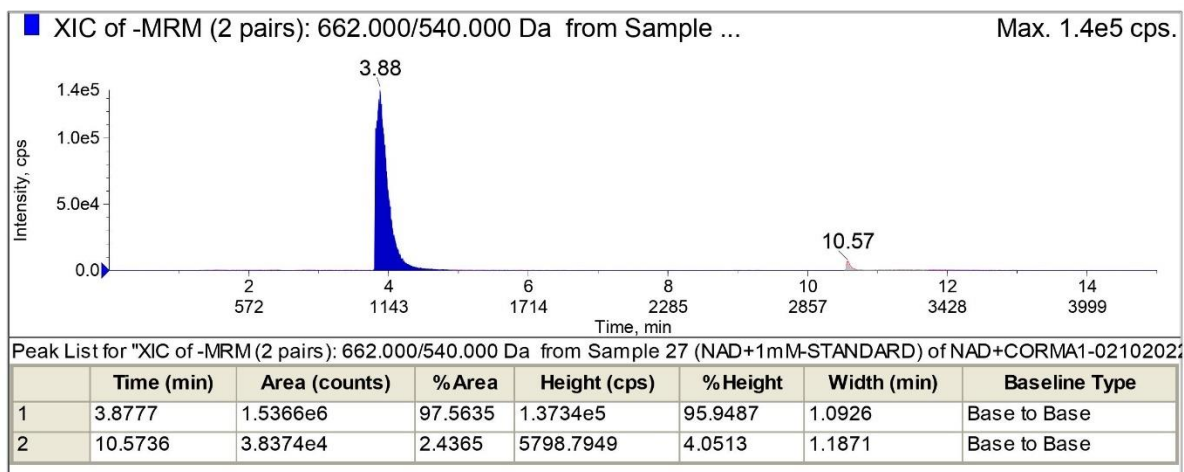
XIC of 1mM NAD⁺ standard in water detecting for NADH



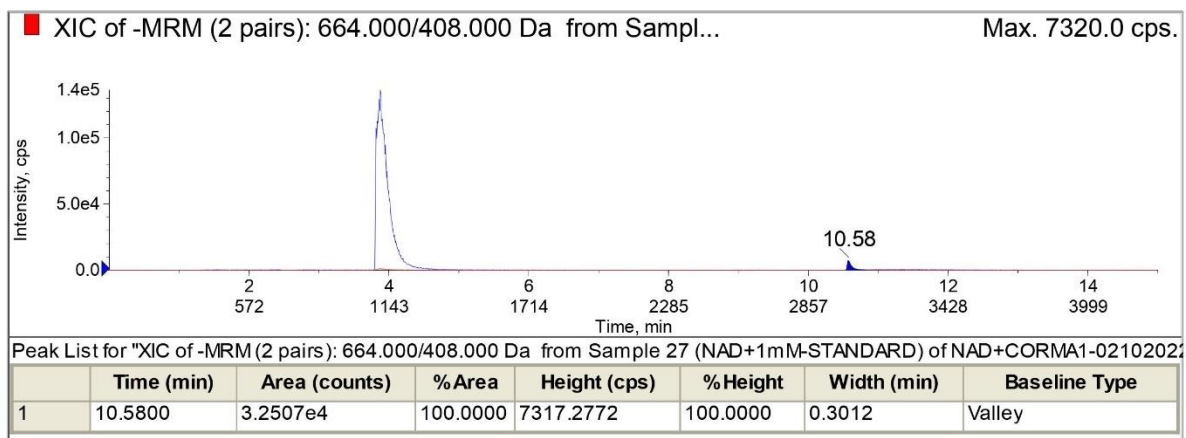
XIC of 2mM NAD⁺ standard in water detecting for NAD⁺



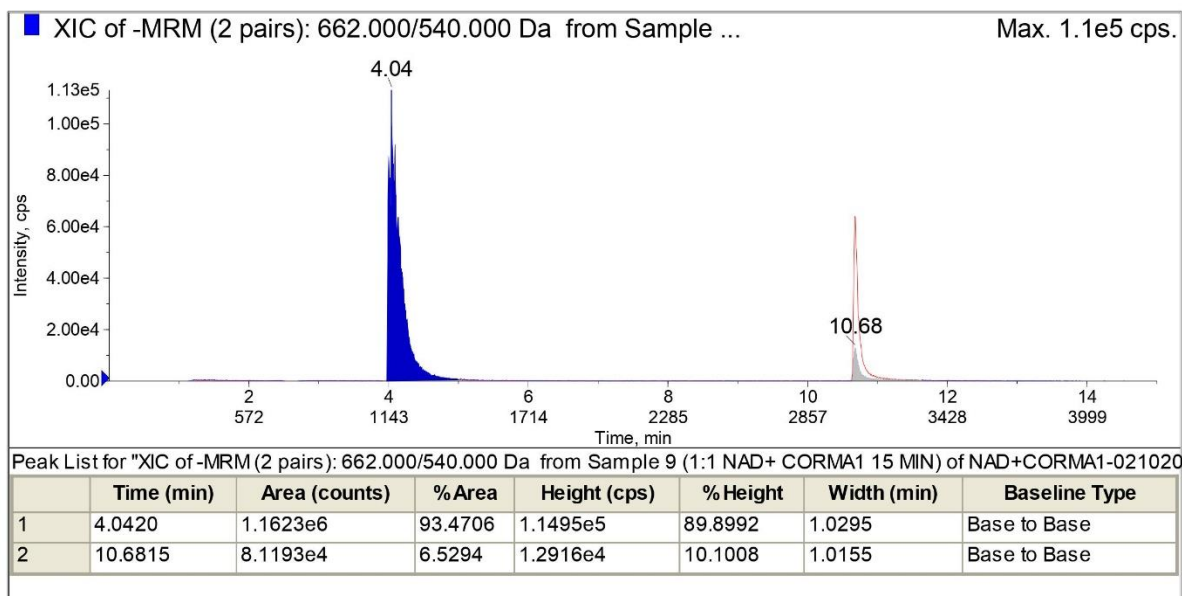
XIC of 2mM NAD⁺ standard in water detecting for NADH



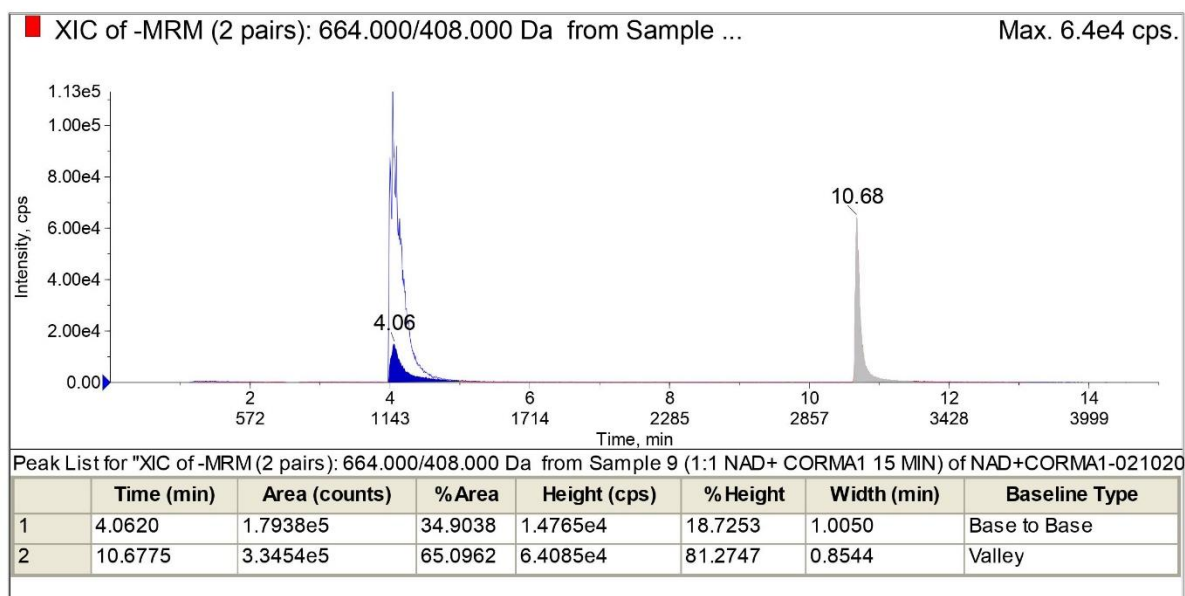
XIC of 1mM NAD⁺ standard in THF detecting for NAD⁺



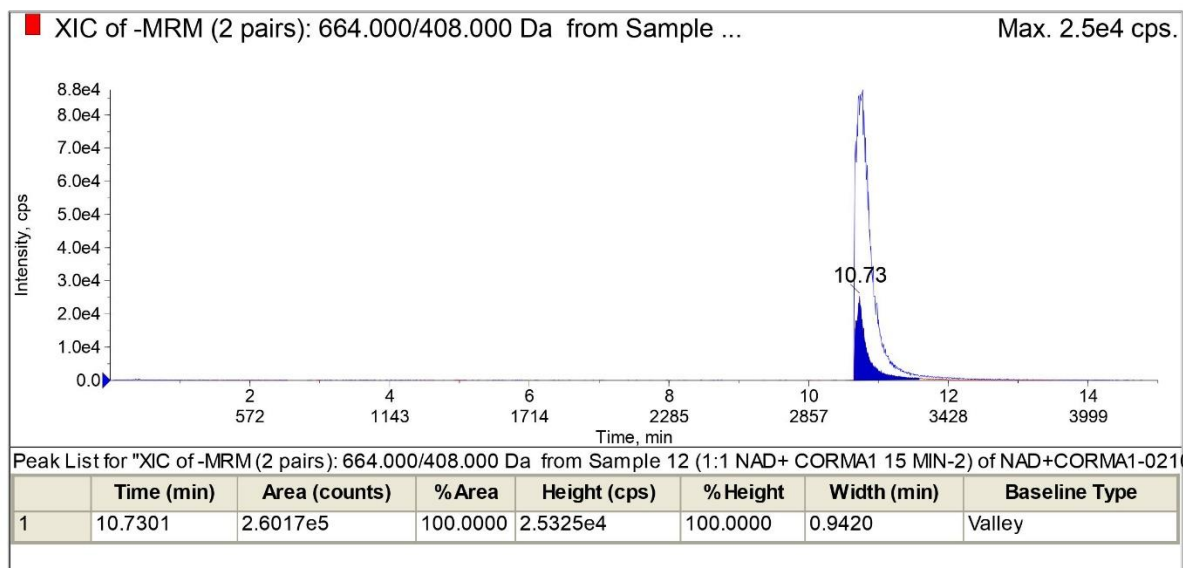
XIC of 1mM NAD⁺ standard in THF detecting for NADH



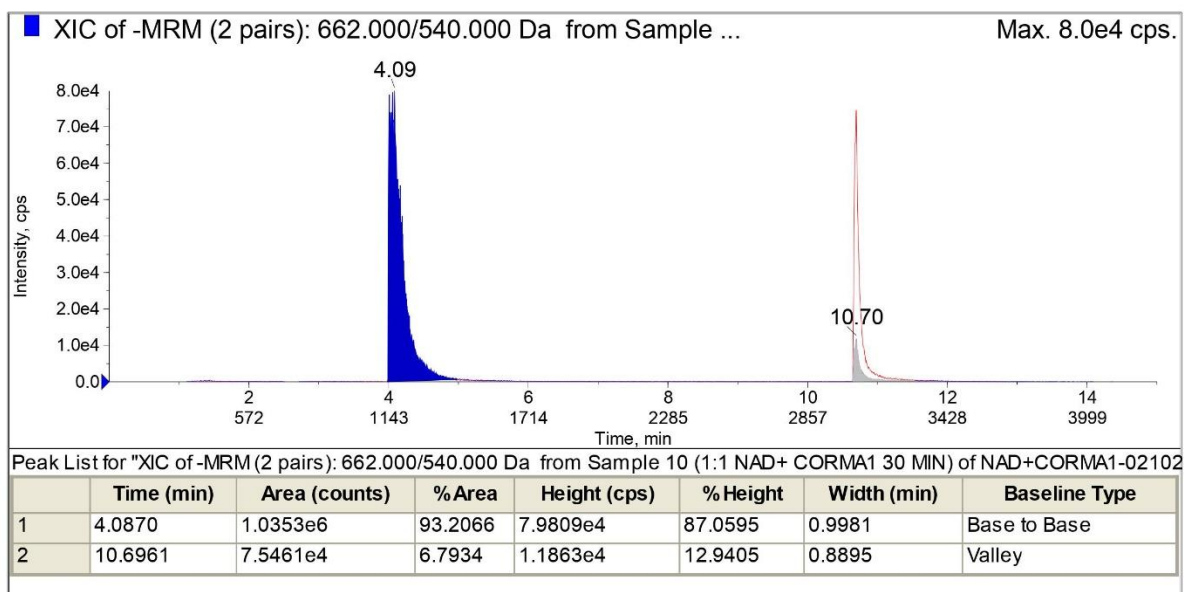
XIC of 1:1 CORM-A1:NAD⁺ at 15min detecting for NAD⁺



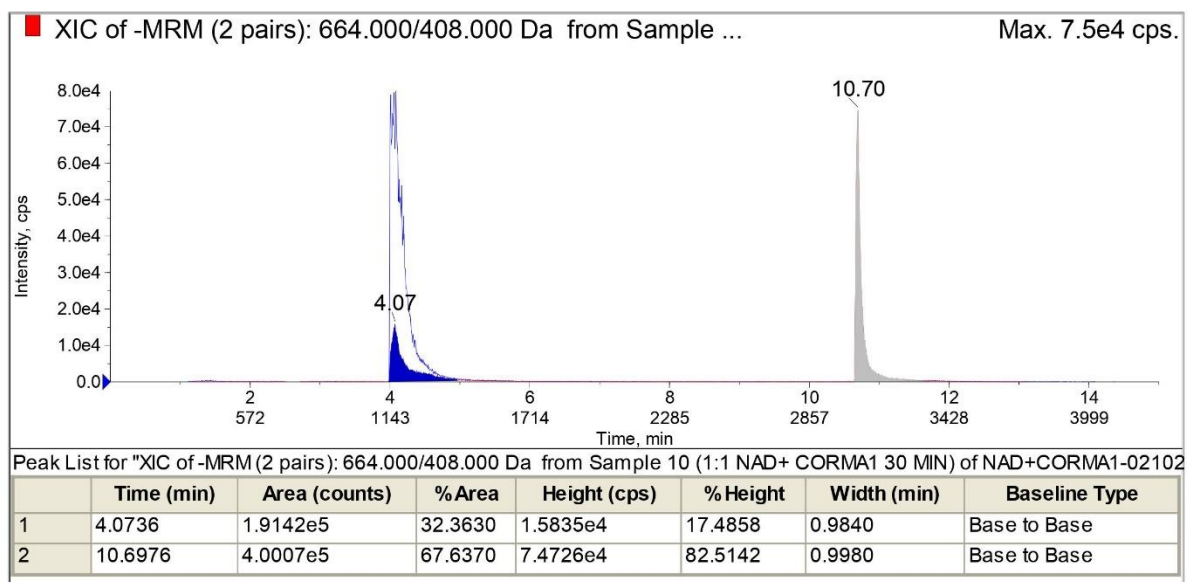
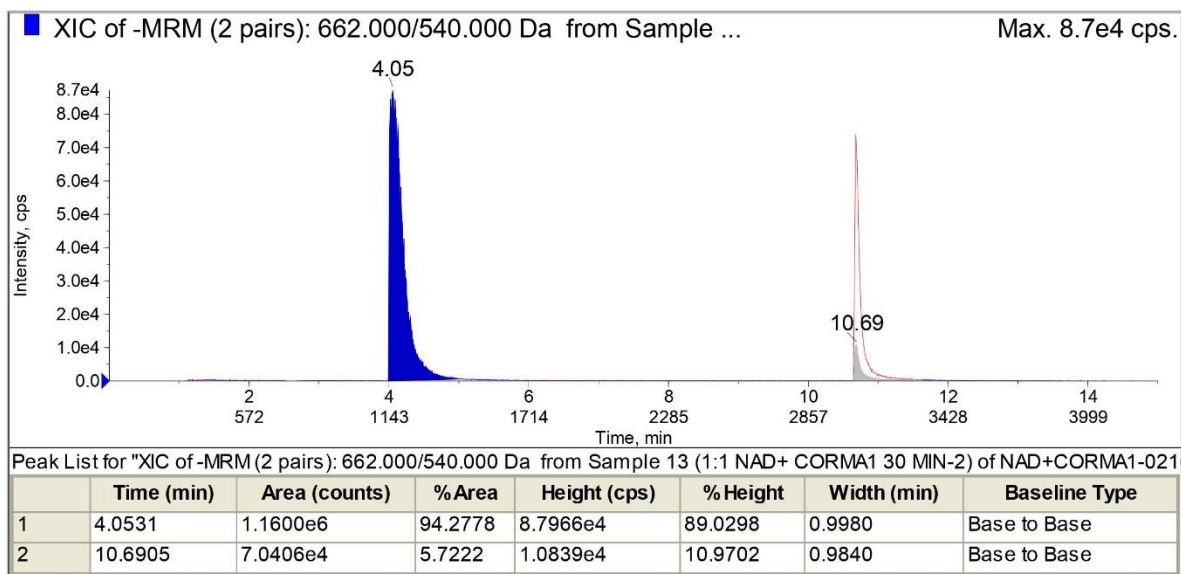
XIC of 1:1 CORM-A1:NAD⁺ at 15min detecting for NADH

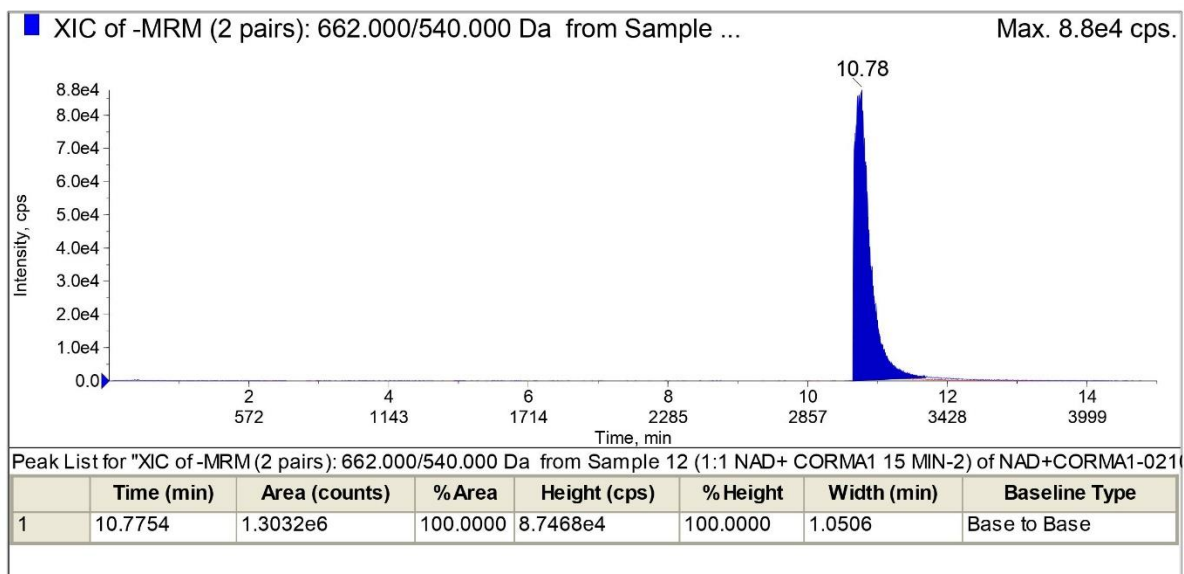


XIC of 1:1 CORM:NAD⁺ (2nd) at 15min detecting for NAD⁺

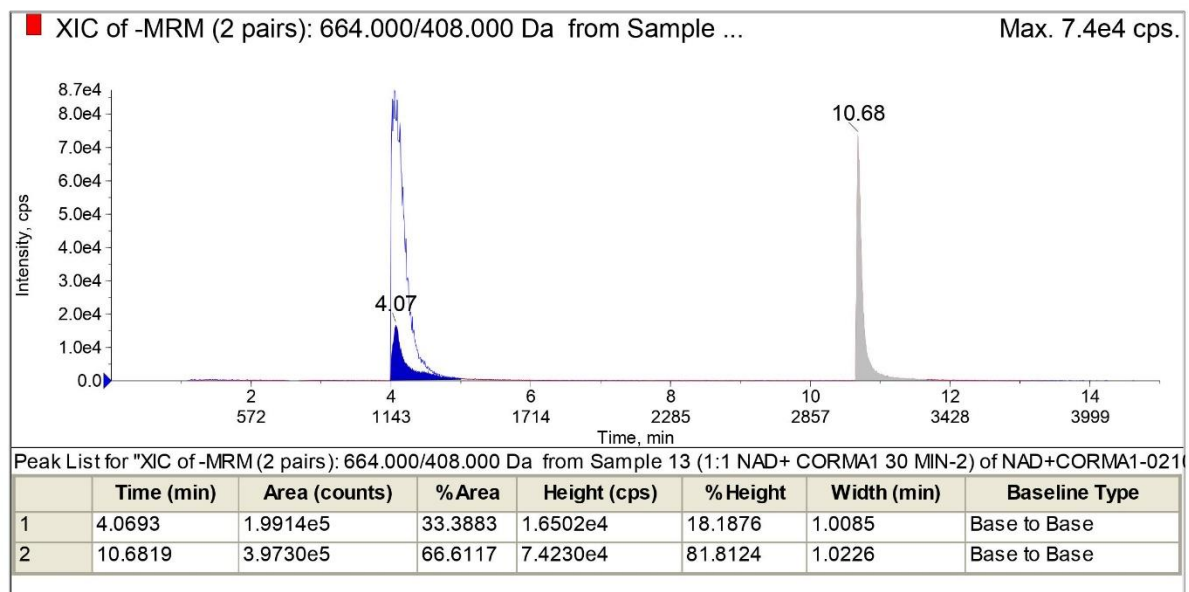


XIC of 1:1 CORM:NAD⁺ (2nd) at 15min detecting for NADH

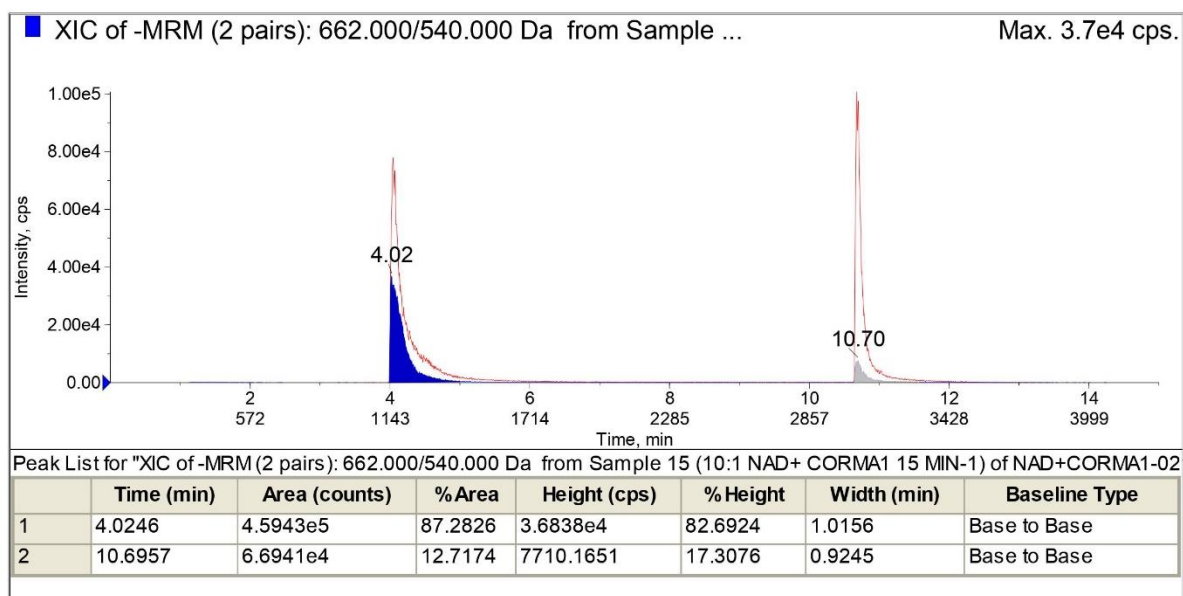




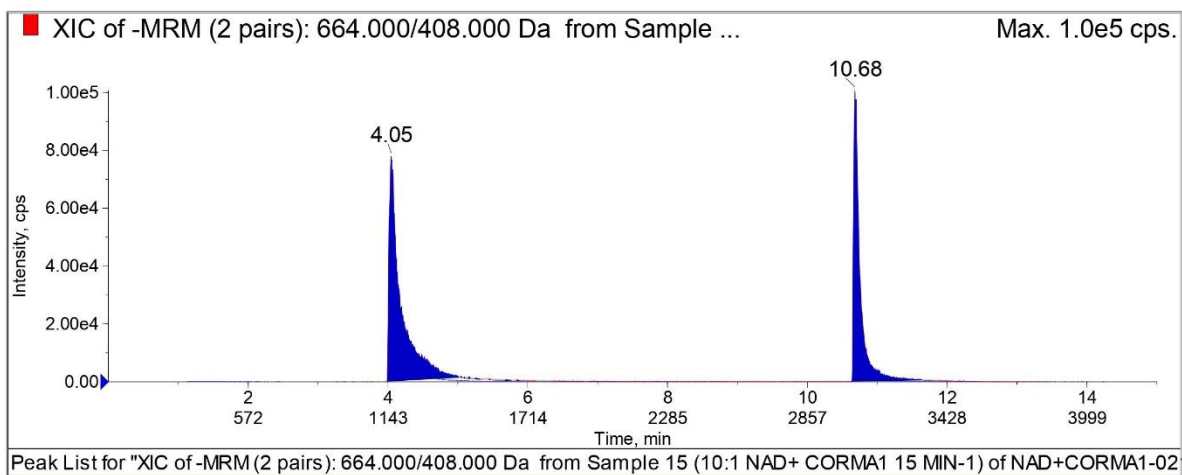
XIC of 1:1 CORM-A1:NAD⁺ (2nd) at 30min detecting for NAD⁺



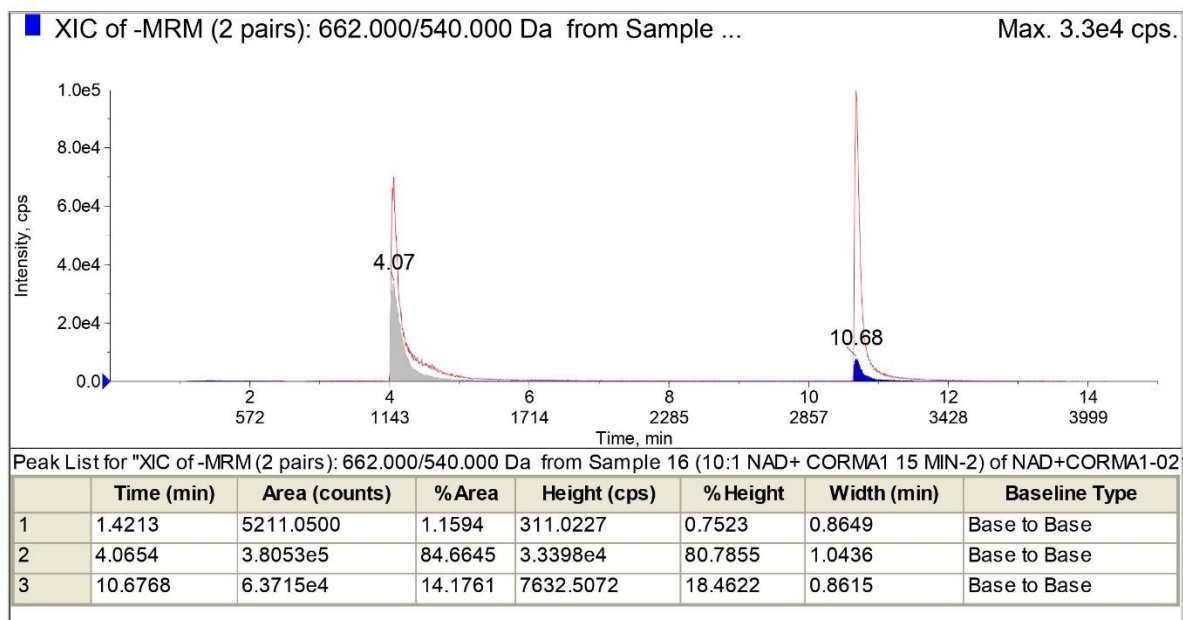
XIC of 1:1 CORM-A1:NAD⁺ (2nd) at 30min detecting for NADH



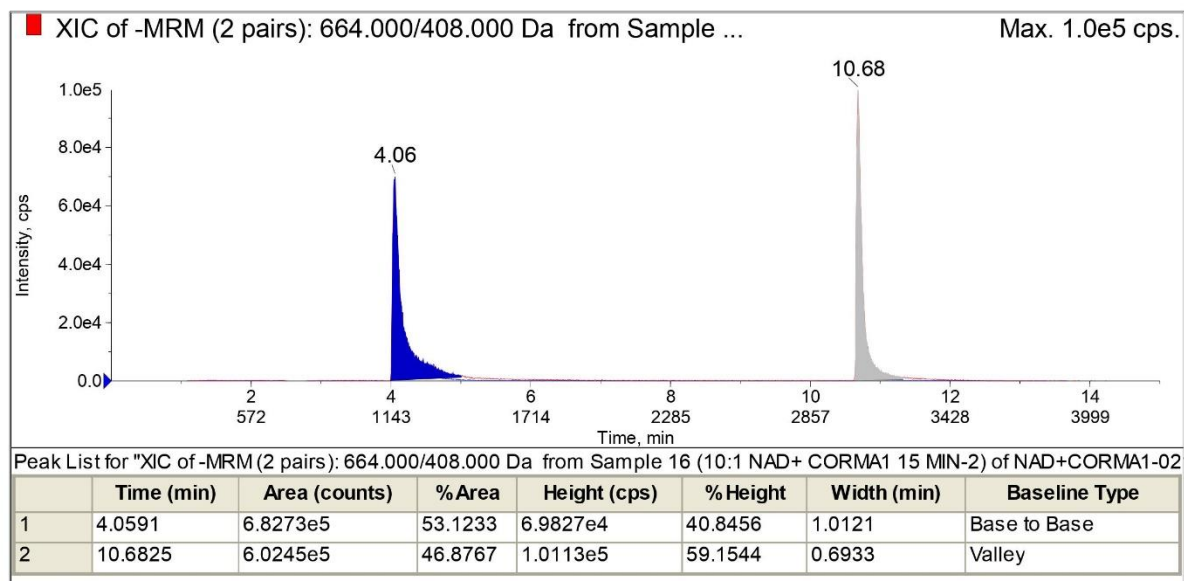
XIC of 10:1 CORM-A1:NAD⁺ at 15min detecting for NAD⁺



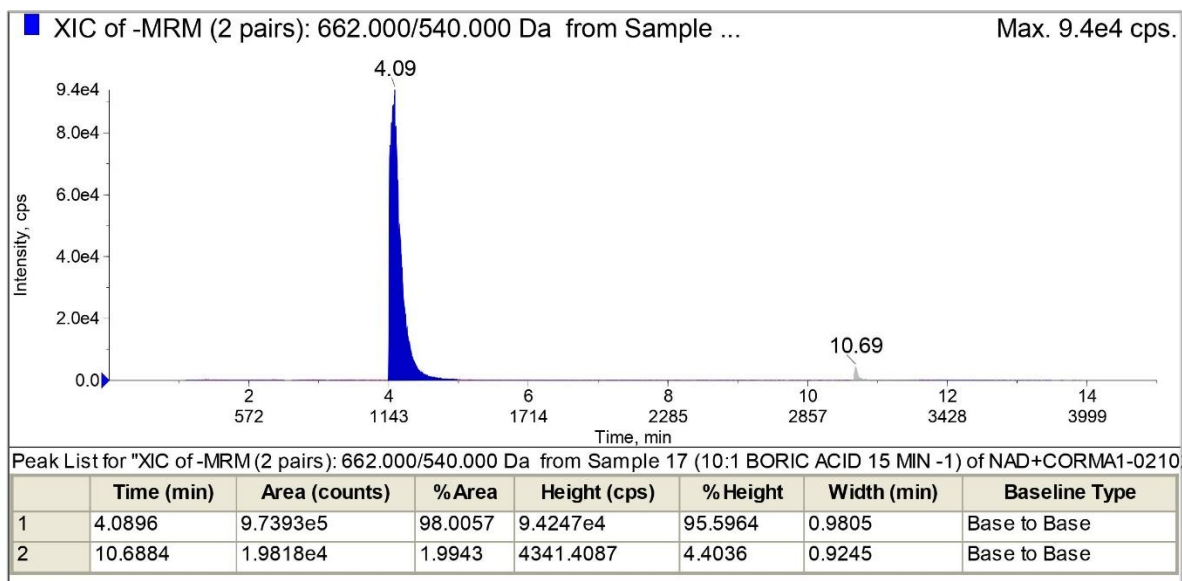
XIC of 10:1 CORM-A1:NAD⁺ at 15min detecting for NADH



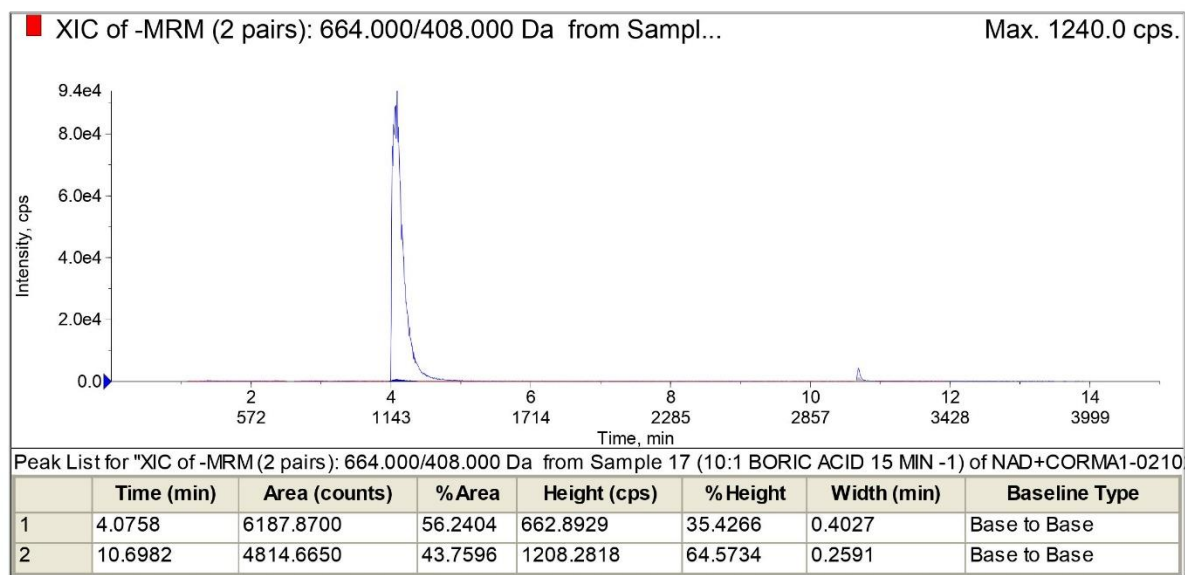
XIC of 10:1 CORM-A1:NAD⁺ (2nd) at 15min detecting for NAD⁺



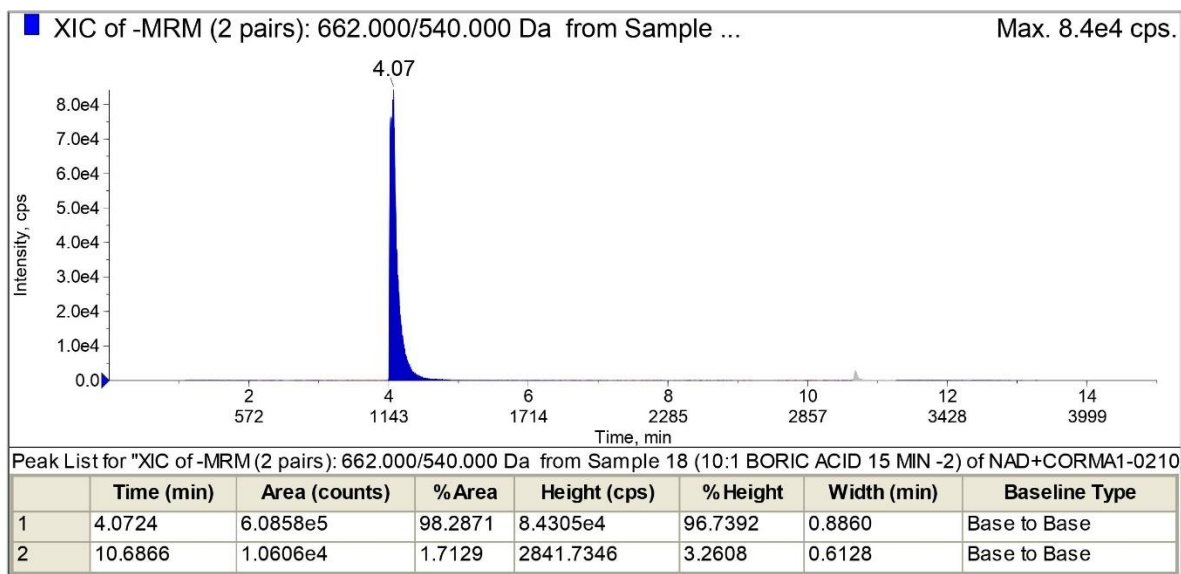
XIC of 10:1 CORM-A1:NAD⁺ (2nd) at 15min detecting for NADH



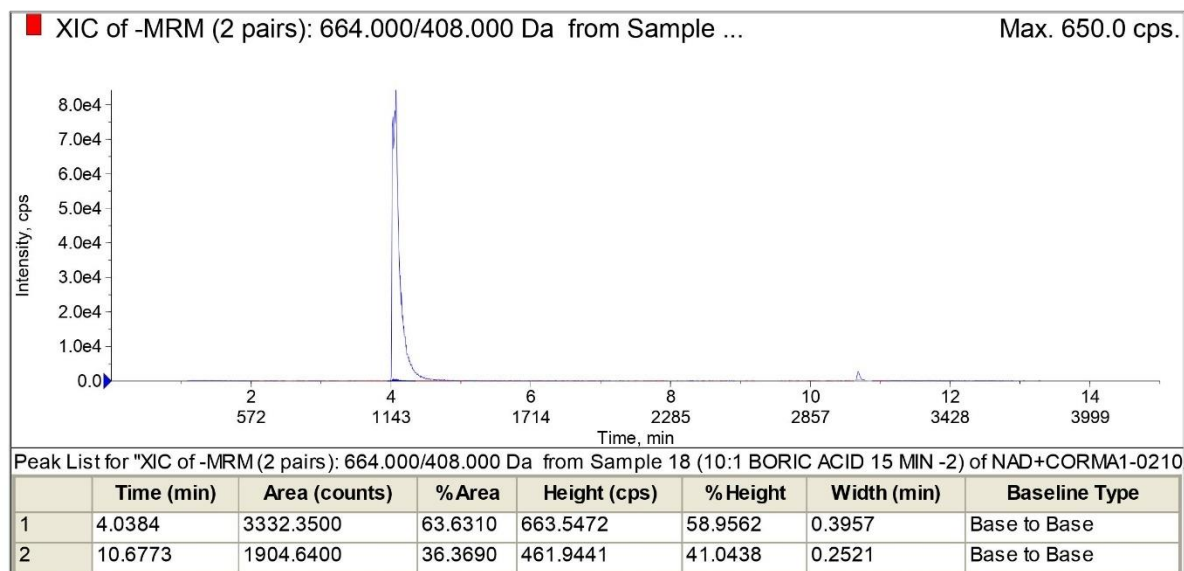
XIC of 10:1 Boric Acid:NAD⁺ at 15min detecting for NAD⁺



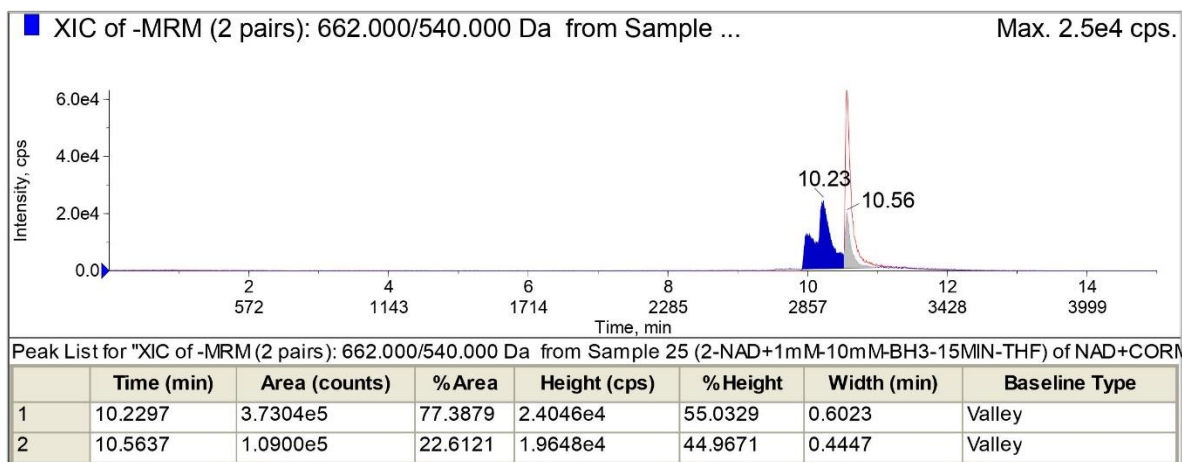
XIC of 10:1 Boric Acid:NAD⁺ at 15min detecting for NADH



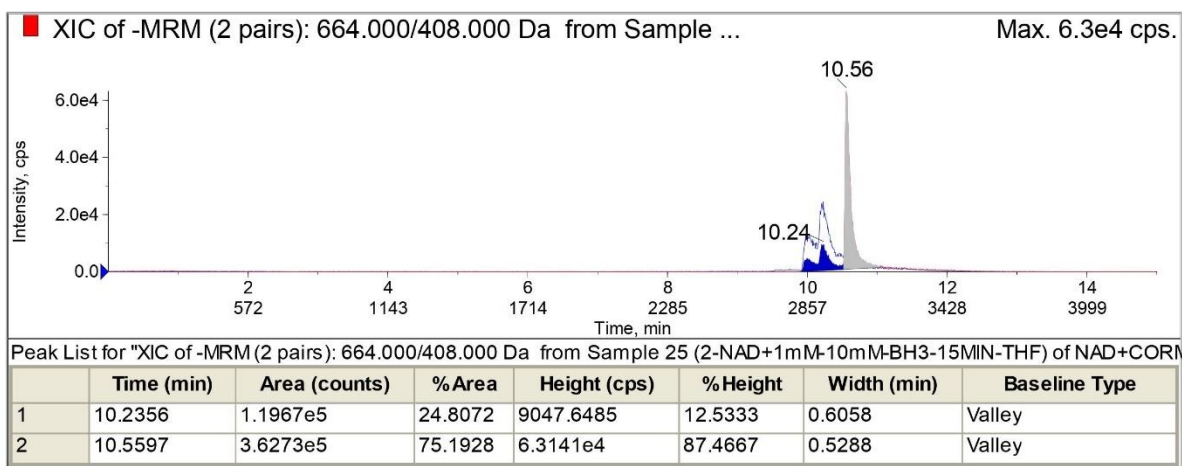
XIC of 10:1 Boric Acid:NAD⁺ (2nd) at 15min detecting for NAD⁺



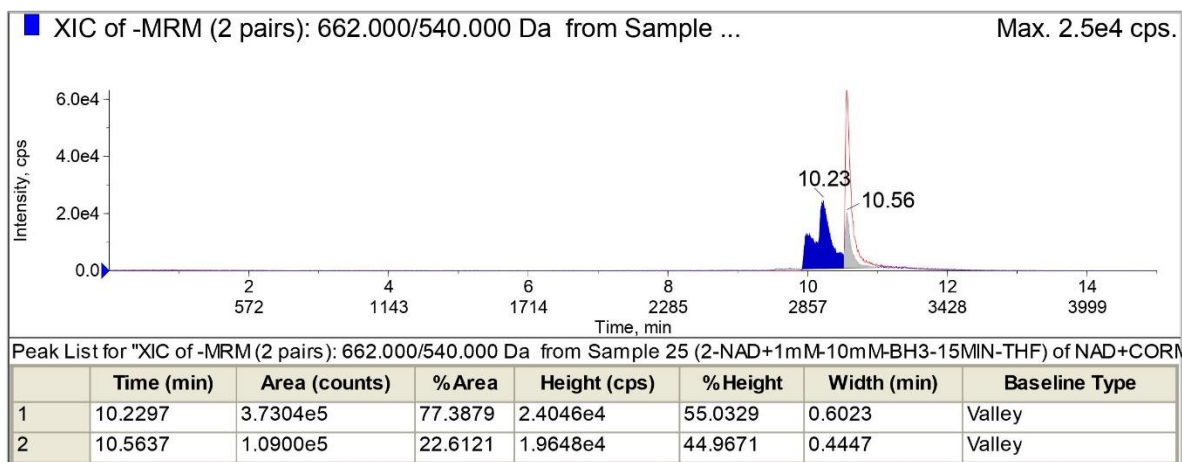
XIC of 10:1 Boric Acid:NAD⁺ (2nd) at 15min detecting for NADH



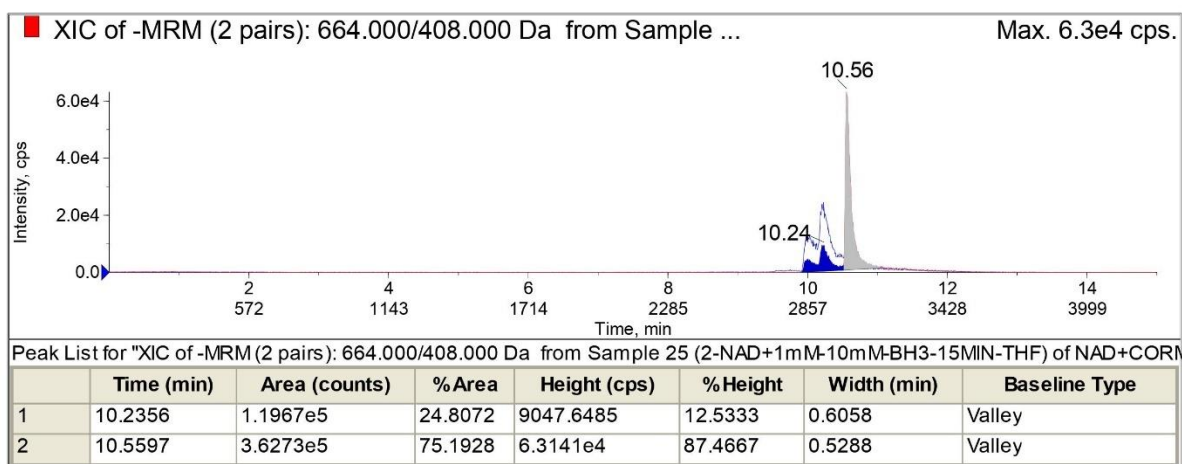
XIC of 10:1 BH₃-THF:NAD⁺ at 15min detecting for NAD⁺



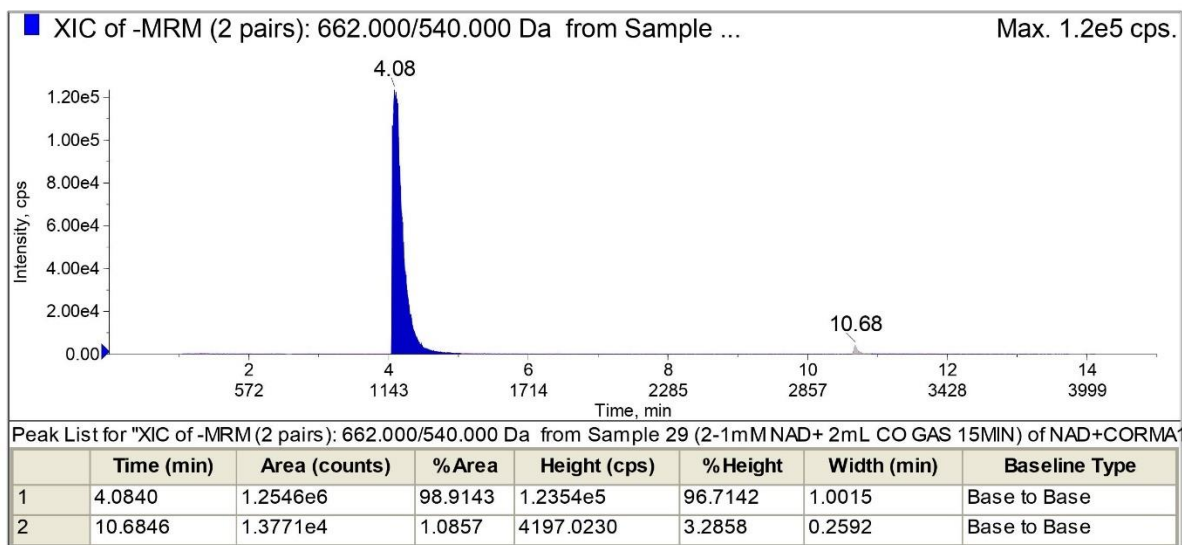
XIC of 10:1 BH₃-THF:NAD⁺ at 15min detecting for NADH



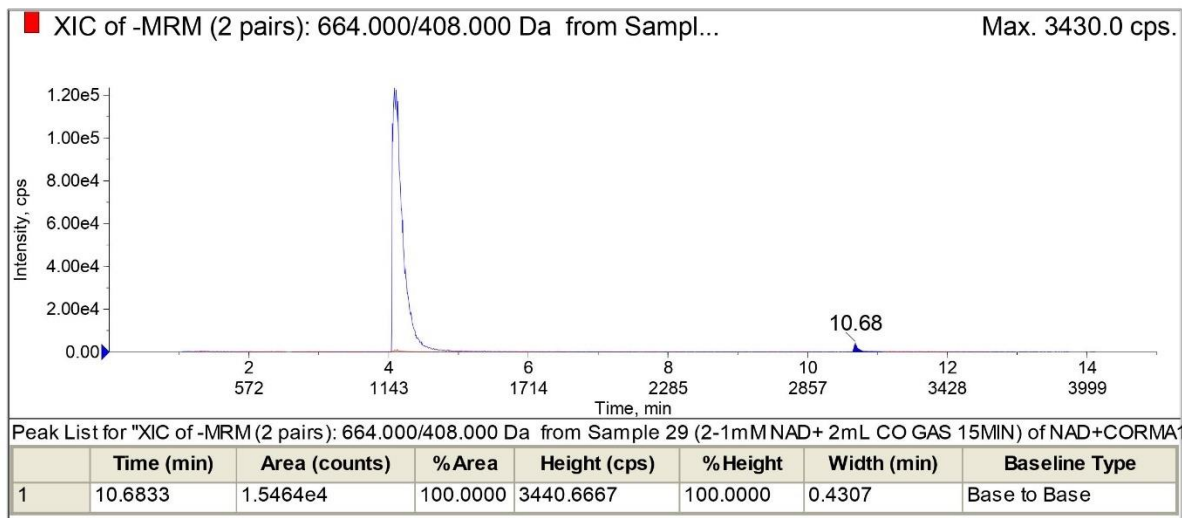
XIC of 10:1 BH₃-THF:NAD⁺ (2nd) at 15min detecting for NAD⁺



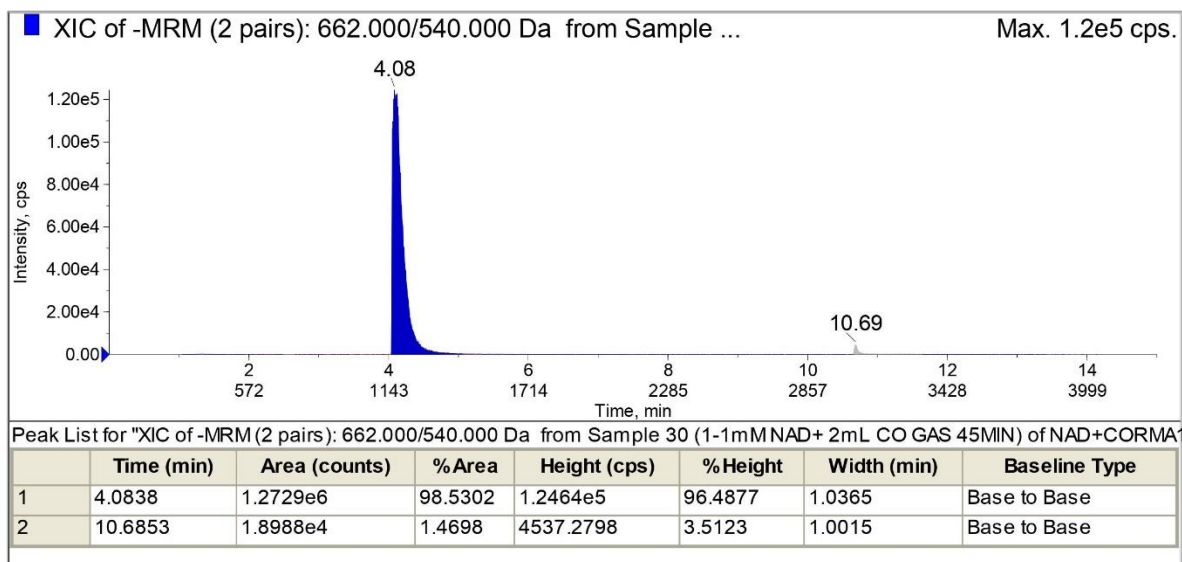
XIC of 10:1 BH₃-THF:NAD⁺ (2nd) at 15min detecting for NADH



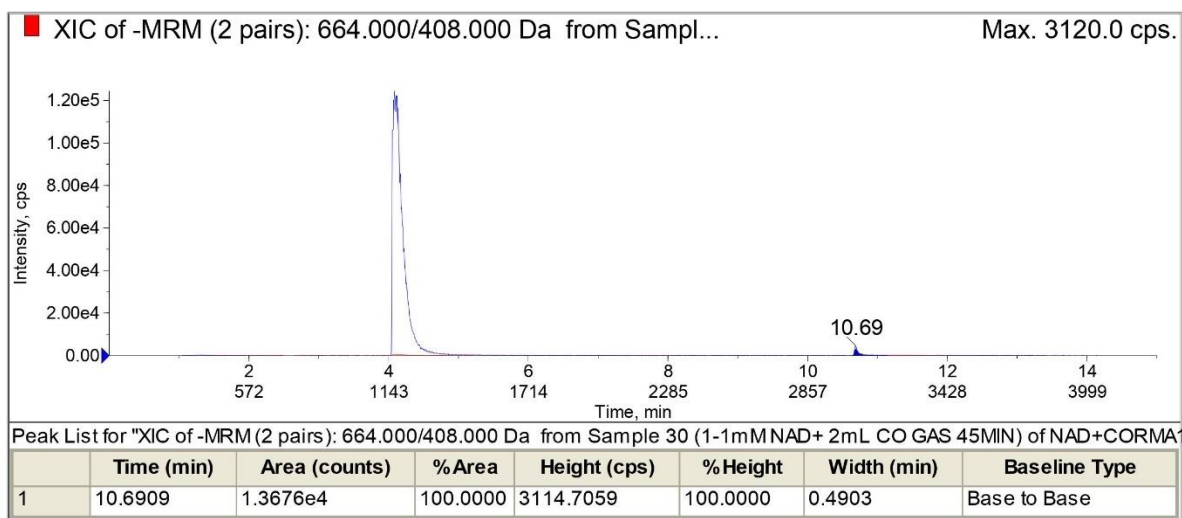
XIC of 2 mL CO Gas in 1mM NAD⁺ at 15min detecting for NAD⁺



XIC of 2 mL CO Gas in 1mM NAD⁺ at 15min detecting for NADH



XIC of 2 mL CO Gas in 1mM NAD⁺ (2nd) at 45 min detecting for NAD⁺



XIC of 2 mL CO Gas in 1mM NAD⁺ (2nd) at 45min detecting for NADH

Appendix A.1 B NMR Spectra for Chapter 1

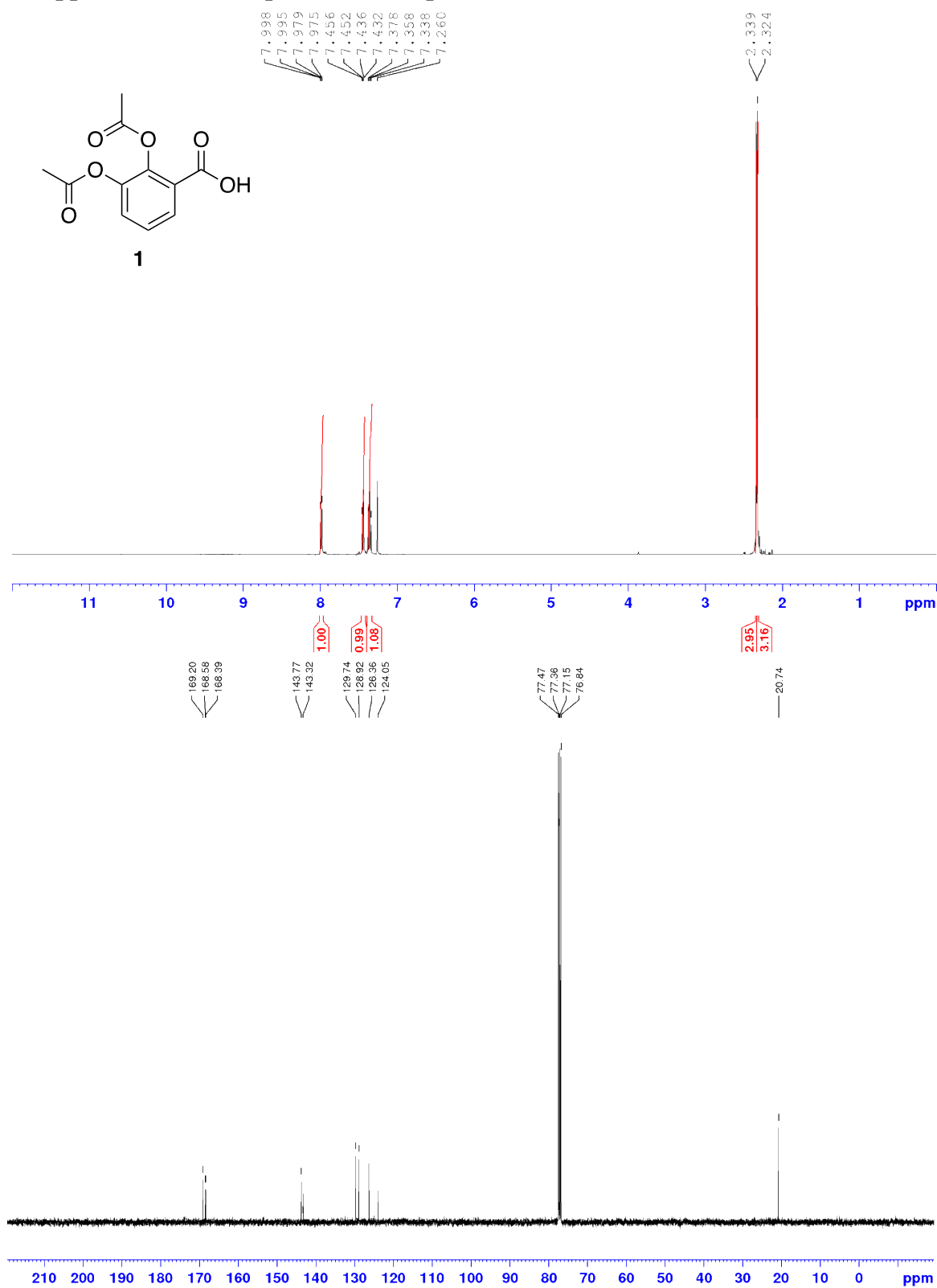
^{11}B NMR Spectra

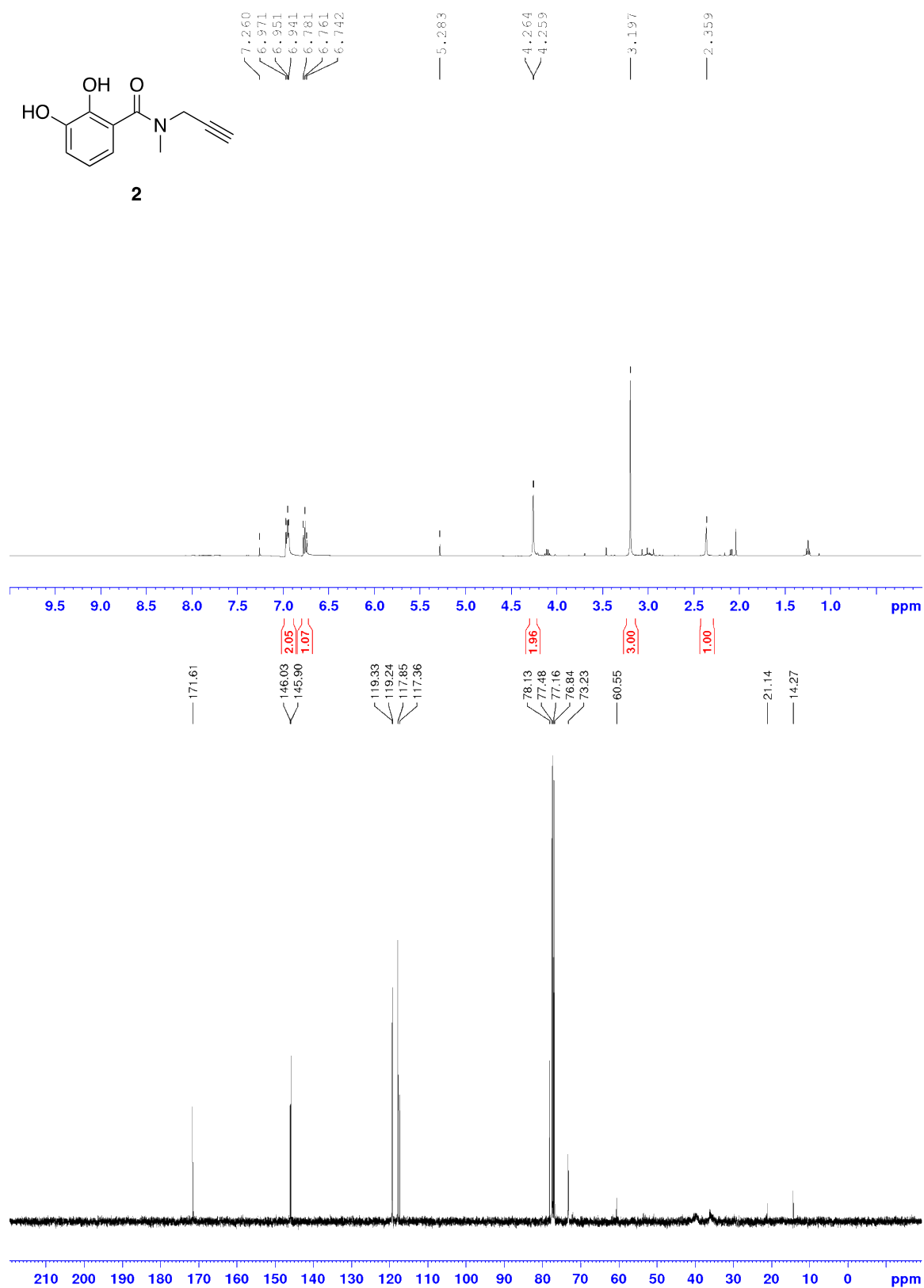


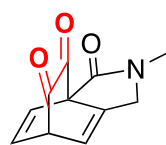
^{11}B NMR of (from top to bottom): 100 mM CORM-A1 in D_2O , the reaction of 100 mM CORM-A1 and 33.3 mM NAD^+ at 10 minutes and 35 minutes, the preceding reaction with an additional 66.6 mM NAD^+ added at 10 minutes and overnight

Appendix A.2

Appendix B: NMR Spectra for Chapter 3







CO-501

